Non-coding RNAs in the Diagnosis of Myocardial Ischemia

Schulte, Christian

Awarding institution:
King's College London

Non-coding RNAs in the Diagnosis of Myocardial Ischemia

PhD Thesis

Christian Schulte

School of Cardiovascular Medicine & Sciences

British Heart Foundation Centre of Research Excellence

January 2023

Submitted for the degree of Doctor of Philosophy from

King's College, London

Supervisors: Prof. M. Mayr & Dr. Anna Zampetaki

1 TABLE OF CONTENTS

ACKNOWLEDGEMENTS

Firstly, I thank Professor Manuel Mayr and Dr. Anna Zampetaki for supporting and enabling this project. Prof. Mayr provided just the right balance of leadership on the one hand and tansfer of responsibility on the other. His unrivalled eye for detail, accuracy and itegrity along with his substantial knowledge and insight were major parts in the foundation of this work. Dr. Zampetaki's perduring support and impressive expertise paved the way for many of the experiments needed to succeed in this PhD.

I must also thank my colleagues in the Mayr laboratory for their social and scientific support. Dr. Temo Barwari was a patient teacher in acquiring numerious lab skills. He was kind and generous with his time and experience. Dr. Abhishek Joshi was a source of ideas and inspiration – in science and in life in general. Dr. Ruifang Lu was kind and supportive. Mr. Christian Kassel was a supportive corner stone in organisation of the lab's necessities.

The Deutsche Forschungsgemeinschft deserve thanks for funding the Fellowship that lead to this Thesis.

I must particularly thank Prof. Tanja Zeller, who has long been and is still my mentor, for preparing and supporting me and putting me into the position to successfully apply for the PhD position, which lead to this thesis.

Finally, enormous thanks to my family: my wife Christin, who agreed to pack bags and travel through Europe with our young and growing family to enable this project; who stepped back on her own career and who waited patiently long hours for me to come home from the lab. My eldest son Johan who moved with us to London at the age of 1 and my second son Leonard who was born during the Fellowship in London. My youngest daughter Emilie, who was born after return to Germany. I thank you all for bringing so much joy.

And my parents Klaus and Brigitte Schulte, who have always been and continue to be as strong a foundation as anyone could wish for.

FIGURES

TABLES

SUPPLEMENTARY MATERIAL

ABBREVIATIONS

AI	Acute myocardial injury
AUC	area under the curve
circRNA	circular RNA
cMyBP-C	cardiac myosin-binding protein-C
cTn	cardiac-specific troponin
cTnT	cardiac troponin T
cTnI	cardiac troponin I
hs-cTn	high-sensitivity cardiac troponin
LIPCAR	long intergenic non-coding RNA predicting cardiac remodeling and survival
lncRNA	long non-coding RNA
MI	myocardial infarction
miRNA/miR	microRNA
ncRNA	non-coding RNA
NSTEMI	Non-ST-elevation myocardial infarction
PEA	proximity extension assay
ROC	receiver operating characteristic

STEMI	ST-elevation myocardial infarction
T1MI	NSTEMI type 1
T2MI	NSTEMI type 2
TASH	transcoronary ablation of septal hypertrophy
UDMI4	fourth universal definition of myocardial infarction

2 ABSTRACT

Rationale. Cardiac-specific troponins (cTns) are excellent circulating biomarkers and considered the current gold standard for a rapid diagnosis of acute myocardial infarction (MI). Nevertheless, abnormal cTn do not differentiate between the different aetiologies of myocardial injury – including type 2 MI (T2MI). In fact, there is no biomarker allowing to differentiate type 1 MI (T1MI) and T2MI. Cardiac myosin-binding protein C (cMyBP-C) was discovered to be released earlier than cTn upon myocardial injury. Initial results of its clinical application in the detection of MI has suggests a potential benefit towards cTn in sensitivity and specificity. The development of more sensitive protein biomarker assays results in continuous improvements of detectability, extending the range of clinical applications to the detection of subclinical cardiovascular disease (CVD). On the other hand, these efforts have not yet led to improvements in risk assessment compared to existing risk scores. Non-coding RNAs (ncRNAs) are expressed in a tissue- and/or cell-type specific manner and show surprising stability in the circulation and ideal properties of circulating biomarkers. They have been assessed as biomarkers, and microRNAs (miRNAs) have attracted most attention. More recently, other ncRNA classes have been identified, including long non-coding RNAs (lncRNAs) and circular RNAs (circRNAs) and have been implicated as novel biomarkers in acute settings of MI but their relationship to myocardial protein biomarkers has not been described. Additionally, ncRNAs have been proposed as prognostic biomarkers for cardiovascular disease. ncRNAs are quantified via quantitative real time polymerase chain reaction (RT-qPCR), which is known to be affected by the presence of heparin in the used biomaterial. Their release kinetics in MI have not been explored without confounding by heparin. Besides their exploration as circulating biomarkers for acute MI, ncRNAs have not yet been reported in the differential diagnosis of specific MI subtypes such as T2MI.

Objective. To compare ncRNA species in heparinase-treated samples with established and emerging protein biomarkers for myocardial injury. To combine protein and ncRNA biomarkers to identify novel biomarker candidates to further discriminate different MI aetiologies.

Methods and Results. Screening of 158 circRNAs and 21 lncRNAs in human cardiac tissue identified 12 circRNAs and 11 lncRNAs as potential biomarkers with cardiac origin. 11 miRNAs were included. Human myocardial tissue was spiked into plasma from healthy individuals and the expression levels of ncRNAs were determined and compared to cardiac proteins. At low spike-in concentrations of myocardial tissue, significantly higher regression coefficients were observed across ncRNA species compared with cTn and cMyBP-C. We transferred our findings to the clinical setting of transcoronary ablation of septal hypertrophy (TASH), in which the exact time point of myocardial injury is known and biomarker kinetics can be assessed in a highly controlled setting. We assessed protein and ncRNA molecules in early time points after TASH as well as in a MI. Heparinase-treatment of serial plasma and serum samples of patients undergoing TASH removed spurious correlations between miRNAs in non-heparinase-treated samples. After TASH, muscle-enriched miRNAs (miR-1 and miR-133a)

showed a steeper and earlier increase than cardiac-enriched miRNAs (miR-499 and miR-208b). Putative cardiac lncRNAs, including previously as a cardiac lncRNA described LIPCAR, did not rise, refuting a predominant cardiac origin. We performed a circRNA microarray screening and assessed candidate circRNAs in MI and myocardial injury samples. Cardiac circRNAs remained largely undetectable. In a validation cohort of acute MI, receiver operating characteristic curve analysis revealed noninferiority of cardiac-specific miRNAs compared with gold standard cTn, but miRNAs failed to identify cases presenting with low cTn values. cMyBP-C was validated as a biomarker with highly sensitive properties, and the combination of muscle-enriched miRNAs with high-sensitivity (hs) cTnT and cMyBP-C returned the highest area under the curve values for the diagnosis of MI. Next, we sought to explore biomarkers for their potential to differentiate different MI subtypes such as T2MI and acute myocardial injury (AI) according to the latest Universal Definition of Myocardial Infarction (UDMI4). While cTn allows for rapid diagnosis of T1MI, its performance to differentiate acute AI or T2MI is limited. The objective was to combine biomarkers to improve discrimination of different MI aetiologies. We determined levels of cTnT and cTnI, cMyBP-C, NT-proBNP and ten miRNAs, known to be associated with cardiac pathology in a total of n=495 serial plasma samples at three time points (on admission, after 1h and 3h) from 57 non-ST-elevation myocardial infarction (NSTEMI), 18 AI, and 31 ST-elevation myocardial infarction (STEMI) patients, as defined by UDMI4 and 59 control individuals. We then applied linear mixed effects model to compare the kinetics of all molecules in these MI subtypes. Established cardiac necrosis markers (cTnT, cTnI) and novel cardiac necrosis markers (cMyBP-C) performed relatively well in discriminating NSTEMI from AI but failed in differentiating T1MI vs T2MI at early time points. All cardiac necrosis markers were higher in T1MI than in T2MI at 3h after admission. Muscle-enriched miRNAs (miR-1 and miR-133a) were correlated with cardiac necrosis protein markers but did not offer better discrimination. Established cardiac stress marker NT-proBNP differentiated AI and T1MI at all time points but failed to discriminate between T1MI and T2MI. However, the combination of NT-proBNP and cTnT along with age presented discriminative potential in differentiating T1MI, T2MI and AI returning an overall AUC of 0.76 [95%CI 0.67 - 0.84].

Conclusions. In a comparative assessment of ncRNAs and protein biomarkers for myocardial injury, cMyBP-C showed properties as the most sensitive cardiac biomarker while miRNAs emerged as promising candidates to integrate ncRNAs with protein biomarkers. Sensitivity of current miRNA detection is inferior to cardiac proteins but a multi-biomarker combination of muscle-enriched miRNAs with cMyBP-C and hs-cTnT could open a new path of integrating complementary characteristics of different biomarker species. Rather than using single biomarkers of myocardial necrosis, a combination of clinical biomarkers for cardiac necrosis (cTn) and cardiac strain (NT-proBNP) might aid in differentiating T1MI, T2MI and AI.

3 INTRODUCTION

3.1 THE BURDEN OF MYOCARDIAL INFARCTION

Recently, the fourth Universal Definition of Myocardial Infarction (UDMI4) re-defined the categories of myocardial infarction (MI) [1]. Importantly, this new definition emphasises the differences of non-ST-elevation MI (NSTEMI) type 1 (T1MI) and NSTEMI type 2 (T2MI). While plaque rupture is the main cause of T1MI, a general imbalance of oxygen demand and supply unrelated to acute coronary athero-thrombosis is supposed to define T2MI. This definition of T2MI comprises numerous different patho-mechanisms, which complicates the reliable diagnosis of T2MI. Yet, T2MI has a similar, if not worse, long-term outcome as T1MI [2]. One of the reasons for the poor prognosis of T2MI may be the lack of early and specific biomarkers differentiating T1MI and T2MI. Thus, there is a need to identify novel biomarker candidates, particularly now that UDMI 4 has redefined T2MI and included a novel subgroup of acute myocardial injury (AI), comprising such disease entities as acute heart failure and Takotsubo cardiomyopathy.

3.2 DIAGNOSIS OF MI

Biomarkers have guided treatment decisions for cardiovascular disease (CVD) over the past 50 years. For cardiac-specific troponin (cTn), this is apparent in the latest and fourth universal definition of MI: for the first time ‘myocardial injury’ is defined alongside ‘myocardial infarction’ as a different disease entity as a result of the ongoing improvements of assay sensitivities allowing for detection of minute changes in circulating cTn levels. Consequently, even settled elevations of cTn levels can be detected [1]. A downside of this increase in sensitivity is an increased likelihood of false positives, requiring new definitions of pathological values in acute and chronic settings, or the definition of new disease states where very low levels of the detected biomarker capture a separate phase of the disease process. Thus, there is still a need to improve upon and complement existing biomarkers for cardiac injury. In this respect, an approach of complementary biomarker combinations seems worth exploring. Circulating non-coding RNAs (ncRNAs) are currently being assessed as biomarker candidates, and initial results, especially for microRNAs (miRNAs), show potential. Further ncRNA species, such as long non-coding RNAs (lncRNAs) and circular RNAs (circRNAs) have properties of circulating biomarkers, but their exploration is still in its infancy [3].

3.2.1 Historical time-line of the identification of biomarkers for MI

The first cardiac-specific protein biomarker, creatine kinase myocardial band (CK-MB) was the biomarker of choice for the detection of MI in the 1980s and 1990s [4]. Up until then, the general muscle marker creatine kinase (CK) was clinically used to determine damage to any type of striated muscle. This obviously involved a high degree of uncertainty, and thus a lack of specificity, with regards to the detection of cardiac damage. In the mid-1990s, the quantification of circulating CK-MB levels allowed for determining quantifiable levels in the circulation 6-10 hours upon onset of myocardial injury. Thus, measurements of CK-MB every 12 hours was defined as an adequate and cost-effective method for the diagnosis of MI [4], earlier than available cTn assays at the time [4]. In the early 2000s, cTnI/T first complemented and later replaced CK-MB as the standard biomarker for acute MI [5]. cTnI/T have been the gold standard in the detection of MI ever since. Good sensitivity and high specificity for the myocardium made cTnI/T superior to CK-MB. Nevertheless, CK-MB may still be used in biomarker-based estimation of the extent of myocardial damage upon MI or after coronary intervention as well as in patients with impaired renal function, where cTn levels can be elevated [6]. Over the past decade, significant improvements in cTn detection assays have led to the development of high-sensitivity assays, which have contributed to changes in clinical practice: The application of hs-cTn assays allows for a sensitive detection of MI within one hour after hospital presentation and thus improves early stratification of patients with suspected MI [7]. A timeline of biomarker discovery for MI is presented in **Figure 1** and illustrates the novelty of RNA-based circulating biomarkers compared to protein-based biomarkers, including a novel protein biomarker candidate: cardiac myosin-binding protein C (cMyBP-C).

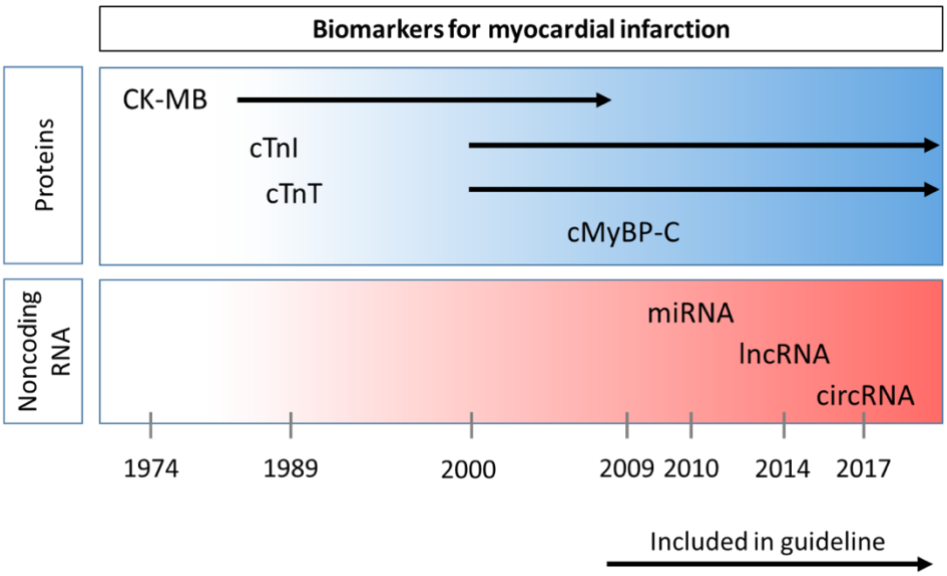

Figure 1. Time Line - Biomarkers for Myocardial Infarction. *While protein-based molecules were discovered in the late 1980s and have been implemented as clinical routine biomarkers for over 20 years, non-coding RNAs have only recently been identified as potential biomarkers for over 20 years, non-coding RNAs have only recently been identified as potential biomarker candidates in acute myocardial infarction. Reproduced from Schulte et al, Trends Mol Med 2020*

3.3 DIFFERENTIATION OF MI SUBTYPES USING BIOMARKERS

The diagnosis of MI relies on the quantification of cTn. Hs-cTn assays offer rapid rule-in and rule-out for MI [1,2]. The recent fourth Universal Definition of Myocardial Infarction (UDMI4) re-defined the categories of MI [3] by emphasising the differences of T1MI and T2MI and including the novel subcategory of AI. While plaque disruption is the main cause of T1MI, T2MI is defined by a general imbalance of oxygen demand and supply. T2MI comprises numerous different patho-mechanisms and lacks a reliable biomarker for diagnosis. T2MI has a similar, if not worse, long-term outcome as T1MI [4,5]. Thus, there is a need to identify novel biomarker candidates, particularly with UDMI4 redefining T2MI to exclude abnormal cTn values without acute ischaemia and grouping this into AI subtype.

Nestelberger et al. have recently compared established cardiac biomarkers as well as cMyBP-C in their potential to differentiate T1MI and T2MI [9]. The authors concluded that current single biomarkers only provide moderate additional value in the discrimination of T1MI and T2MI. However, patients with AI were excluded from their analysis. AI represents a clinically important subgroup, including predominantly patients with heart failure and heart failure-like phenotypes. More recently, Neumann et al. compared 29 biomarkers measured at baseline to discriminate MI and myocardial injury [10]. The authors propose a panel of 4 biomarkers to discriminate T1MI and T2MI and a combination of 6 biomarkers to distinguish NSTEMI from myocardial injury. However, AI was not segregated from chronic injury and biomarker combinations were not explored to differentiate all the 3 subtypes i.e., T1MI, T2MI and AI. Additionally, protein biomarkers were measured solely at baseline [10] while biomarker kinetics are important in the clinical evaluation of myocardial damage[11].

3.4 PROTEIN BIOMARKERS

3.4.1 Troponin

Troponins are a component of thin myofilaments of the contractile apparatus (together with actin and tropomyosin). The troponin complex consists of TnC, TnI, and TnT. cTnI and cTnT are cardiac-specific and amongst the most widely used biomarkers. They are the gold standard for detection of myocardial injury due to their cardiac specificity and the exceptionally high sensitivity of current assays [8]. The assays performance is a result of extensive optimization since their first identification as circulating biomarkers almost three decades ago [9]. While only a few years ago, any detectable cTn values implied a pathological process, the latest hs-cTn assays return detectable values in a large proportion of healthy individuals. Before expanding the application of this assay to diagnosis of subclinical disease and risk prediction [10], it remains to be determined if such very low cTn levels reflect clinically relevant myocardial injury or just myocyte protein turn-over. New cut-offs for pathological cTn values will have to be defined in acute and chronic disease settings. As an example illustrating how hs-Tn assays are transforming cTn from a diagnostic to a potential prognostic marker for CVD risk assessment [11], cTn

levels were assessed in 22,000 individuals with suspected MI. Within the MI group the 1- and 2-year risk for further CVD events gradually increased with the cTn level at presentation – even at values below the 99th percentile. The same trend was observed in 8,345 matched-pair individuals from a data set comprising 70,000 individuals from the general population, exemplifying the potential use of cTn as a biomarker for primary CVD risk assessment. Yet, the use of cTn in addition to existing CVD risk scores offered little improvement upon risk assessment using conventional risk factors [12]. Therefore, complementary biomarkers are needed.

3.4.2 Cardiac myosin-binding protein C (cMyBP-C)

cTn has revolutionized the diagnostics of MI over the past two decades, but with the exceptional sensitivity of the latest cTn assays there is a need for improvements in specificity. Peak cTn levels are reached 24h after onset of MI. Cardiac biomarkers with an earlier release and faster clearance could add value in clinical decision making. cMyBP-C is a sarcomeric, thick filament-associated protein which is more abundant in cardiomyocytes than cTn [13]. Using proteomics, it was discovered that cMyBP-C is released earlier than cTn upon myocardial injury [14,15]. Ischemia-induced proteolysis and the generation of N-terminal fragments of cMyBP-C provide a likely explanation for this earlier release. In patients undergoing trans-coronary ablation of septal hypertrophy (TASH), cMyBP-C rose more rapidly after onset of myocardial injury than cTn [16]. In ROC analysis, cMyBP-C outperformed hs-cTnT and hs-cTnI after TASH [3]. Subsequent studies in patients with MI, where cTn serves as the adjudicator of the diagnosis, showed that cMyBP-C offered comparable performance to cTn. Testimony to the high sensitivity of this assay, cMyBP-C was detectable in all healthy individuals serving as controls, while one fifth had hs-cTnT levels below the lower limit of detection [3]. This suggests cMyBP-C as a candidate biomarker for early and subclinical disease states as well as for risk prediction. Anand *et al*. reported cMyBP-C to be associated with myocardial hypertrophy and fibrosis in aortic stenosis patients and an increased risk of mortality in these patients [17]. However, no data for cMyBP-C are available so far in a primary preventive setting. In this respect the evaluation of cTn in subacute CVD entities and risk prediction has been assessed more thoroughly, not least because cTn assays are widely available and extensively validated. cMyBP-C measurements still need to be performed in larger cohorts with defined cut-off values, to address the risk of false positives for cardiac biomarkers with high sensitivity.

3.5 NCRNA BIOMARKERS

Among the 20,000 protein-coding genes, surprisingly few proteins have cardiac tissue specificity: 12 proteins are considered to be cardiac-specific and some have already been implemented in clinical applications, i.e. cTns and natriuretic peptides (**Table 1**, adapted from https://www.proteinatlas.org/humanproteome/tissue/heart). With the completion of the Human

Genome Project, an increasing number of ncRNAs have been identified. ncRNAs constitute the largest proportion of the RNA pool [18]. They are functional RNA molecules considered to play key regulating roles in cell biology. Several subcategories of ncRNAs have been described and numerous ncRNAs have been studied in the context of cardiovascular disease (CVD). ncRNAs are generally categorised into short ncRNAs with <200 nucleotides in length and long ncRNAs (lncRNAs) (>200 nucleotides). The best-studied short ncRNAs are miRNAs. miRNAs are single-stranded, usually 18-25 nucleotides long RNA molecules, which are transcribed in the nucleus, before they are processed and transported into the cytosol, where they exert their biological function. circRNAs can be considered a sub-category of lncRNAs and are characterised by their circular shape, created in a process called 'back-splicing' from precursor mRNA, which leads to formation of a covalent binding of the 5' and the 3' end of the linear transcript [19] (**Figure 2**). ncRNAs play important roles in heart development and aging [20] and are key regulators of cardiomyocyte proliferation and heart regeneration [21]. This has led to their exploration in different CVD entities such as heart failure and ischemic heart disease.

Gene	Description	Clinical Use as Biomarker
NPPB	Natriuretic peptide B	Established: Heart Failure, Novel/Potential: CVD risk
MYL7	Myosin, light chain 7	No
NPPA	Natriuretic peptide A	No
MYBPC3	Cardiac myosin-binding protein C	Novel: Diagnostic in AMI, Potential: CVD risk
TNNT2	Troponin T type 2 (cardiac)	Established: Diagnostic in MI, Novel: Post MI risk Potential: CVD risk
BMP10	Bone morphogenetic protein 10	No
TNNI3	Troponin I type 3 (cardiac)	Established: Diagnostic in MI, Novel: Post MI risk Potential: CVD risk
MYH6	Myosin heavy chain 6 (cardiac)	No
ANKRD1	Ankyrin repeat domain 1 (cardiac)	No
RD3L	Retinal degeneration 3-like	No
SBK2	SH3 domain binding kinase family member 2	No
MYL4	Myosin, light chain 4	No

Table 1. 12 cardiac-specific genes with the highest expression in the heart. *Reproduced from Schulte et al, Trends Mol Med 2020*

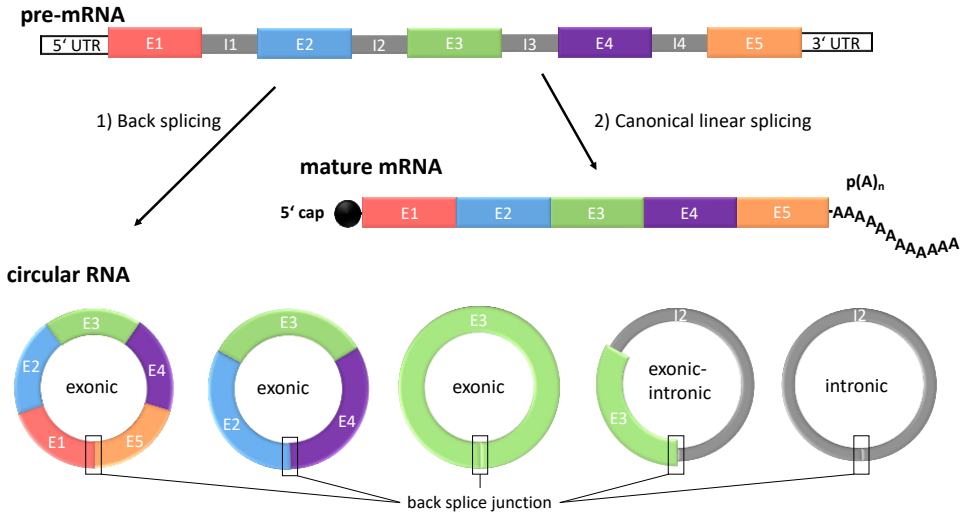

Figure 2. circRNAs are generated via back-splicing. *Both, mRNA and circRNA are spliced from pre-mRNA. circRNA generation requires the specific process of back-splicing in order to achieve the generation of a circular shape with the 3' and the 5' end joining in a back-splice junction, where the two free ends are joined to form a complete circle. CircRNAs can be made up either exclusively of exons or of exons and introns or of an intron only. circRNA = circular RNA; lncRNA = long non-coding RNA; RNA = ribonucleic acid. Amended from Schulte et al, Trends Mol Med 2020*

3.5.1 ncRNAs as circulating biomarkers for cardiovascular disease

Apart from their important intracellular function, ncRNAs, can also be detected in the circulation with surprising stability [22] – freely circulating but also encapsulated in extravesicular bodies,

microvesicles, bound to proteins and associated with and derived from circulating cells such as platelets. This has opened up new avenues of biomarker research to complement protein measurements [19]. ncRNAs have been assessed for their application as circulating biomarkers in CVD [23]. Given their tissue-specific expression, a subset of ncRNAs could serve as 'companion biomarkers' [24] to existing protein biomarkers or as signatures comprising a combination of different ncRNAs to increase specificity [25]. Recently, ncRNAs have been implicated as biomarkers of MI. Plasma and serum levels of muscle- and cardiac-enriched microRNAs (miRNAs) increase markedly after MI [26,27]. Circulating levels of the Long Intergenic ncRNA Predicting Cardiac Remodeling (LIPCAR) were reported to predict adverse cardiac remodelling and death after MI [28]. circRNAs as a different ncRNA species are less susceptible to Rnase activity and may offer tissue specificity with >15,000 circRNAs being present in the human heart [29,30].

3.5.2 miRNAs

miRNAs are single-stranded, usually 18-25 nucleotides long RNA molecules, which are transcribed in the nucleus, before they are processed and transported into the cytosol. miRNAs are expressed in a tissue- and cell type specific fashion [31,32]. They are located in the cytosolic compartment of the cell where they exert their major function: miRNAs function as repressors of gene expression via binding to mRNA and inhibition of protein translation [33]. It is widely recognized that miRNAs are involved in cardiac ischemia signaling and regulation processes [34]. Furthermore, miRNAs have been explored as therapeutic candidates for treatment of CVD, such as miR-92a, which has entered phase I clinical trial for the treatment of ischemic heart disease [35] (NCT03603431) or the first antisense oligonucleotide against a miRNA (miR-132), which recently entered clinical trials for treatment of heart failure (NCT04045405) [36]. A landmark study by Mitchell *et al* revealed that miRNAs are not just confined to the intracellular space, but are also present in the circulation [22]. In contrast to messenger RNAs (mRNAs), circulating miRNAs are protected from degradation through several mechanisms including binding to protein complexes and lipoproteins as well as being encapsulated in microvesicles [37–39]. In this respect miRNAs have been explored as biomarkers for cardiac ischemia and myocardial injury [19]. However, the copy numbers of circulating miRNAs are low. Without a receptor or another amplification mechanism, it is difficult to envisage how the stoichiometry of circulating miRNAs to intracellular mRNA targets can result in major changes in gene expression. Regardless of their function, their potential use as circulating biomarkers for CVD has been studied over the past years [40,41].
Hundreds of miRNAs can be detected in plasma and serum samples from healthy volunteers. However, a subset of miRNAs with cardiac enrichment is only detectable in the circulation after MI. miRNAs that are highly expressed in the heart include miR-1 and miR-133. Similar to myofilament proteins, miR-1 and miR-133 are also present in skeletal muscle. In contrast, miR-499 and miR-208 are less abundant

in the heart but more specific for cardiac versus skeletal muscle injury [32]. A study by van Rooij *et al* [42] described dysregulated miRNAs in failing hearts of humans and mice. A subsequent study in the context of MI showed dysregulation of miRNAs after myocardial injury [43]. Muscle- and cardiac-enriched miRNAs were low or even undetectable in plasma from healthy volunteers, whereas in patients with MI, an increase was detectable as soon as one hour after onset of ischemia [26]. Detectability of changes in miRNA levels thereby preceded that of cTnI. To determine release of miRNAs upon myocardial injury in a well-controlled model of myocardial injury, Liebetrau *et al* studied patients undergoing TASH [44]. As the precise onset of myocardial injury in this procedure is known, this setting allows for a well-controlled assessment of release kinetics of cardiac miRNAs upon MI. In line with previous studies, plasma levels of muscle-enriched miR-1, miR-133a and cardiac-enriched miR-208a increased during the first four hours after TASH. The authors also demonstrated that miRNA release kinetics correlated with cTn levels. However, cardiac biomarker release after TASH may differ from ischemia. With regards to the available publications on miRNAs as biomarkers for cardiac injury, there are two important considerations. First, quantification methods for miRNAs rely on quantitative real time polymerase chain reaction (qPCR) assays. Not only are these measurements time-consuming and expensive, they can also be confounded by the presence of heparin [45]. Surprisingly, even a single bolus injection of heparin is sufficient to alter the results from qPCR assays [45]. Yet, most key publications reporting miRNAs as potential biomarkers for acute MI have not accounted for the presence of heparin, although it is routinely administered in cases with suspected MI (**Table 2**).

Author	**Heparin**	**Temporal assessment**	**Troponin comparison**	**Cq cutoff**	**Individual data points**	**Low hs-cTnT measures**
Ai et al.	?	no	no	30	yes	no
Adachi et al.	?	no	no	?	no	no
D'Alessandra et al.	?	yes	yes	40	no	no
Wang et al.	?	no	no	40	yes	no
Da Rosa et al.	Not administered	no	no	?	no	no
Kuwabara et al.	?	yes	no	40	yes	no
Corsten et al.	?	no	no	?	yes	no
Devaux et al.	?	no	yes	?	no	no
Long et al.	?	late	non-hs only	40	no	no
Oerlemans et al.	?	no	no	?	no	yes
Cheng et al.	?	animals only	no	?	no	no
Liebetrau et al.	?	yes	no	?	no	no

Olivieri et al.	Not administered	no	no	35	no	yes
Vogel et al.	?	yes	no	?	no	yes

Table 2. Publications on circulating miRNAs and their utility as biomarkers in the detection of acute myocardial infarction. *Reproduced from Schulte et al. Circ Res 2019*

ncRNA detection was reported to be inhibited even in conditions with high endogenous heparin levels, such as thoracic aortic aneurysm [46]. Treatment of RNA samples with heparinase can overcome this confounding issue [47], but this finding awaits clinical confirmation. Second, detectability of trace amounts of cardiac miRNAs, analogous to very low cTn levels, is still an unmet need. Finally, in addition to the release of miRNAs from cardiac tissue, acute MI is accompanied by a systemic response that may well be reflected in changes of circulating ncRNAs but is not directly the result of the myocardial injury. The first prospective community-based cohort study examining the predictive value of circulating miRNAs with respect to MI in a primary prevention setting was performed by Zampetaki *et al.* [48]. The authors found a signature of three miRNAs, platelet-enriched miR-223 and miR-197 as well as endothelial cell and platelet-enriched miR-126. Importantly, none of these miRNAs were predictive on their own, but instead only their combination returned significant associations with future CVD events. The prognostic value of these three miRNAs as circulating biomarkers was further explored in a cohort of 873 patients with diagnosed CAD in a secondary prevention setting. Unlike in primary prevention, a combination was of miRNAs was not required: elevated levels of miR-126 were predictive for future cardiovascular death [49,50]. Interestingly, miR-197 and miR-223 were also positively associated with an adverse outcome [50]. Given that these miRNAs are platelet-associated, it is plausible that anti-platelet treatment in secondary prevention influences circulating miR-126, miR-197 and miR-223 levels. Higher levels of these miRNAs may reflect less efficient platelet inhibition on anti-platelet therapy. Bye *et al* evaluated several miRNAs as potential predictors of future MI, proposing a panel of five miRNAs that could enhance the predictive strength of conventional algorithms [51]. Interestingly, the authors were not able to validate the abovementioned, previously identified [48] platelet and endothelial cell miRNAs as predictors of CVD outcome. As a potential reason, the authors discuss different normalization methods applied in the studies. Altogether, these studies indicate that: 1) miRNAs could be informative on *in vivo* platelet activation or treatment response to anti-platelet therapy; and 2) emphasize the importance of harmonized miRNA quantification methods in an attempt to facilitate comparability across studies.

3.5.3 lncRNAs

lncRNAs are a large group of ncRNAs defined by being >200 nucleotides in length [52]. Thus far, there is no agreement on sub-classification for lncRNAs. Unlike miRNAs, lncRNAs are mainly located within the nucleus or in mitochondria [28,53]. Their biosynthesis shares similarities with mRNAs with regards to transcription, polyadenylation, capping and splicing [54]. For the majority of identified lncRNAs, the function remains unclear. Nuclear lncRNAs are involved in regulation of

neighbouring loci through transcriptional regulation or by inhibiting expression of a gene through sequestration of transcription factors [55]. Conversely, other lncRNAs were shown to enhance gene transcription. lncRNAs were recently investigated as regulators of protein function [56]. They are more tissue-specific than protein coding genes [53] and compared with miRNAs, many more transcripts have been identified [57]. They have emerged as mediators of protein translation, mostly via inhibition of other RNA species [58]. Data is available, suggesting key regulatory roles of lncRNAs in cardiac and vascular tissue with respect to ischemic heart disease and MI [58]. In this respect, lncRNAs were shown to regulate hypoxia-inducible factor 1 (HIF1) [59] – an important regulator of ischemia response [60]. Several lncRNAs are also detected in the circulation. This either indicates the presence of protective mechanisms against RNase-mediated degradation similar to those of miRNAs [52] or an abundant source with constant release. The plasma level of Long Intergenic ncRNA Predicting CArdiac Remodeling (LIPCAR) was found to predict adverse cardiac remodeling and death after MI [28]. Many of the reported findings of lncRNAs as biomarkers for CVD are confined to small-size cohorts and require independent validation.

3.5.4 circRNAs

circRNAs are characterised by their circular shape, created in a process called 'back-splicing' from precursor mRNA, which leads to formation of a covalent binding of the 5' and the 3' end of the linear transcript [19]. They can either emerge from exons or introns of primary gene transcripts (pre-mRNA) [29,61] (**Figure 2**). circRNAs are endogenous to mammalian cells and expressed in a tissue- and developmental-specific context [29,62]. circRNAs are resistant to degradation by the exonuclease RNase R – a type of RNase that cleaves linear RNA (**Figure 3**). RNase R treatment is therefore used to enrich circRNAs over their linear counterparts [63,64]. In combination with the use of divergent primers in

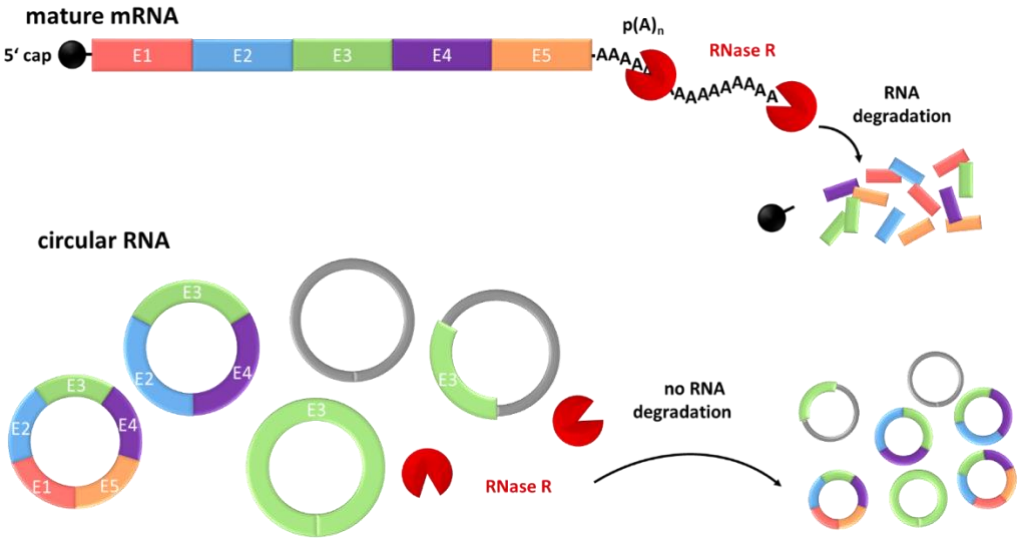

***Figure 3*. circRNAs are resistant to RNase R degradation.** mRNA contains a poly-A tail which is targeted by RNase R to cause degradation. circRNAs on the other hand do not contain poly-A tails and are therefore protected from this particular way of degradation, which is used to prove the circularity of a targeted RNA by degradation of all linear transcripts. circRNA = circular RNA; lncRNA = long non-coding RNA; RNA = ribonucleic acid. *Amended from Schulte et al, Trends Mol Med 2020*

polymerase chain reaction amplification, this approach ensures specificity for the detection of circular transcripts. Functionally, circRNAs may act as miRNA sponges – thereby decreasing the inhibitory effect of miRNAs on protein synthesis [65]. There are few circRNAs with many miRNA binding sites. More recently, circRNAs were reported to be translated into proteins [66]. At the same time, their expression is regulated by proteins such as RNA-binding proteins. circRNAs appear to influence gene expression by competing with splicing of their linear counterparts [31,64,67]. circRNAs show a certain degree of conservation across species [31,68]. They have recently been characterized in the heart [30], but at the same time are highly enriched in platelets relative to nucleated tissues.

Sequencing data revealed the presence of more than 15,000 circRNAs in the human heart, some in high abundance [30]. While intron-derived circRNAs are primarily found in the nucleus [65], the majority of circRNAs, in particular those with exonic origin, are located in the cytoplasm [69]. This may increase the likelihood of their early release into the circulation upon myocardial injury. Some studies have also described a mechanistic role for cardiac circRNAs in MI-induced apoptosis [70,71]. Other reports implicate circulating circRNAs as biomarkers for CVD in less acute settings [72] [73]. Interestingly, the authors did not use plasma or serum samples but instead used RNA isolated from whole blood, increasing the likelihood of the detected transcripts being blood cell-derived. Similar to lncRNA LIPCAR, the findings may reflect changes in inflammatory or other hematopoietic cells either as a potential consequence of a systemic response after MI [72] or effects of medication. Other studies evaluating circRNAs as biomarkers were either small in size [74], or performed normalization using a transcript of a commonly used intracellular reference gene [75]. The latter results could reflect plasma levels of residual blood cells such as platelets or leukocytes. Overall, circRNAs are difficult to detect in cell free body fluids, which currently hampers their evaluation as biomarkers. On the other hand, circRNA detection assays are in their infancy and improvements may lead to better strategies in their evaluation as circulating biomarkers.

3.5.5 Confounding of ncRNA quantification by Heparin

miRNAs have been investigated as biomarkers in the setting of acute MI over the last decade. Several publications reported that miRNAs might challenge cTn in their potential as early biomarkers for MI [26,27,76]. Heparin, an anticoagulant commonly administered in the clinical setting of MI, is a major confounding factor for measurements of ncRNAs by real-time polymerase chain reaction (qPCR). Especially, the widely for normalisation purposes used spike-in Cel-miR-39 is strongly affected by the presence of heparin [45,77]. No publication has taken into account that RNA quantification can be affected by the presence of heparin, which is routinely administered in AMI patients (**Table 2**). Few studies on the release of ncRNAs after MI used heparinase treatment to overcome this confounding effect by heparin, a prerequisite for comparative analysis of ncRNA and protein biomarkers. While circulating levels of muscle- and cardiac-enriched miRNAs have been shown to correlate to cTn after

MI, the release of ncRNAs and novel protein biomarkers such as cMyBP-c have not been compared in the clinically most relevant setting of MI patients presenting early with low cTn values (**Table 2**).

4 AIMS AND PROJECT DESIGN

ncRNAs have been proposed as promising novel biomarkers in the detection of acute MI. The overarching aim of this thesis is to assess novel protein biomarkers and different ncRNAs with respect to their clinical applicability as biomarkers for acute T1MI and for MI subtypes. In the latter setting, the objective of this study was to compare the discriminative ability of biomarker trajectories for MI subtypes including AI.

4.1 HYPOTHESIS

1. Novel protein and ncRNA biomarker candidates can aid in improving sensitivity and specificity in the detection of MI.

2. The confounding effect of heparin in clinical samples can be overcome by heparinase-treatment.

3. A systemic biomarker assessment including promising protein and ncRNA biomarker candidates can help to improve early differentiation of specific MI subtypes.

4.2 AIMS

4.2.1 Aim 1: Overcoming the heparin-induced confounding of qPCR detection methods

Heparin, an anticoagulant commonly administered in the clinical setting of MI, is a major confounding factor for measurements of ncRNAs by real-time polymerase chain reaction (qPCR). Few studies on the release of ncRNAs after MI used heparinase treatment to overcome this confounding effect by heparin, a prerequisite for comparative analysis of ncRNA and protein biomarkers. So far, the question has not been answered whether the confounding effect of heparin in clinical samples can successfully be addressed to enable qPCR-based methods to be applied in detecting circulating biomolecules. Aim 1 is to use heparinase-treatment in clinical samples in order to enable potential clinical use of qPCR-based detection of circulating biomolecules in the detection of acute MI.

4.2.2 Aim 2: Assessment of ncRNAs as circulating biomarkers in acute T1MI

Despite advances in biomarker-based detection of acute MI, there is still a need for biomarkers that facilitate early rule-out/rule-in of clinically relevant MI. Recently, a new cardiac-specific protein, cMyBP-C, was proposed as a promising novel biomarker, which is released earlier upon myocardial ischemia than cTn [14] and allows for an earlier detection and better rule-in/rule-out of MI, showing even higher sensitivity than Tn [111]. On the other hand, recent results have shown that a further increase in sensitivity does not necessarily improve the clinical diagnosis of AMI[5]. While circulating levels of muscle- and cardiac-enriched miRNAs have been shown to correlate to cTn after MI, the release of ncRNAs and novel protein biomarkers such as cMyBP-C have not been compared in the

clinically most relevant setting of MI patients presenting early with low cTn values. Aim 2 is to establish the release kinetics of three different ncRNA species (miRNAs, lncRNAs, circRNAs) in serial samples from patients undergoing transcoronary ablation of septal hypertrophy (TASH) as well as in patients with acute MI presenting with a wide range of hs-cTn levels in the Biomarkers in Acute Cardiac Care study (BACC study, n>2500). The performance of ncRNAs will be compared with hs-cTn and cMyBP-C as established and novel protein biomarkers of cardiac injury, respectively.

4.2.3 Aim 3: Assessment of blood-based proteins and ncRNAs as potential circulating biomarkers in T2MI

UDMI4 emphasizes the heterogeneity of different types of MI[6], which currently are not conveniently distinguishable with cTn. Aim 3 is to compare the discriminative ability of biomarker trajectories for MI subtypes including AI. Measurements of protein biomarkers alongside miRNA-based biomarker candidates will be performed at three serial time points. Then linear mixed effects models will be applied to compare patient subgroups and biomarker kinetics. Machine learning methods will be used to combine independent biomarkers and identify the best serial biomarker combination in discriminating T1MI, T2MI and AI.

5 METHODS

5.1 T1MI ASSESSMENT

5.1.1 RNA extraction

Total RNA was extracted using the miRNeasy Mini kit (Qiagen, Hilden, Germany) according to the manufacturer's recommendations, with some modifications. In brief, 100µl of serum or plasma were combined with 694.75µl of Qiazol lysis reagent, 4µl of diluted synthetic *Caenorhabditis elegans* miR-39 (cel-miR-39-3p) spike-in and 1.25µl carrier RNA from bacteriophage MS2 (Roche). Following brief incubation at room temperature, 140 µl of chloroform was added and the solution was mixed vigorously. Samples were then centrifuged at 13,500 x *g* for 15 minutes at 4°C. 280 µl of the upper (aqueous) phase were transferred to a new tube and mixed with 1.5 volumes (420 µl) of 100% ethanol and applied to columns and washed according to the manufacturer's protocol. Total RNA was eluted in 35 µl of nuclease-free H_2O by centrifugation at 8500 x *g* for 1 minute at 4°C.

In order to assess the reliability and efficiency of the RNA extractions Cel-miR-39 spike-in raw Cq values were plotted for TASH and MI cohort (**Figure 4**). The standard deviation was below 0.5 and the coefficient of variation below 2% in both groups, confirming good RNA processing and consistency of the RNA isolation.

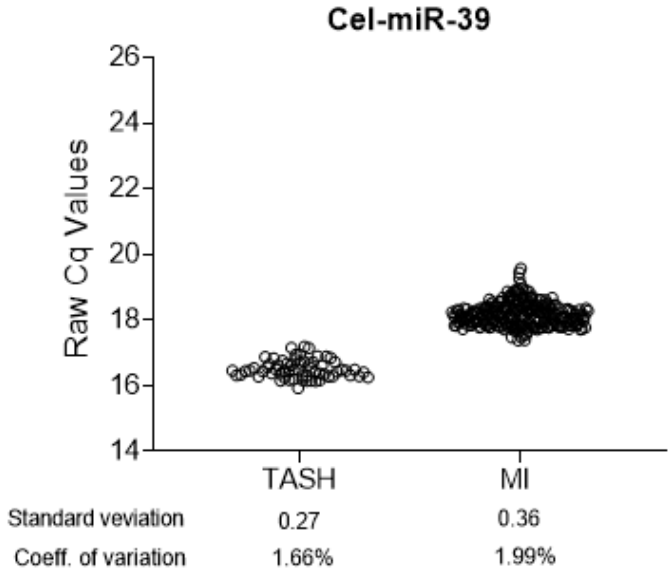

Figure 4. Raw Cq value distribution of the spike-in normalisation control in the TASH and MI cohort. *The distribution of Cel-miR-39 raw Cq values after spike-in in the TASH and MI cohort returned standard deviations < 0.5 and coefficients of variation of <2% indicating good RNA extraction performance and its suitability as normalisation control for relative quantification analysis. Reproduced from Schulte et al. Circ Res 2019*

5.1.2 Heparinase treatment

ncRNA analyses. Prior to reverse transcription, the extracted RNA was treated with heparinase 1 from Flavobacterium (Sigma) according to the following protocol: 5µl of each sample were combined with 1.25µl heparinase, 0.25µl of RNase inhibitor (Ribo Lock 40U/µl, Thermofisher) and 3.5µl of heparinase buffer (pH 7.5) and thoroughly mixed, then incubated at 25°C for 3 hrs. The samples were then immediately used for reverse transcription. For comparison, a buffer-only group was treated with heparinase buffer devoid of heparinase, which was incubated under the same conditions as the heparinase-treated samples. The untreated group received neither heparinase nor buffer, nor was it left for incubation, but instead was used for further reverse transcription together with the treated samples.
Proximity Extension Assay (PEA). cTnI was part of the organ damage panel offered by Olink (Uppsala, Sweden). Human plasma samples were treated by adding 0.1U (concentration: 0.2U/µl) of heparinase 1 from Flavobacterium (Sigma) per 1µl of plasma. 0.5µl of the heparinase solution was added per 1µl of plasma. The mixture was then incubated for 1h at 30°C as previously described [79].

5.1.3 Reverse transcription

To verify the use of highly sensitive miRNA detection methods, we compared two of the most widely used kits from 1) Qiagen and 2) Thermo Fisher. **Figure 5** shows a higher sensitivity to detect miR-1 in clinical samples of the TASH cohort for the Qiagen kit, which is based on a system using locked nucleic acids and which does not require pre-amplification of the cDNA product.

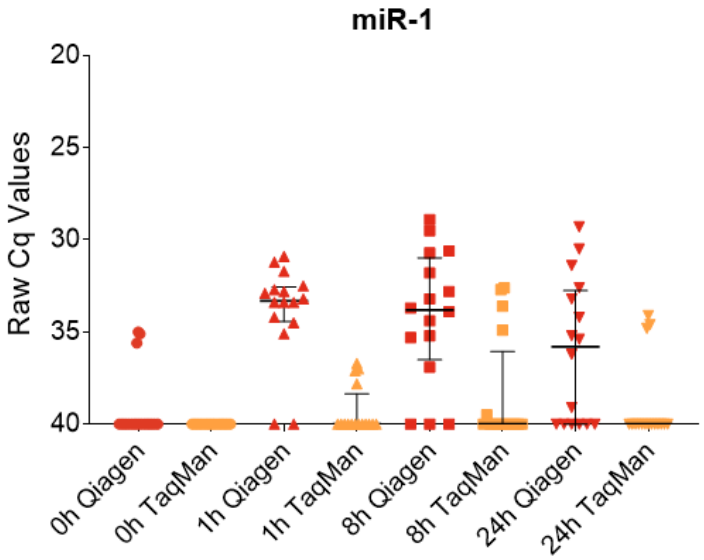

***Figure 5. Comparison of two of the most widely-used miRNA quantification systems**. The Qiagen ™ System shows higher sensitivity for muscle miRNA-1.*

For lncRNAs and circRNAs the highly sensitive Thermo Fisher platform was used. Thus, for reverse transcription two different platforms 1) for miRNAs (miRCURY LNA RT kit (Qiagen)) and 2) for lncRNAs and circRNAs (SuperScript VILO cDNA Synthesis Kit (Invitrogen)) were used.

Analysis of miRNAs. 3 µl of RNA from plasma/serum RNA was used as input in each reverse transcription (RT) reaction. RT reactions were set up according to the manufacturer's recommendations. Briefly, miRNAs were reverse-transcribed using the miRCURY LNA RT kit (Exiqon), combining 3µl RNA with 5x reaction buffer, 1µl enzyme mix, 0.5µl UniSp6 synthetic spike-in and 3.5µl nuclease-free water. The RT-PCR reaction was set as follows: reverse transcription, 42°C for 60 minutes; inactivation, 95°C for 5 minutes using a Veriti Thermal Cycler (Applied Biosystems).

Analysis of lncRNAs and circRNAs. RT was performed using the SuperScript VILO cDNA Synthesis Kit (Invitrogen). 2 µl of VILO RT Master Mix were combined with 8 µl of sample. Thermal cycler stages were set as follows: incubation at 25°C for 10 minutes and synthesis at 42°C for 120 minutes, followed by termination of the reaction at 85°C for 5 minutes. cDNA products were stored at -20ºC.

5.1.4 Real-time PCR Assays

Custom-designed primers for detection of lncRNAs and circRNAs were produced by IDT Oligos (Integrated DNA Technologies, Inc., 8180 N. McCormick Blvd., Skokie, Illinois 60076, USA). A list of primers used for qPCR detection and their sequence is provided in **Supplemental Table 1**. miRCURY SYBR Green qPCR in combination with miRCURY LNA miRNA PCR Assays (for miRNAs, both Qiagen) and SYBR Select Master Mix (Applied Biosystems) in combination with custom-made primers were used to assess relative expression levels of miRNAs and lncRNAs/circRNAs, respectively. For miRCURY SYBR Green, cDNA was diluted 1:30 according to the manufacturer's recommendations, then 3µl of the diluted cDNA were combined with 5µl miRCURY SYBR Green Mastermix, 0.05µl ROX reference dye, 1µl PCR Primer Mix and 0.95µl of RNase-free water to a 10µl reaction volume. For SYBR Select Master Mix, cDNA was diluted 1:20, then 2µl of diluted cDNA were combined with 2.5µl of SYBR Select Master Mix and 0.1µl of 10µM forward primer and 0.1µl of 10µM reverse primer. Reactions were loaded using a Bravo Automated Liquid Handling Platform (Agilent). qPCR was performed on a ViiA7 Real-Time PCR System (Applied Biosystems) at 95ºC for 2 minutes followed 40 cycles of 95ºC for 10 seconds and 56ºC for 1 minute for miRCURY SYBR Green (miRNA) and at 50 ºC for 2 minutes, then 95ºC for 2 minutes, followed by 40 cycles of 95ºC for 15 seconds and 60ºC for 1 minute for SYBR Select Master Mix (lncRNAs and circRNAs), respectively.

5.1.5 RNA quantification

In the analyses of raw Cq data, any measurements beyond 35 cycles were considered undetectable. In order identify unreliable measurements of miRNAs we set a Cq threshold of 35. The threshold was set

so that we exclude Cq values which follow uniform distribution and can thus be considered random noise. To make these calculations we used the one-way Kolmogorov-Smirnov test for all cohorts of this paper. For all four muscle/cardiac-enriched miRNAs of interest the p-value of the test for the Cq values greater than 35 was smaller than 0.05 and bigger than 0.05 for the Cq values smaller than 35.
The relative quantitation for RNAs was performed as follows:
Analysis of miRNAs. In TASH samples as well as the MI cohort the delta-delta Cq method was used for relative quantification, using cel-miR-39-3p as a normalisation control. Quantification results were calibrated against the median of three identical replicates consisting of equal volumes from all TASH or all MI samples, respectively. Relative quantification was performed with Microsoft Excel, version 15.32 for MacOS. In the myocardial tissue *in vitro* spike-in experiment normalisation was also performed using *Cel-miR-39* spike in. Calibration was performed using the median value of all samples per individual RNA assay to remove assay-related biases.
Analysis of circRNAs and lncRNAs. Calibration of circRNAs and lncRNAs in the TASH samples was performed against the median of all samples for each assay. In the myocardial tissue spike-in experiment the same method was used. The relative quantity was calculated as described above for miRNAs.

5.1.6 Myocardial tissue spike-in

5.1.6.1 Myocardial Tissue

For cardiac tissue spike-in analyses and primer testing, samples from human myocardial tissue were obtained from an explanted failing heart under Ethical Approval from the Royal Brompton and Harefield Trust BRU Biobank and from nonfailing hearts under Ethical Approval approval from the local Research Ethics Committee and institutional Research and Development office for St George's Hospital and King's College London. The study was performed in accordance with the Declaration of Helsinki. All patients gave written informed consent. All samples were frozen at −80 °C.

5.1.6.2 Myocardial Tissue Spike-In Experiment

In order to assess the detectability of RNAs with cardiac origin, different amounts of human cardiac tissue were spiked into human plasma before extracting RNA. Tissue was lysed in Qiazol at a concentration of 1µg/µl. Lysis was performed in a FastPrep-24 Homogeniser (MP Biomedicals) at 6000 rpm for two rounds of 20 seconds using Lysing Matrix D beads (MP Biomedicals). Then the desired concentration was added to the RNA extraction process as described above using 100µl of plasma from healthy volunteers (**Figure 6**). For protein analyses, human myocardium was weighed, and the tissue was crushed in a percussion mortar for 10 seconds as previously described[80]. Buffer solution [50 mL Tris, pH 7.5, containing a protease inhibitor cocktail (cOmplete EDTA-free, Roche)] was added to the pulverized tissue (1 mL of buffer per 100 mg of tissue). The subsequent solution was subject to

ultrasonication on ice (6 × 10-second bursts on ice, with 10-second intervals on ice). Following ultrasonication, the solution was centrifuged at 21,130g for 30 minutes at 4 °C. The supernatant was frozen in liquid nitrogen and then stored at −80 °C. Dilutions of this solution were then spiked into 400µL of human serum.

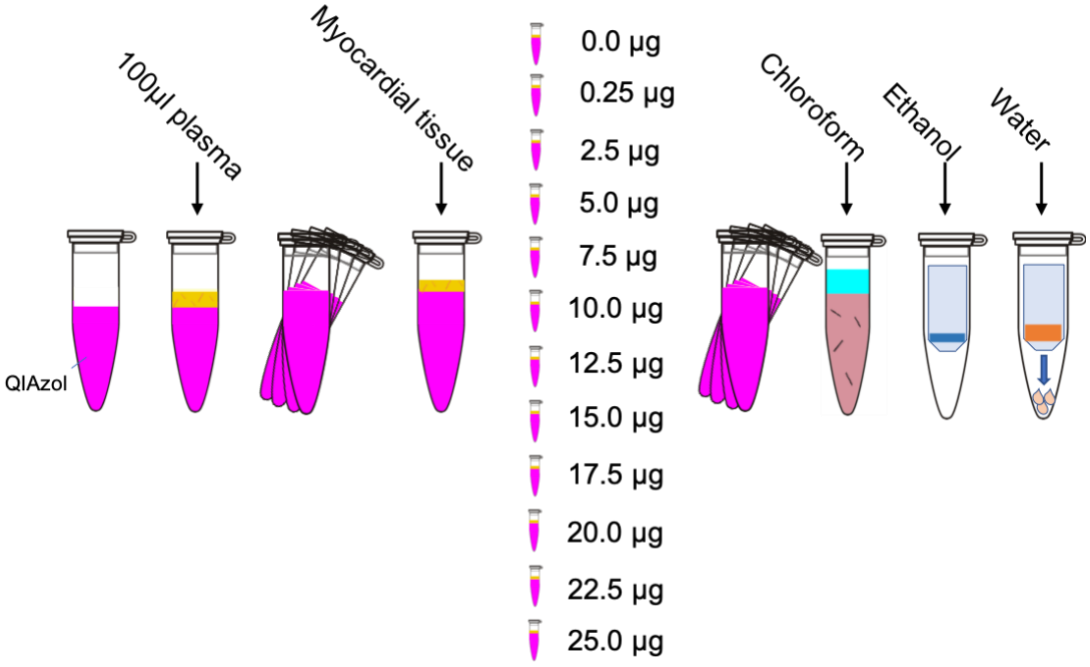

Figure 6. Workflow of myocardial tissue spike-in. *100µl of plasma from healthy control individuals was first spiked into Qiazol lysis buffer (Qiagen, Hilden, Germany) and shaken vigorously before human cardiac tissue (also already lysed in Qiazol) was added at different concentrations and again shaken vigorously. RNA extraction was then performed according to the manufacturer's recommendations and as described in the methods section. Reproduced from Schulte et al. Circ Res 2019*

5.1.7 Selection of ncRNAs

We selected the most promising ncRNA species to analyse, including those for which at least some preliminary data on their assessment in human circulation and related to cardiovascular disease was reported. Within each ncRNA class, starting from screening results, we stepwise narrowed the candidate ncRNAs down based on detectability in the heart, in human plasma and taking into account their association with cardiac genes (**Figure 7**). In the myocardial spike-in experiment, those ncRNAs were selected that returned the highest Pearson correlation with increasing spike-in volume. lncH19 was furthermore included to account for its nucleus origin as opposed to mitochondrial origin of lncLIPCAR and lncuc004cov.4. All RNAs/lncRNAs included in the spike-in experiment are presented in **Supplemental Figures 1 and 2**. For clinical assessment in TASH, those circRNAs and lncRNAs with Cq<25 cycles in cardiac tissue were selected for further analyses, that were detectable in >50% of 12 pooled TASH samples or detectable in all samples of one time point (n=3 per time point) (see below '**5.1.9 Tash cohort**'). In all TASH samples, only circSMARCA and circPCMTDL were detectable in >50% per time point, and therefore possible to evaluate in terms of kinetics (**Figure 10**).

5.1.7.1 miRNAs

Two cardiac-enriched miRNAs (miR-208b-3p, miR-499a-5p), two muscle-enriched miRNAs (miR-1, miR-133a-3p) and 7 additional miRNAs were included in the analyses for their good detectability in human plasma as non-cardiac/non-muscle counterparts.

5.1.7.2 circRNAs

To broaden our search for cardiac-enriched circRNAs that are detectable in plasma, we performed a microarray-based screening of circRNAs in pooled TASH plasma samples (n=4 per time point, n=16 samples in total) screening for 13,617 circRNAs (Arraystar Human Circular RNA Array, Arraystar INC, 9430 Key West Avenue 128, Rockville, MD 20850). To complement this screening, a literature search was performed. circRNAs were selected from four deep sequencing datasets reporting >15,000 circRNAs, of which 158 circRNAs were RNase-R treated and validated by qPCR. These 158 circRNAs plus their linear transcripts were first tested in 12 human cardiac tissue samples. For circRNAs with more than one transcript from the same gene, the one with the best detection based on Cq values was chosen. Only circRNAs with Cq values of < 25 cycles that were derived from cardiac and/or muscle-associated genes (n=12) were included.

In detail, total RNA from each TASH sample was quantified using spectrophotometry (NanoDrop ND-1000). The integrity of RNA was assessed by electrophoresis on a denaturing agarose gel. The sample preparation and microarray hybridization were performed based on the Arraystar's (Arraystar, Inc., Rockville, MD, USA) standard protocols as previously described (Huang et al., 2017). Briefly, total RNAs were digested with Rnase R (Epicentre, Inc.) to remove linear RNAs and enrich circRNAs. Then, the enriched circRNAs were amplified and transcribed into fluorescent cRNA utilizing a random priming method (Arraystar Super RNA Labeling Kit; Arraystar). The labeled cRNAs were hybridized onto the Arraystar Human circRNA Array v2 (8x15K, Arraystar). After having washed the slides, the arrays were scanned by the Agilent Scanner G2505C. Agilent Feature Extraction software (version 11.0.1.1) was used to analyze acquired array images. Quantile normalization and subsequent data processing were performed using the R software limma package. Differentially expressed circRNAs with statistical significance between two groups were identified through Volcano Plot filtering. Differentially expressed circRNAs between two samples were identified through Fold Change filtering. Hierarchical Clustering was performed to show the distinguishable circRNAs expression pattern among samples. Detectability was defined as present or marginal in at least three or more of 16 TASH plasma samples. 6812 circRNAs were detectable in plasma of TASH patients. Of these, 4106 circRNAs showed an increase in expression levels between time point 0 hours and 1 hour, whilst 4225 and 4255 circRNAs showed an increase between 0 hours and 8 hours and between 0 hours and 24 hours, respectively. Anova test was used to determine statistically significant changes in circRNAs in the TASH cohort. Correction

for multiple testing was conducted with Benjamini-Hochberg method. None of the circRNAs was significantly regulated with an FDR threshold of 10% **(Figure 7).**

5.1.7.3 lncRNAs

lncRNAs were selected based on microarray screening of 33,045 lncRNAs in human plasma[28]. Of these, 768 lncRNAs showed differential plasma levels in patients developing heart failure after MI. 21 lncRNAs with high signal intensity were validated by qPCR. As for circRNAs, only lncRNAs with Cq values < 25 (n=11) were selected for further analyses. A graphical depiction of the selection process including references is shown in **Figure 7**.

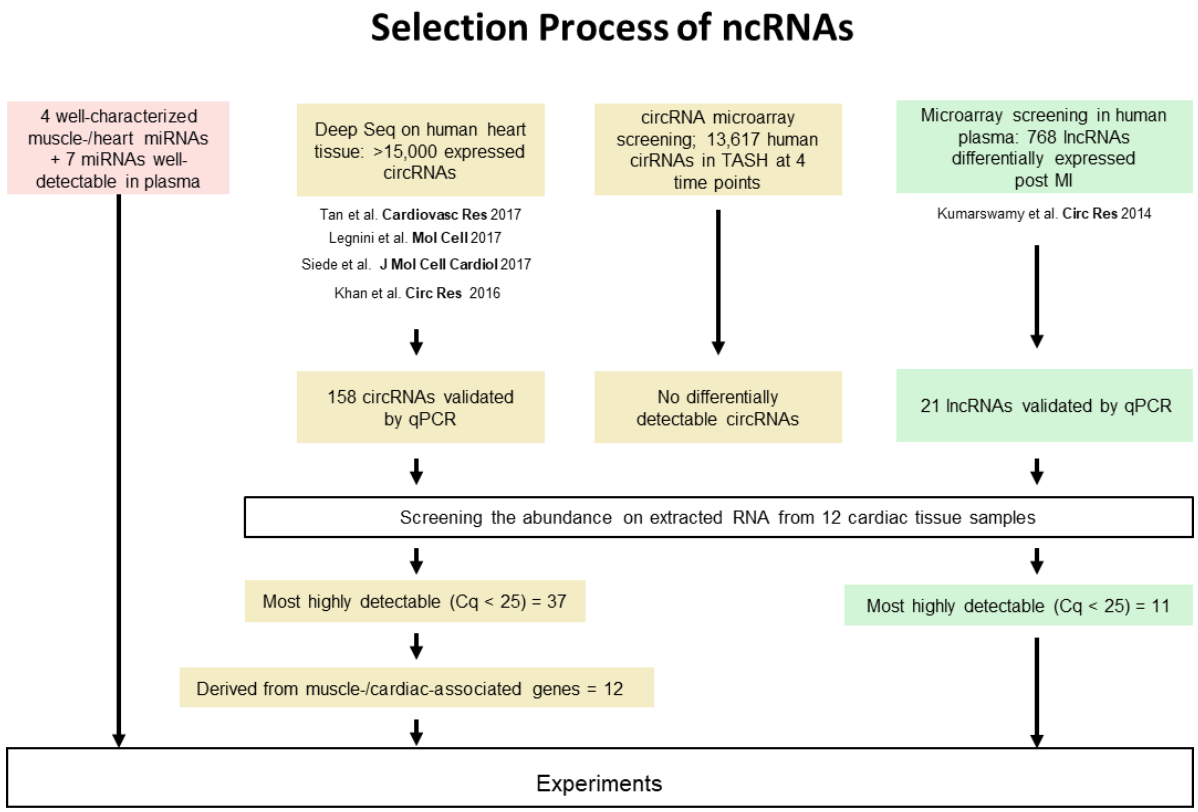

Figure 7. Selection process of ncRNAs used in the experiments. *miRNAs have previously been studied in the context of myocardial injury, and we selected muscle-/cardiac miRNAs plus other miRNAs that are well detectable in human plasma. circRNAs are the least well-studied class of ncRNAs. We interrogated the literature on deep RNA sequencing data of human cardiac tissue and selected the circRNAs that were reported to be detectable via qPCR. circRNA primers were further selected for the muscle-/cardiac specificity of their related gene. Additionally, we performed a circRNA array screening of 13,617 circRNAs detectable in plasma in TASH samples (n=4 per time point). None of the screened circRNAs were differentially detectable after TASH. lncRNAs were chosen from published microarray data on human cardiac tissue and selected based on qPCR validation. Both, custom-made circRNA and lncRNA primers were tested on extracted RNA from human cardiac tissue; only the most abundant RNAs in myocardial tissue were chosen for further analyses in plasma and serum. Reproduced from Schulte et al. Circ Res 2019*

5.1.7.4 Selection of appropriate miRNA normalisation method

In order to identify potential endogenous candidates as normalisation controls, we analysed expression levels of some of the most abundant plasma miRNAs in the TASH cohort. None of them returned

expression profiles, which can be considered stable enough for use as normalisation controls, especially compared with Cel-miR-39 (**Figure 8**). Next, we performed normalization using the average of all ncRNAs instead of Cel-miR-39 as normalizer. For the four miRNAs of our interest we conducted correlation analysis between the RQ values obtained from each one of the normalization strategies. A strong correlation (R2>0.5) indicated that the selection of the normalization method had no major influence on the overall RQ results.

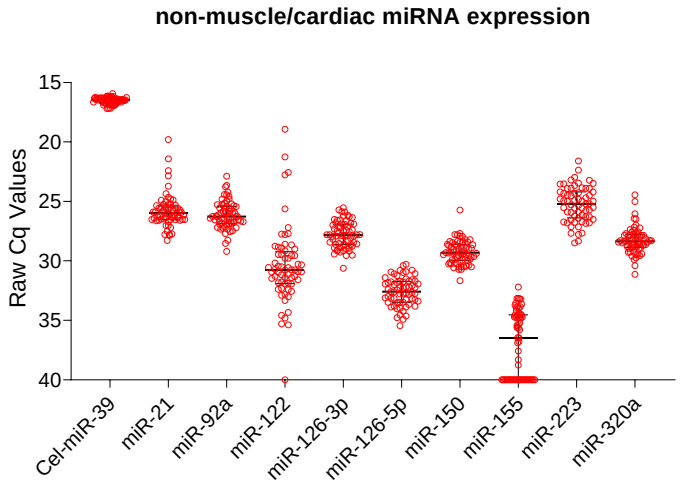

Figure 8. Raw Cq value distribution of non-cardiac/-muscle miRNAs in TASH. *Compared to endogenous miRNAs, the Cel-miR-39 spike-in control showed the most stable expression profile across all TASH samples. Reproduced from Schulte et al. Circ Res 2019*

5.1.8 TASH cohort

The TASH cohort patient characteristics and procedure as well as the blood sampling methods have previously been described [81]. Samples from 20 patients undergoing this procedure were chosen based on adequate sample volumes and complete data sets from four different time points (baseline, 1 h, 8 hrs and 24 hrs after onset of myocardial injury). For ncRNA analyses samples from a subset of 16 patients were available. hs-cTnT and cMyBP-C data were available from 15 and 20 patients, respectively. For clinical assessment in TASH, those circRNAs and lncRNAs with Cq<25 cycles in cardiac tissue were selected for further analyses, that were detectable in >50% of 12 pooled TASH samples or detectable in all samples of one time point (n=3 per time point) (**Figure 9).** Results from the evaluation of the selected circRNAs and lncRNAs are depicted in **Figure 10 and 11**, respectively. Only, circSMARCA and circPCMTDL were detectable in >50% per time point, and therefore evaluated in terms of kinetics.

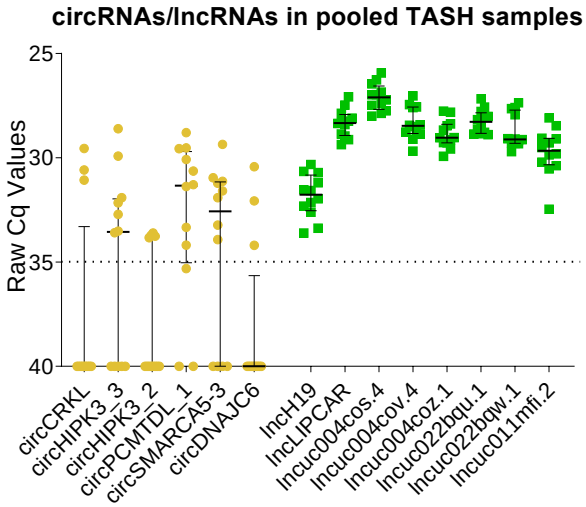

Figure 9. Selection of circRNAs and lncRNAs in pooled TASH samples. *The figure displays those circRNAs and lncRNAs that were detectable in >50% of 12 pooled TASH samples (4 per time point) or detectable in all samples of one time point (n=3 per time point). The ncRNAs were selected based on detectability (Cq<25 cycles) in cardiac tissue. Reproduced from Schulte et al. Circ Res 2019*

5.1.9 The Biomarkers in Acute Cardiac Care (BACC) study

The BACC study has been described before [82]. Briefly, the study prospectively included 2,335 patients presenting to the emergency department and chest pain unit of the University Hospital Hamburg. The inclusion criteria were suspected acute MI, age above 18 and the ability to provide written informed consent. All patients were triaged according to local standard of care: A standard ECG was collected at admission. cTn was routinely measured using the local standard of care cTnT assay (Elecsys® troponin T high-sensitive, Roche Diagnostics, Basel, Switzerland, LLoD 5.0ng/L, values are reported up until the limit of blank 3.0ng/L) at admission and after 3 hrs. A study-specific additional blood draw was ascertained 1 hour after admission and for cTnI (Troponin I hs STAT Abbott Arcitect, LLoD 1.9ng/L) at all time points. The 99th percentile is set to 14ng/L (hs-cTnT) and 27ng/L (hs-cTnI), respectively[83,84]. The self-reported onset of pain was obtained from a study-specific questionnaire or medical records and then categorised to time intervals as follows: 0-1 h, 1-3 hrs, 3-6 hrs, 6-12 hrs, 12-24 hrs, 24-72 hrs. The final diagnosis was adjudicated by two cardiologists independently, taking to account the cTnT results (Roche) and all available clinical and imaging results, ECG and routine laboratory testing. In cases of disagreement, a third cardiologist reviewed the case. A subset of patients was selected for this study, excluding T2MI patients and balancing patients with STEMI (n=20) and T1MI (n=18). The BACC study was registered at www.clinicaltrials.gov (NCT02355457), complied with the Declaration of Helsinki and was approved by the local Ethics Committee.

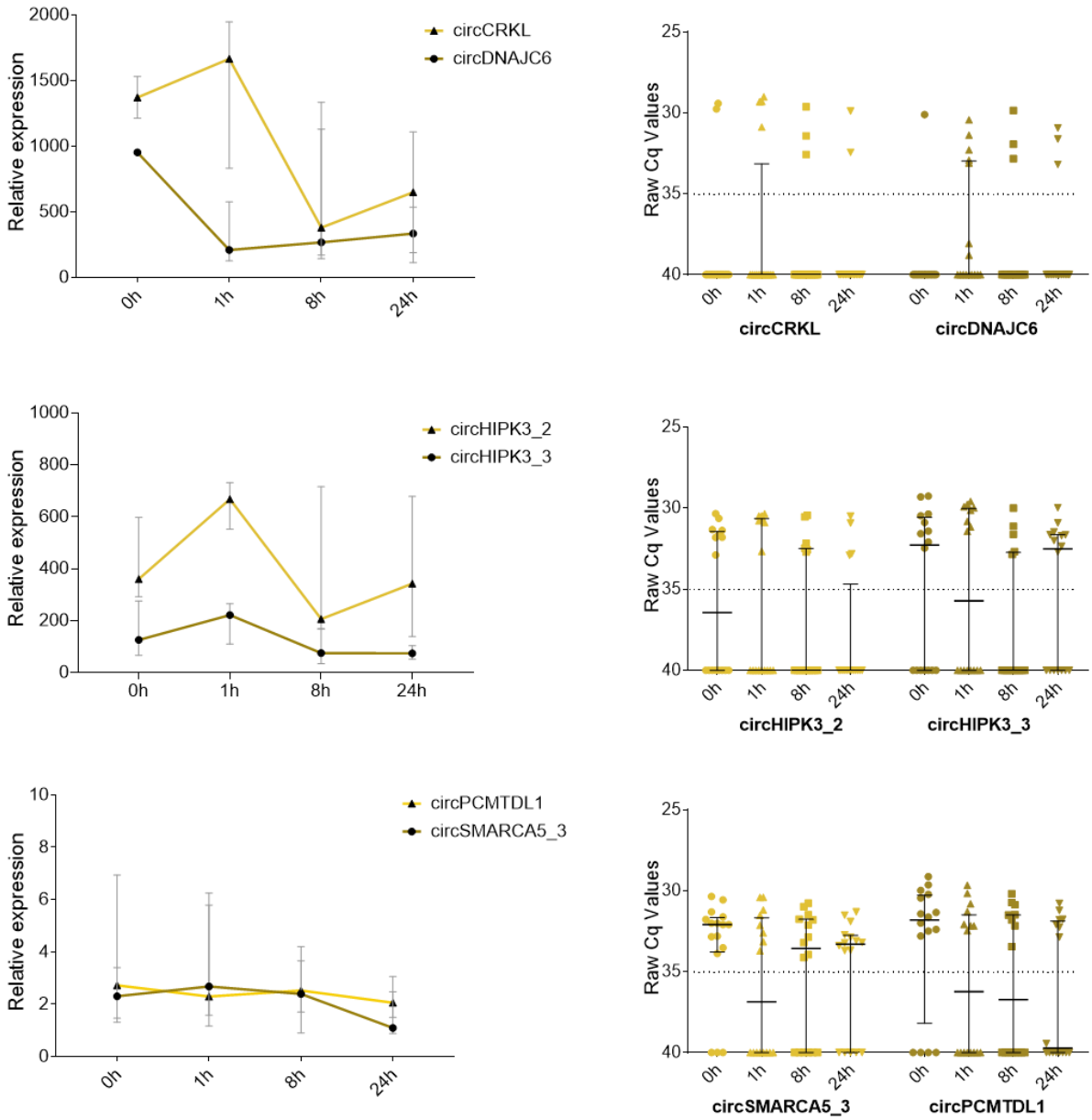

Figure 10. Selected circRNAs tested in the TASH cohort. *Results from the evaluation of the selected circRNAs. Only, circSMARCA and circPCMTDL were detectable in >50% per time point, and therefore evaluated in terms of kinetics but showed no dysregulation after myocardial injury. Reproduced from Schulte et al. Circ Res 2019*

5.1.10 Measurements of cTnI by proximity extension assays (PEA)

In order to quantify cardiac cTnI in TASH plasma samples using a qPCR-based method, proximity extension assays (PEA) were performed as previously published [85,86]. cTnI was part of the 'organ damage panel' from Olink (Uppsala, Sweden).

5.1.11 Antibody-based measurements of cardiac proteins (cTnI, cTnT, cMyBP-C)

All antibody-based measurements of cTnI, cTnT and cMyBP-C were performed on assays proprietary to the manufacturer.

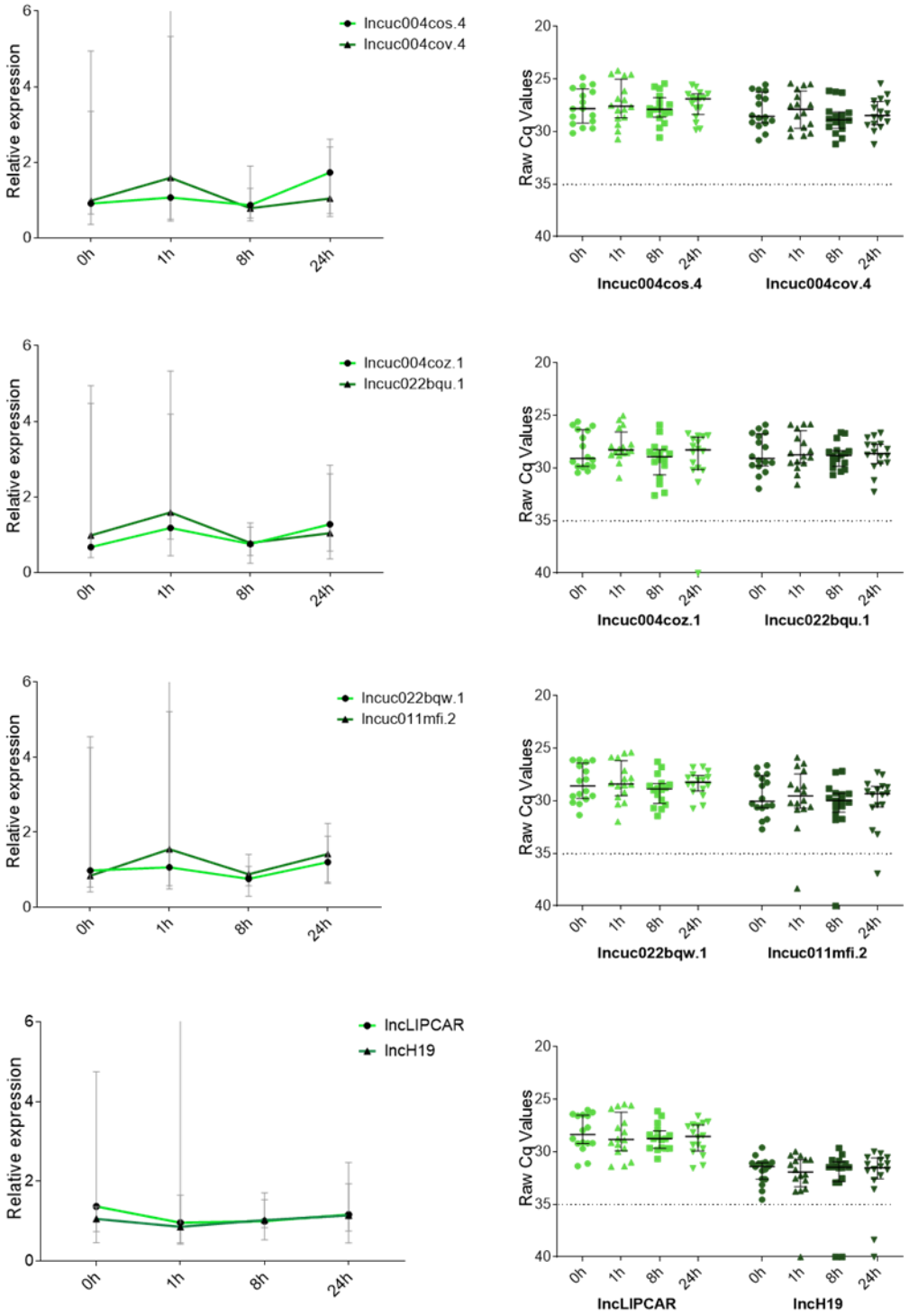

Figure 11. Selected lncRNAs tested in the TASH cohort. *Results from the evaluation of the selected circRNAs. All tested lncRNAs were well-detectable at all time points, but showed no dysregulation after onset of myocardial injury (0h). Reproduced from Schulte et al. Circ Res 2019*

5.1.12 Myocardial Tissue Spike-In

The concentrations of cTnI and cTnT were measured using contemporary high-sensitivity assays [Abbott Architect, limit of detection (LoD) 1.9 ng/L; and Roche Elecsys, LoD 5 ng/L, respectively] as previously described [80]. cMyBP-C was measured by EMD Millipore on the Erenna® platform using proprietary reagents as recently described (LoD of 0.4 ng/L)[80].

5.1.13 TASH samples

cMyBP-C was quantified using an electrochemiluminescence (ECL) SECTOR imager 2400 instrument (MesoScale Discovery), by utilizing capture and detection monoclonal antibodies that recognized discrete epitopes on the C0C2 peptide as previously described [16]. In brief, the capture antibody (Clone 3H8/30 µL/1 µg/mL) was coated onto 96-well SECTOR® plates (MesoScale Discovery) in 10 mM Tris pH 9.6 overnight at 4°C, washed three times with PBS/0.05 % Tween, and blocked with 1 %BSA/PBS for 1 hour at room temperature on a platform shaker. Serum samples (30 µL/well) were diluted 1 in 2 with Diluent 7 (MesoScale Discovery) and were added to the plate along with recombinant C0C2 standards also diluted with Diluent 7, before incubation for 1 h at room temperature. Afterwards, the plates were washed three times with PBS/0.05 % Tween to reduce non-specific binding. Detection antibody (Clone 1A4/30 µL/PBS pH 7.4), which had been conjugated to ruthenium (MesoScale Discovery) according to the manufacturer's instructions, was then added to the wells and incubated for 2 h at room temperature with shaking at 300 rpm. Finally, the plates were washed three times with PBS/0.05 % Tween, and 150 µL 1× read buffer was added to the wells prior to ECL analysis on the SECTOR imager 2400. The standard curve generated was then used to quantify the cMyBP-C concentration present in serum samples and expressed as ng/L. hs-cTnT measurements were performed as previously described [81]. In brief, hs-cTnT was measured in serum with the hs-electrochemiluminescence immunoassay (hs-cTnT assay, Elecsys Analyzer 2010, Roche Diagnostics). The lower detection limit for the hs-cTnT assay is 3.0 ng/L, with the 99th percentile at a concentration of 14.0 ng/L.

5.1.14 MI cohort (BACC)

cMyBP-C was measured by Merck Millipore using the Erenna platform with a lower limit of detection (LLoD)of 0.4 ng/L and a lower limit of quantification (LLoQ of 1.2 ng/L. The 99th percentile cut-off point was previously determined at 87 ng/L[87]. cTn was routinely measured using the local standard of care cTnT assay (Elecsys® troponin T high-sensitive, Roche Diagnostics, Basel, Switzerland, lower limit of detection 5.0ng/L, values are reported up until the limit of blank 3.0ng/L) at admission and after 3 hrs. A study specific additional blood draw was ascertained 1 hour after admission and for cTnI (Troponin I hs STAT Abbott Arcitect, lower limit of detection 1.9ng/L) at all time points. The 99th percentile is set to 14ng/L (hs-cTnT) and 27ng/L (hs-cTnI), respectively[83,84].

5.1.15 Statistical analyses

Tissue spike-in experiment

To enable comparisons of the relative expression values for ncRNAs and the absolute concentrations for protein biomarkers, relative quantities have been calculated for all molecules by dividing their values with the median quantity for each molecule. Then linear regression curves were calculated for all

miRNAs, circRNAs, lncRNAs and cardiac proteins study their release kinetics by comparing the regression curves slopes. All R^2 values were >0.9, therefore, the used linear model provides a good fit to the data. Next, the slopes of the regression curves of the three molecules with the highest scores were selected from each category: for miRNAs miR-133a, miR-208b and miR-499; for circRNAs: circALPK2, circMYBPC3, and circSLC8A1; for lncRNAs: lncDANCR, lncH19, and lncRNACOX2; for proteins: hs-cTnT, hs-cTnI, and cMyBP-C. Mann-Whitney U-tests [88] were used to perform pairwise statistical comparisons between the slopes of proteins and ncRNAs.

TASH cohort

To study the release kinetics of proteins and ncRNAs at 1h after TASH, absolute protein measurements and relative RNA measurements were both transformed into relative values on the same scale by dividing each value by the overall maximum value of the single biomarker across all time points. The data for each molecule and each patient were curve-fitted using linear regression and slopes of the curves were calculated. Mann-Whitney U-tests were used to perform pairwise statistical comparisons between the slopes of the regression curves of protein and ncRNA molecules.

BACC study

Analyses to study release kinetics after acute MI were performed analogous to the TASH cohort for the first hour after hospital presentation. Correlation analyses of biomarkers in the acute MI cohort were performed with Graph Pad Prism 7.0d for MacOS. Nonparametric Spearman correlation was used since none of the biomarkers were normally distributed. P-values in the correlation analyses were two-tailed and approximate values were calculated.

ROC analyses

For training and testing regression models for predicting the time from onset of MI combining miRNAs and proteins we used a hybrid of a heuristic algorithm and Support Vector Regression models (details are provided in the Supplementary Material).

Predictive analytics with TASH and BACC cohorts

Quantitative values of both miRNAs and proteins from samples of TASH and BACC cohorts were arithmetically normalized to range in the interval [0,1]. Missing values were imputed using the K-Nearest Neighbours imputation method[89] with k=20 (default value).

The markers measured in TASH cohort, were combined considering all meaningful combinations and using the Support Vector Regression method [90] to construct regression models which can predict a score that corresponds to the time passed in hours from the onset of the injury. Non-linear Radial Basis

Functions and linear kernels [91] were explored as the more suitable kernel functions to be used for Support Vector Machines.

The Nondominated Sorting Genetic Algorithm (NSGA) optimization method [92] was used to select the optimal kernel function and to tune the Regularization parameter C of SVM and the gamma parameter of Radial Basis Functions. The parameters used for the NSGA algorithm were: Population Size: 50, Maximum Number of Generations: 200, Crossover probability: 90%, Mutation probability: 1%. Three different competitive optimization goals were set to guide the optimization function, two related with the prediction accuracy and one related with the complexity of the prediction model. These goals were formulated to the following fitness functions:

- Fitness function 1: 1/(1+Root Mean Square Error)
- Fitness function 2: Squared correlation coefficient
- Fitness function 3: Number of Samples of the Dataset/Number of Support Vectors of Trained Model

For the evaluation of the individual models we utilized the leave-one-out cross validation approach[93][14]. The libSVM implementation [94] was used for training and testing the SVR models and for the NSGA algorithm an open python implementation was used (https://github.com/haris989/NSGA-II).

TASH cohort was used as the training cohort and the fitness functions were measured using the leave one-out-approach. BACC cohort was used as a validation cohort. The most promising predictive models according to their performances in the TASH dataset were applied on the BACC dataset without retraining them for this dataset to measure the generalization performance of the trained model on an independent validation cohort. ROC curves analysis was conducted using the LABROC4 algorithm [95].

5.2 Additional Methods used in Differential Assessment of specific MI subtypes

5.2.1 Patient and sample selection

For the study, we assessed human plasma samples from a chest pain cohort comprising of patients presenting with suspected MI (BACC study, see below). This sub-cohort was derived from the BACC cohort as a selection of patients comprising 1) STEMI, 2) T1MI, 3) T2MI, 4) AI and 5) non-cardiac chest pain. The distribution of the available samples is as follows: 1) n=31 STEMI patients with serial sampling across 3 time points totalling 93 samples; 2) n=26 T1MI patients with sequential specimens across 3 time points adding up to 78 samples; 3) n=31 T2MI patients with serial sampling across 3 time points making 93 samples; 4) n=18 AI patients with serial specimens across 3 time points totalling 54

samples; 5) n=59 non-cardiac chest pain patients with repeat sampling across 3 time points adding up to177 samples.

5.2.2 Protein measurements

We used proximity extension assays (PEA, Olink®, Olink Proteomics, Uppsala, Sweden) to measure NT-proBNP in serial samples. In PEA, oligonucleotide-labelled monoclonal or polyclonal antibodies (PEA probes) are used to bind target proteins in a pair-wise manner using only 1 µL of sample. PEA assay was used to address the high levels of 44% missingness in baseline clinical NT-proBNP measurements. NT-proBNP is not measured routinely in clinics for these patients. Additionally, serial measurements (1hr and 3hr) of NT-proBNP are not done in the clinics and thus was not available. To obtain kinetics for all the three time-points we measured NT-proBNP with the PEA assay. Importantly, results from the PEA assay showed a positive and significant correlation to clinical NT-proBNP (Pearson r=0.64, P value <0.001; Spearman rho=0.82, P value <0.001, **Figure 12**).

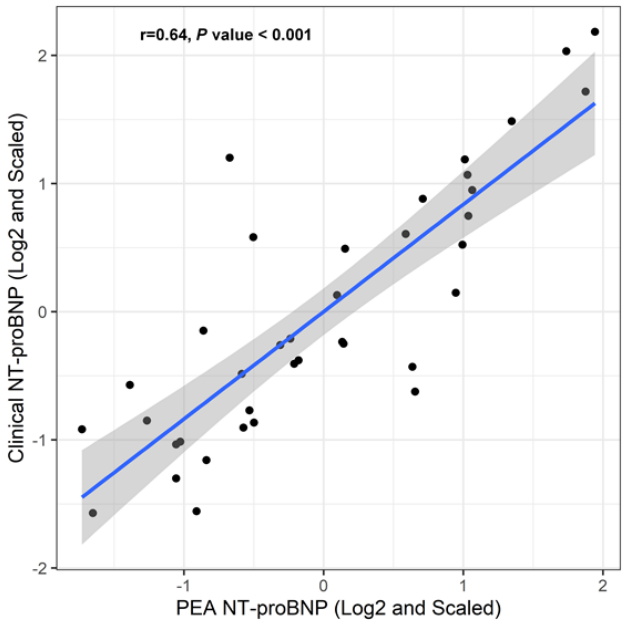

Figure 12. Association between clinical and PEA NT-proBNP baseline measurements. *A positive and significant Pearson (r=0.64, P value <0.001) and spearman correlation (rho=0.82, P value <0.001) exists between PEA and clinical NT-proBNP. Lines show fitted linear regression with grey bands indicating the 95% confidence interval. Abbreviations - PEA: Olink proximity extension assay. Reproduced from Schulte et al. J Mol Cell Cardiol Plus 2022*

5.2.3 Statistical analyses

The serial release kinetics of proteins and miRNAs were analysed using linear mixed effect model with individuals as the random effect to factor within subject variance. Linear mixed effect model was selected to allow heteroscedasticity and imbalanced repeats across various timepoints i.e., baseline (0 hr), 1h and at 3h. Release kinetics model for proteins and miRNAs were performed without data scaling. Given the insignificant association between demographics and biomarkers (proteins and miRNAs), release kinetics were not adjusted for age and sex (**Figure 13**). R package lme4 was used to implement linear mixed effect model. Post-hoc pairwise comparisons were performed using R package 'emmeans'

with "tukey" adjustment for comparing a family of 9 estimates (3 groups, 3 timepoints). Satterthwaite degrees-of-freedom method was used. Correlation between continuous variables was performed using Spearman correlation adjusted for individual effects. Correlation between continuous and binary variables was performed using point-biserial correlation adjusted for individual effects. *P* values were adjusted for multiple-testing using Benjamini-Hochberg FDR correction. Correlation plot with dendrogram was generated using R package heatmaply [96] with Ward's minimum variance method (‘ward.D2’) as the hierarchical clustering method. Baseline characteristics significance test was undertaken using Mann-Whitney U test for continuous variables and Fisher exact test for binary variables. Box plots to show raw data distribution of biomarkers (proteins and miRNAs) were generated using R package ggboxplot. Statistical analysis and associated figures were generated with R programming environment (version 4.0.2).

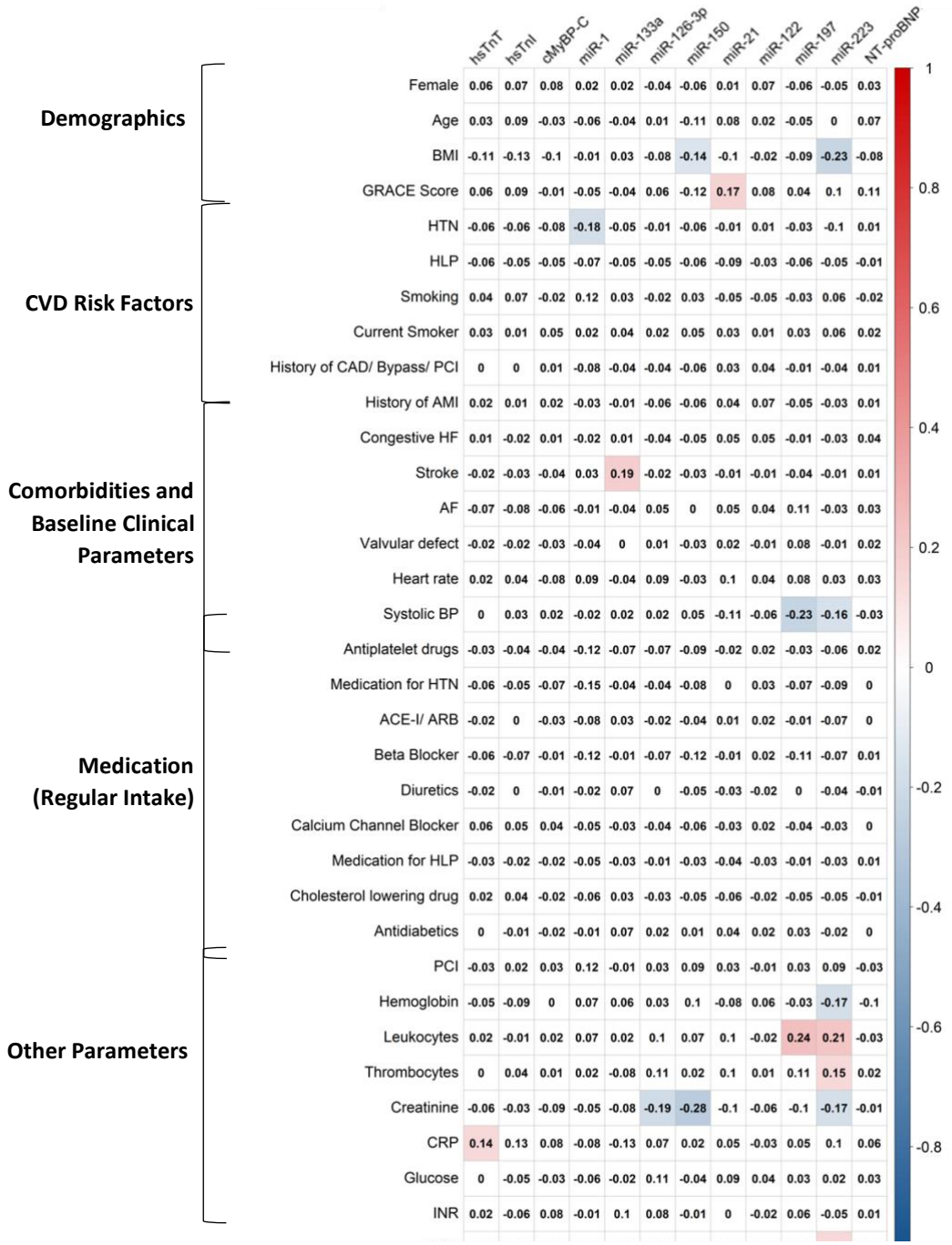

***Figure 13. Pairwise Spearman correlation for continuous variables**, and point-biserial correlation for pairwise correlation of continuous and binary variables adjusted for individual effects (repeated measure) in T1MI, T2MI and AI groups. White indicates no significant correlation (P value >0.05). Red indicates positive and blue negative correlation with P value < 0.05. P value is adjusted for Benjamini-Hochberg FDR correction. Abbreviations - CRP: c-reactive protein; TSH: thyroid stimulating hormone; INR: standardized prothrombin time; GRACE: Global Registry of Acute Coronary Events; CK: creatine kinase; hs-TnT: high-sensitivity Troponin T; hs-TnI: high-sensitivity Troponin I. Reproduced from Schulte et al. J Mol Cell Cardiol Plus 2022*

5.2.4 Machine learning

Biomarkers with statistically significant release kinetics (*P* value <0.05) across the three time points in at least one pairwise comparison were assessed for their power to discriminate T1MI, T2MI and AI. This resulted in selection of hs-TnT and NT-proBNP. Hence, the predictive performance of hsTnT, NT-proBNP and their combination were evaluated in T1MI, T2MI and AI. Boruta stability selection [97]

was used as a wrapper to multi-class random forest for feature selection in individual as well as combination biomarkers design along with demographics i.e., age and sex. For internal validation, leave-one-out cross validation was performed such that samples from the same individual are grouped into the same fold and thus avoid leakage into model performance metrics. Majority voting was applied to aggregate sample level classification into patient level final grouping. Performance metrics were computed using one-vs-all comparison with weightage to account for data imbalance. The implementation of multi-class random forest was done using Scikit-learn 0.23.2 Python package.

6 RESULTS

6.1 BIOMARKERS FOR ASSESSING T1MI

6.1.1 Detectability of ncRNAs in human plasma

To compare detectability of different ncRNAs, human myocardial tissue was spiked into plasma of healthy volunteers at defined concentrations of 0.25µg to 25µg/100µl plasma (**Figure 6, methods part**). Based on published data, we selected 158 circRNAs and 21 lncRNAs that were reported as abundant in human myocardium (for details see Methods section and **Figure 7**). circRNAs associated with cardiac-specific proteins such as cTnT, cTnI and cMyBP-C were amongst the least well-detectable circRNAs in plasma (data not shown). Muscle- (miR-1, miR-133a) and cardiac-enriched miRNAs (miR-208b, miR-499) were chosen for comparison. These four miRNAs showed comparable overall regression curves to cardiac circRNAs (circSLC8A1, circMyBPC3, circALPK2) and lncRNAs (lncLIPCAR, lncH19 lncuc004.cov4) as well as protein markers (**Figure 14, 15**).

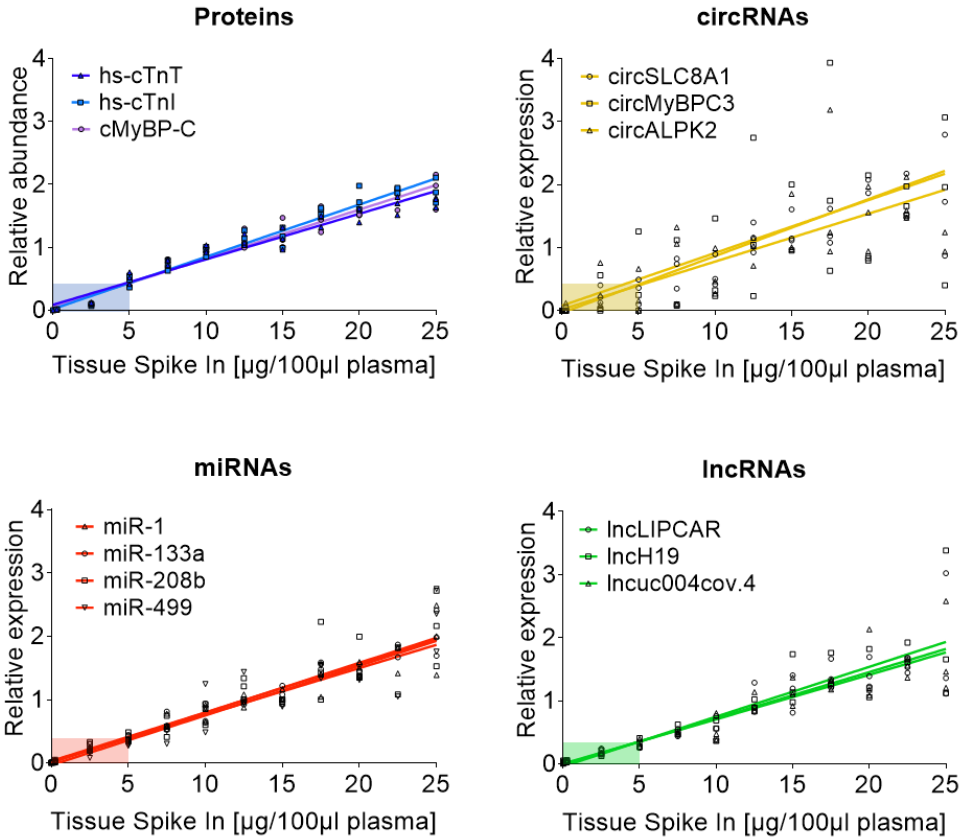

Figure 14. Myocardial tissue spike-in – best marker selection. *Linear regression curves of each of the three ncRNA classes with the highest coefficient of determination (R-squared) values. At low spike-in concentrations, the measured protein concentrations were markedly below the regression curve (coloured boxes). Reproduced from Schulte et al. Circ Res 2019*

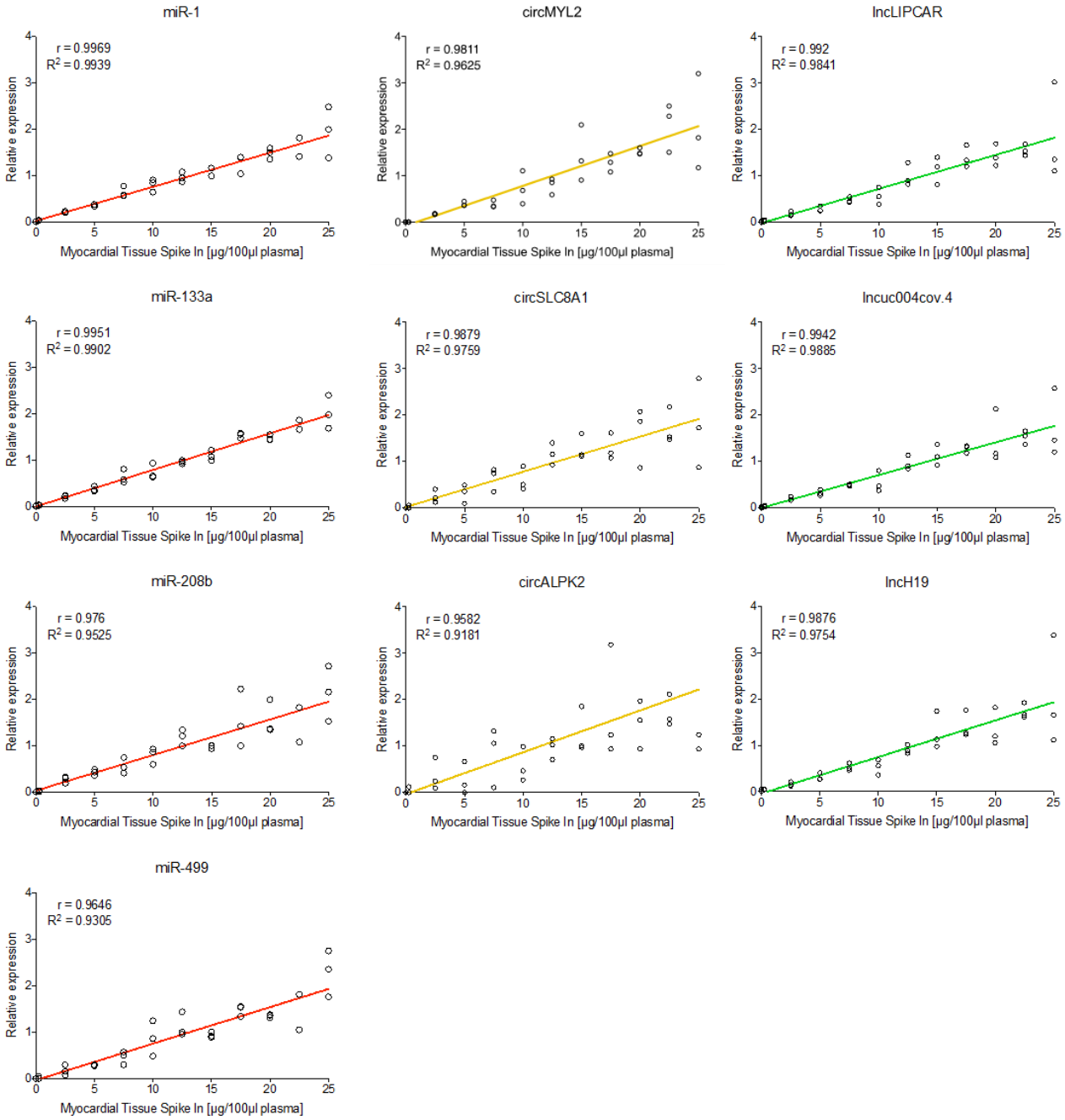

Figure 15. Myocardial tissue spike-in – selected ncRNAs. *Regression curves for a selection of ncRNA biomarkers with the highest r and R^2 values. Left Y-axis depicts relative expression referenced to the individual biomarker's median relative expression value. r = Pearson correlation coefficient; R^2 = Coefficient of determination. Reproduced from Schulte et al. Circ Res 2019*

Levels of other miRNAs remained unaltered upon spiking human myocardial tissue into plasma (**Figure 16**). Next, ncRNA spike in results were compared with measurements of established and novel cardiac protein biomarkers as previously described [80] (**Figure 17**).

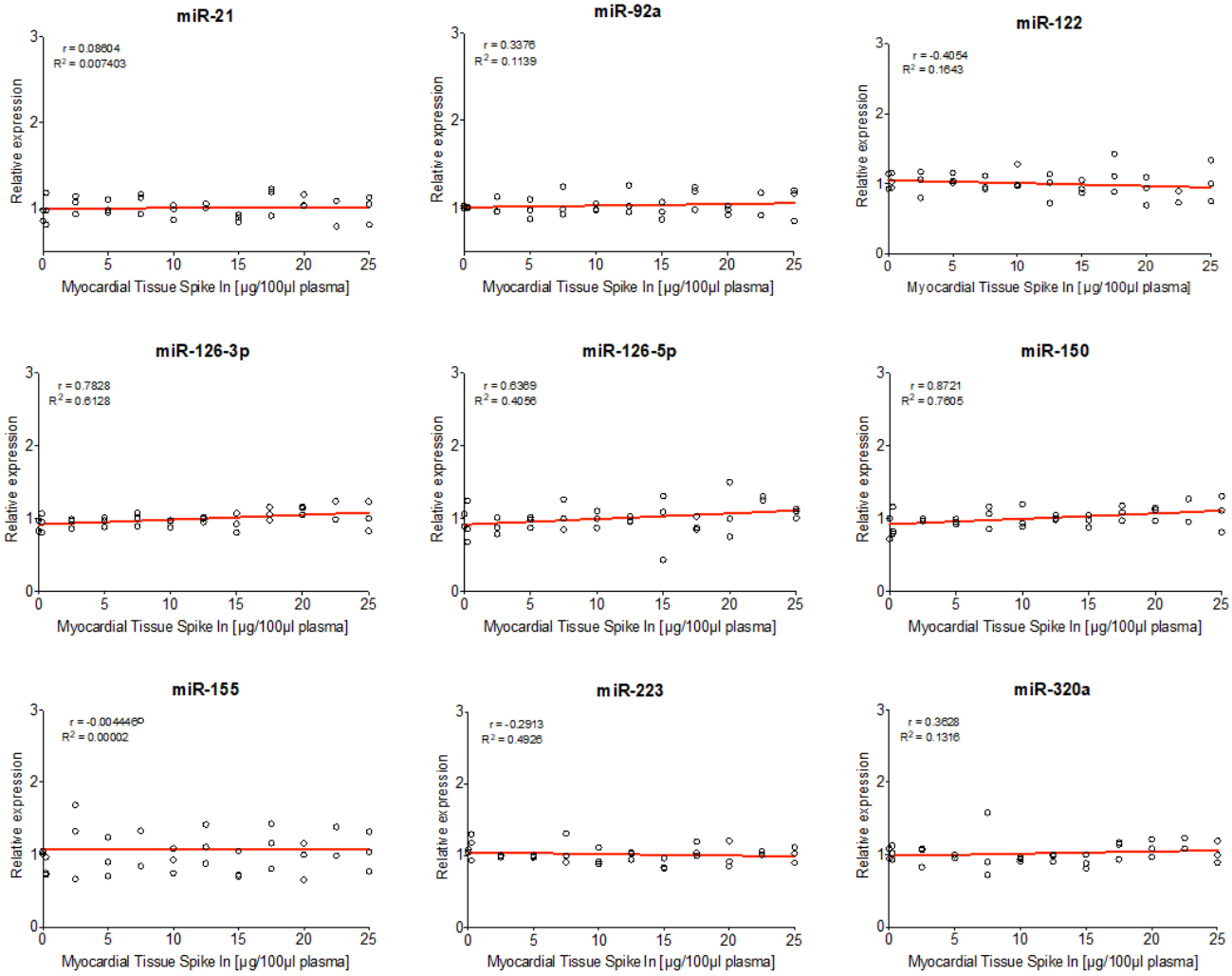

Figure 16. Myocardial tissue spike-in - non muscle-/cardiac enriched miRNAs. *miRNAs that are not enriched in muscle or myocardium fail to show an increase in plasma after myocardial tissue spike-in at different concentrations. r = Pearson's correlation coefficient, R^2 = Coefficient of determination. Reproduced from Schulte et al. Circ Res 2019*

Whilst ncRNAs demonstrated a continuous, linear dose-response-curve across all spike-in concentrations, measurements of cardiac proteins (hs-cTnT, hs-cTnI, cMyBP-C) remained below their regression curve at low spike-in concentrations (0.25µg and 2.5µg/100µl plasma) (**Figure 14,** coloured boxes). At low spike-in concentrations, ncRNA regression curves were steeper compared with cardiac protein biomarkers (**Figure 18A**). Curve fitting analyses for low spike-in concentrations returned significantly higher regression coefficients for ncRNA species (**Figure 18B**, Mann-Whitney test for comparison against cardiac protein biomarkers: miRNAs $p<0.0001$, fold-change 2.6; circRNAs $p=0.0028$, fold change 2.8; lncRNAs $p=0.0028$, fold-change 1.6).

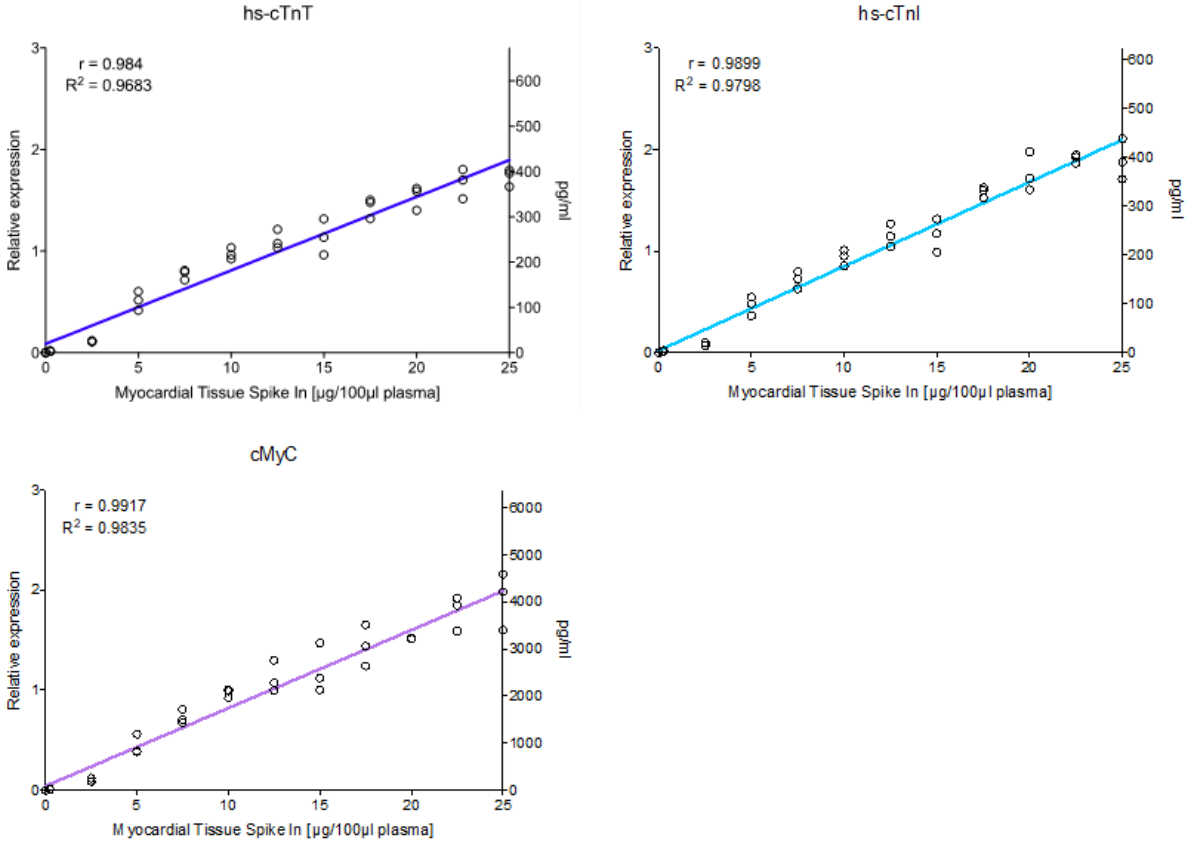

Figure 17. Myocardial tissue spike-in – protein cardiac biomarkers*. Regression curves for protein cardiac biomarkers. Left Y-axis depicts relative expression referenced to the median value of the individual protein biomarker. Right Y-axis depicts the absolute concentration in pg/ml. cMyBP-C = cardiac myosin-binding protein C, hs-cTnT = high sensitivity cardiac troponin T; hs-cTnI = high sensitivity cardiac troponin I; r = Pearson correlation coefficient, R^2 = Coefficient of determination. Reproduced from Schulte et al. Circ Res 2019*

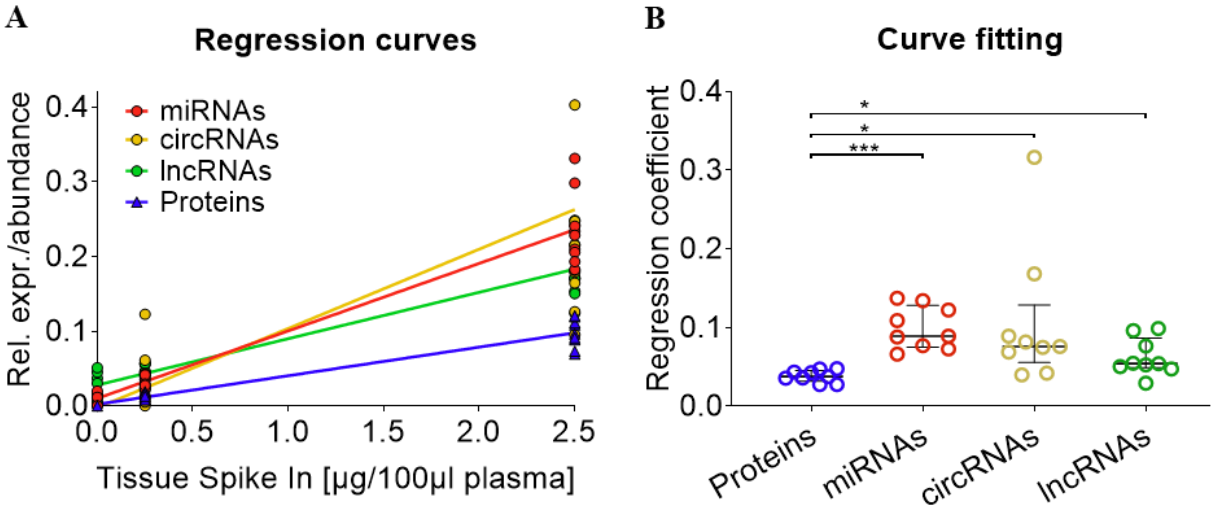

Figure 18. Myocardial tissue spike-in – regression curves and curve fitting*. **A)** Linear regression curves of all biomarker entities, combining the single biomarkers from panel A per class. ncRNAs showed steeper regression curves compared with protein biomarkers. **B)** At low spike-in concentrations, significantly higher regression coefficients, indicating higher sensitivity, were observed for all ncRNA species compared with proteins. ***: p<0.0001; *: p<0.0028 (Mann Whitney test). Reproduced from Schulte et al. Circ Res 2019*

6.1.2 Confounding by heparin in ncRNA analysis

The derangements of ncRNA biomarker measurements after heparin administration can be addressed by heparinase treatment as demonstrated in two examples: First, human plasma was spiked with 10 IU of heparin per 1ml plasma. Heparin reduced the detectability of the exogenous spike-in control *Cel-miR-39* and endogenous miRNAs resulting in spuriously elevated raw Cq values, which was rectified by heparinase treatment (**Figure 19**).

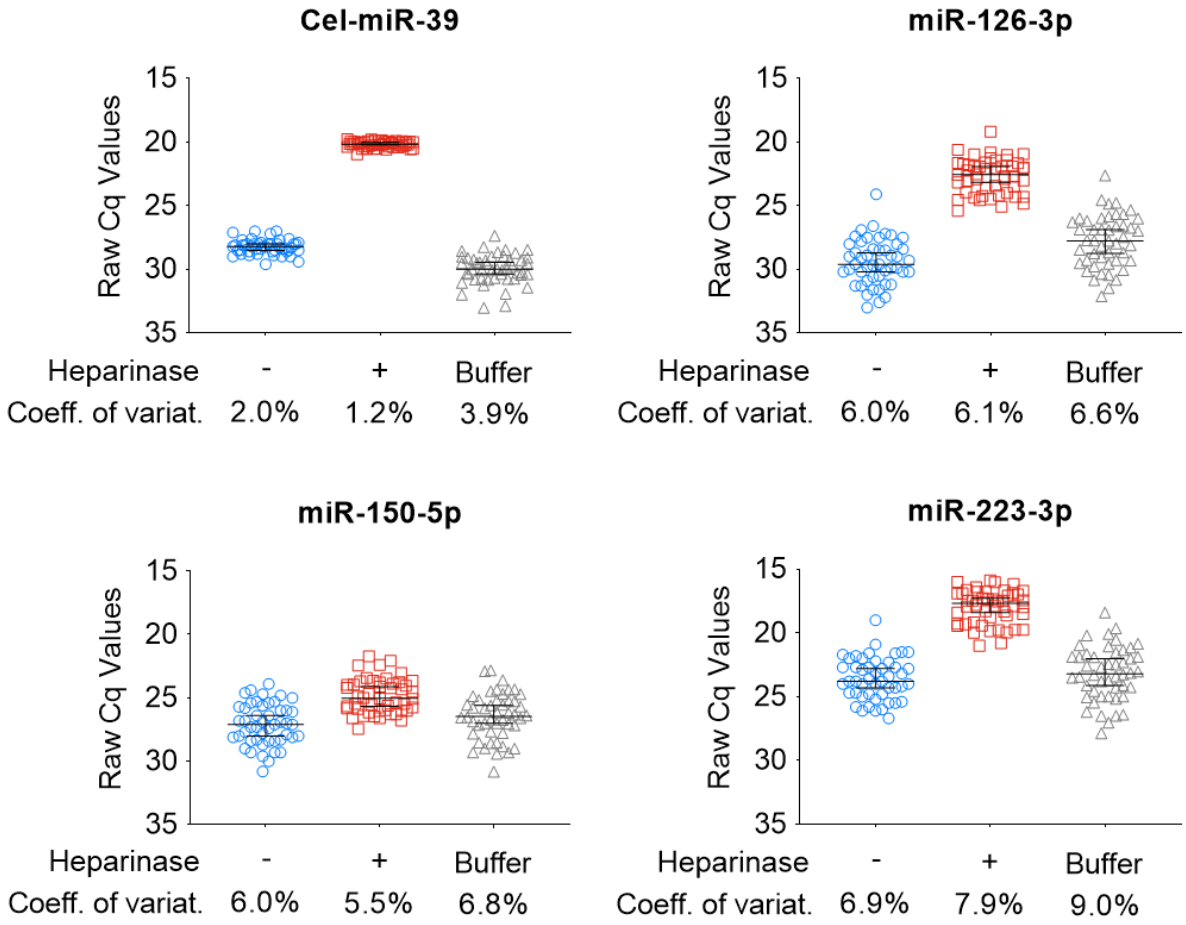

Figure 19. Heparin effect on selected miRNAs and results after heparinase treatment. *Human plasma samples were treated with heparin after blood was drawn, then miRNA expression was measured (blue). The measurements were repeated in the same samples after they were treated with heparinase (red) or with a buffer solution lacking heparinase (grey). Reproduced from Schulte et al. Circ Res 2019*

Second, we assessed samples from a cohort of patients undergoing TASH [44], where the exact time of onset of myocardial injury and heparin administration were known. In this setting, samples could be obtained before myocardial injury. We evaluated plasma miRNA levels before, and 1h, 8 and 24hrs after induced myocardial injury in TASH patients (n=16). In non-heparinase-treated samples we discovered a dense miRNA correlation network, which consists of spurious correlations between miRNAs independent of their cellular origin. This observation contradicts the well-known cell- and tissue specific expression of miRNAs **(Figure 20)**. Notably, liver-specific miR-122 and red blood cell-

enriched miR-486 appeared in the same cluster area. Heparinase treatment resolved the clustering of the network removing the correlations between miRNAs in non-heparinase-treated samples. Thus, the distinct cellular origins of non-cardiac derived plasma miRNAs became readily apparent: as visualised in **Figure 21**, the clustering shows liver miR-122 and red blood cell miR-486 separate from previously reported platelet-enriched miRNAs (miR-126, miR-223, miR-191).

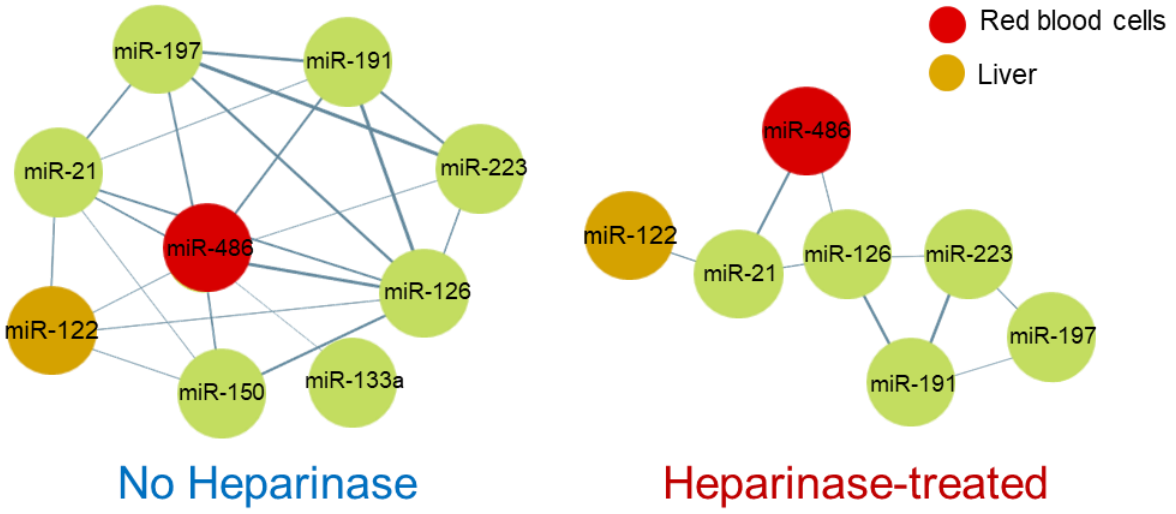

Figure 20. Heparin effect on selected miRNAs and results after heparinase treatment. *Clustering networks of miRNAs in the TASH cohort: before heparinase treatment the analysed miRNAs showed a dense correlation network. Heparinase treatment resolved this clustering of miRNAs, removing spurious correlations between miRNAs in non-heparinase-treated TASH samples. The distinct cellular origin of miRNAs, i.e. liver-specific miR-122 versus red-blood cell derived miR-486, became more readily apparent. Reproduced from Schulte et al. Circ Res 2019*

6.1.3 Release kinetics of ncRNAs after TASH

To assess the release of ncRNAs after myocardial injury, serial samples were obtained from patients undergoing TASH[81]. Upon heparinase treatment, the release of ncRNAs was compared with hs-cTnT and cMyBP-C at baseline, 1h, 8 hrs, and 24 hrs after induced myocardial injury. The clinical characteristics of the TASH patients were reported previously [81]. Plasma and serum from 16 patients at 4 time points were available for comparative analyses of the release of muscle- (miR-1, miR-133a) and of cardiac-enriched miRNAs (miR-208b, miR-499) (**Figure 21**). Unlike muscle-enriched miRNAs, the two cardiac-enriched miRNAs were undetectable at baseline. MiR-208b became detectable at 1h after TASH. For miR-499, detectable levels were only reached at 8h after TASH. circRNAs (circSMARCA, circPCMTDL) and lncRNAs (lncLIPCAR, lncH19) were chosen for their best detectability in plasma and serum. Neither mitochondrial lncRNA LIPCAR nor nucleus-derived lncRNA H19 changed after TASH (**Figure 22**). Thus, LIPCAR and lncRNA H19 levels are not of cardiac origin.

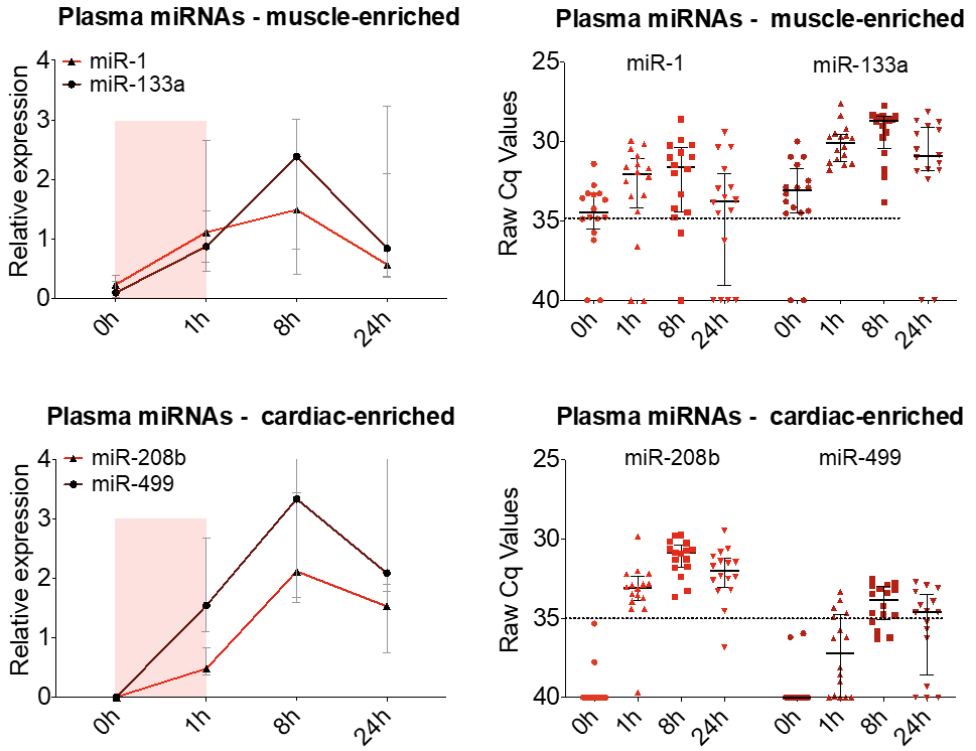

Figure 21. miRNAs after TASH. *Relative plasma levels as well as raw Cq values for muscle-enriched and cardiac-enriched miRNAs after TASH for time points before (0h) and after myocardial injury (1h, 8hrs, 24hrs). Dotted line indicates the detectability threshold; Cq-values above 35 were considered as undetectable. Of particular interest is the time course of the first hour after TASH with respect to biomarker sensitivity (coloured boxes). Depicted are median values, error bars indicate interquartile range. Reproduced from Schulte et al. Circ Res 2019*

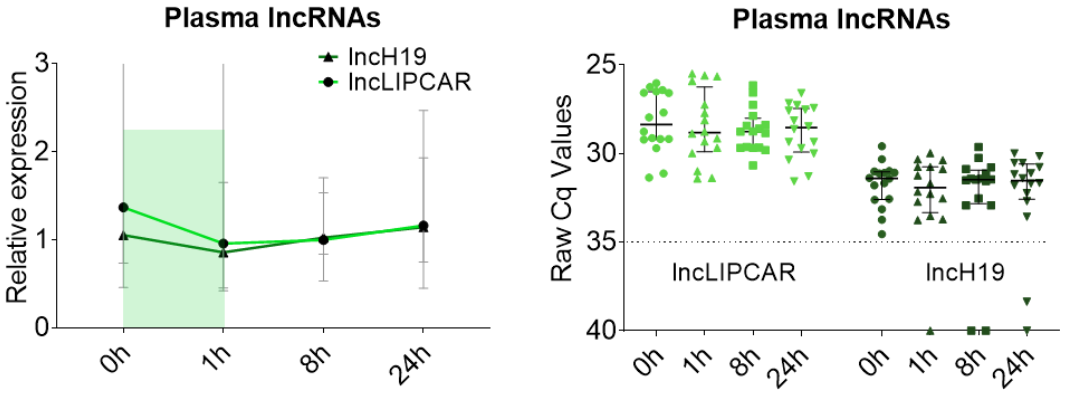

Figure 22. lncRNAs after TASH. *Relative plasma levels as well as raw Cq values for lnRNAs after TASH for time points before (0h) and after myocardial injury (1h, 8hrs, 24hrs). Dotted line indicates the detectability threshold; Cq-values above 35 were considered as undetectable. Depicted are median values, error bars indicate interquartile range. Reproduced from Schulte et al. Circ Res 2019*

Unlike other ncRNA classes, cardiac circRNAs showed poor detectability at baseline and after TASH (**Figure 23)**, despite the fact that these circRNAs were readily detectable in cardiac tissue (**Figure 24)**. An additional circRNA microarray screening of 13,617 circRNAs performed at all 4 time points did not return any significantly dysregulated circRNAs after TASH (**Figure 25**).

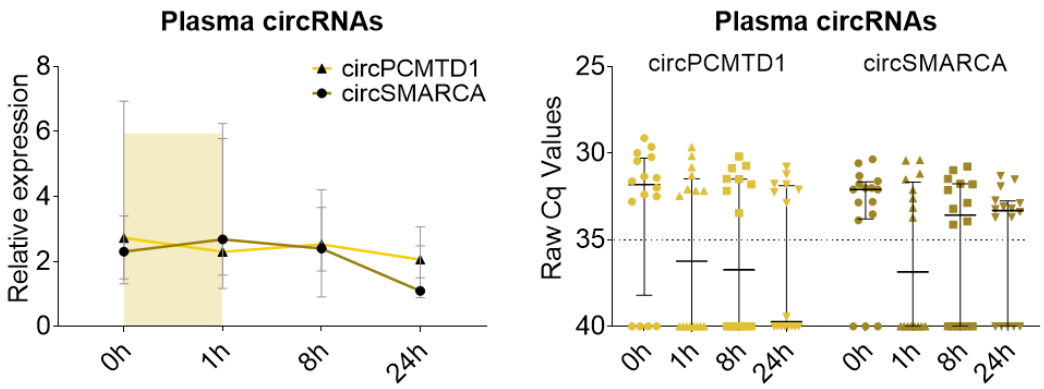

Figure 23. circRNAs after TASH. *Relative plasma levels as well as raw Cq values for circRNAs after TASH for time points before (0h) and after myocardial injury (1h, 8hrs, 24hrs). Dotted line indicates the detectability threshold; Cq-values above 35 were considered as undetectable. Depicted are median values, error bars indicate interquartile range. Reproduced from Schulte et al. Circ Res 2019*

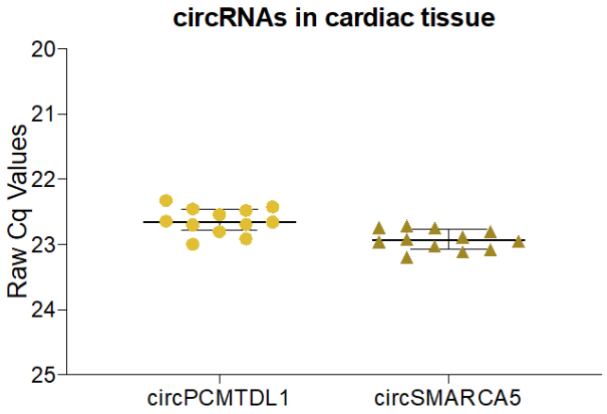

Figure 24. Raw Cq-values of selected circRNAs in human cardiac tissue. *circPCMTDL1 and circSMARCA5 were detectable in 12 human cardiac tissue samples. Their expression was stable and abundant based on raw Cq values. Reproduced from Schulte et al. Circ Res 2019*

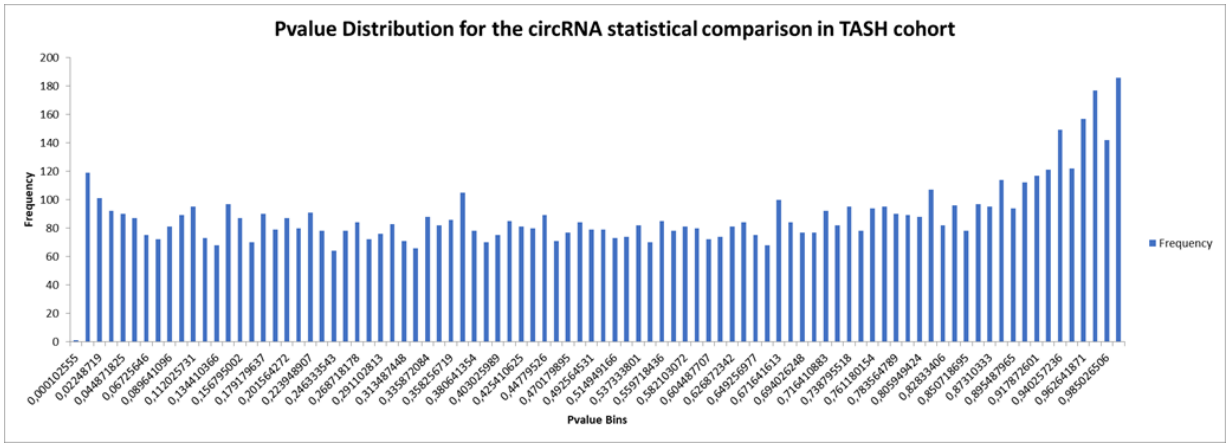

Figure 25. P-value distribution for the statistical comparison of changes in circRNAs after TASH. *An Anova test was used to test for statistically significant changes of circRNAs at 0, 4, 8 and 24 hours after TASH (n=4 pools at each time point, respectively). Correction for multiple testing was performed with Benjamini-Hochberg adjustment. None of the circRNAs was found significant with an FDR threshold of 10%. The distribution of the p-values after correcting for multiple testing, which would we expected to be skewed towards the 0 value of the x-axis in case of true significance. This is not the case, indicating that all initial significant changes are lost. Reproduced from Schulte et al. Circ Res 2019*

6.1.4 Comparison of cardiac protein versus ncRNA biomarkers in TASH

Figure 26 depicts the time course of serum levels of cardiac protein biomarkers (hs-TnT, cMyBP-C, **Figure 26A**) and circulating muscle-enriched miRNAs after TASH (miR-1, miR-133a, **Figure 26B**). As reported previously [16], cMyBP-C levels peaked before hs-TnT. Similarly, muscle-enriched miRNAs (miR-1, miR-133a) peaked earlier than cardiac protein biomarkers. When the measurements of cardiac proteins and the two muscle-enriched miRNAs, miR-1 and miR-133a, were expressed as proportions of the maximum detected value (**Figure 26C**), cMyBP-C showed a significantly higher regression coefficient compared with hs-cTnT ($p<0.0001$, Mann-Whitney test, **Figure 26D**). Similarly, higher regression coefficients were observed for muscle-enriched miRNAs compared to cardiac protein biomarkers within the first hour after induced myocardial injury (Mann-Whitney test; hs-TnT vs. miR-1 $p<0.0001$, hs-TnT vs. miR-133a $p<0.0001$, cMyBP-C vs. miR-1 $p=0.0091$, cMyBP-C vs. miR-133a

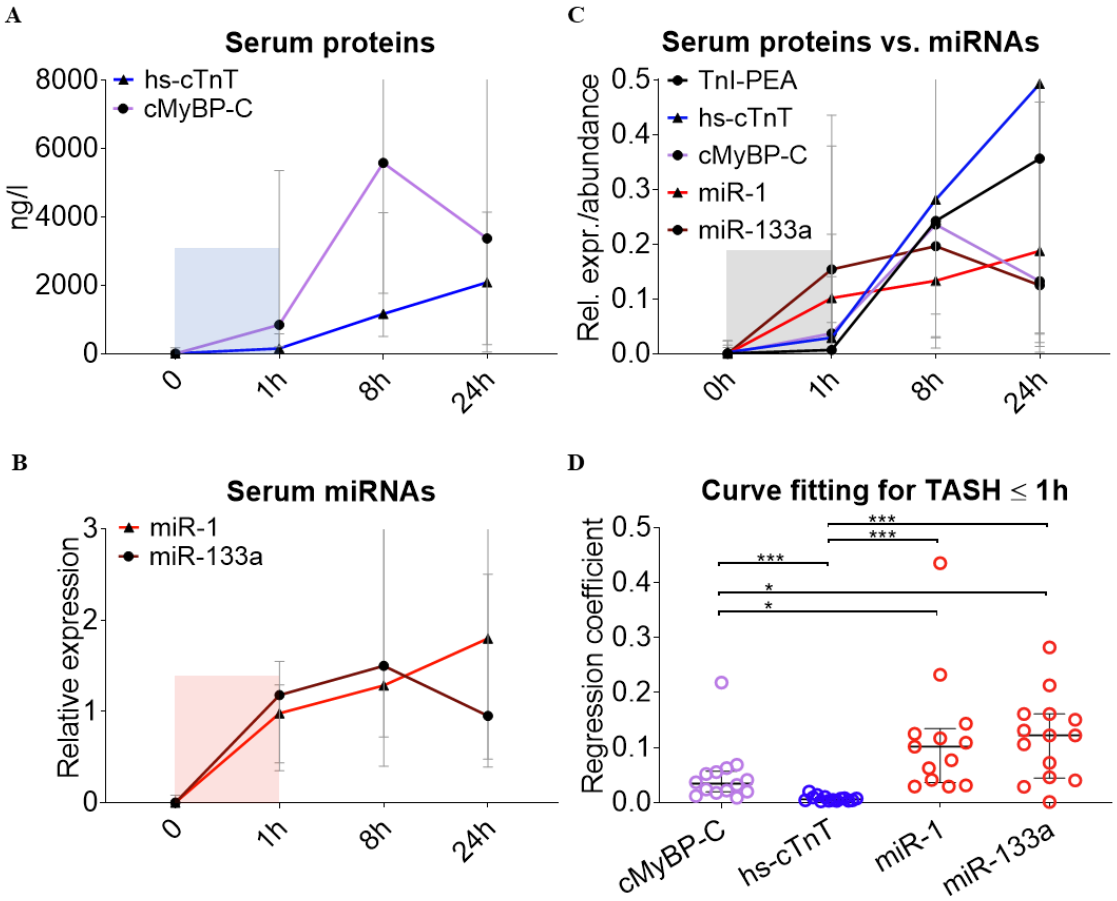

Figure 26. Comparison of ncRNAs and protein biomarkers after TASH. A) *Levels of cardiac protein biomarkers and muscle miRNA (the ncRNA group with the best overall detectability and steepest increase in the first hour after onset of myocardial injury) in the TASH cohort, depicted as median plus interquartile range. B) Transformation of absolute protein quantification measures and relative miRNA quantification measures to the same scale by dividing each value by the maximum value of each biomarker. C) Slope statistics on the relative expression of miRNA species after transformation according to panel B revealed significant differences in the regression coefficients between muscle-enriched miRNAs (miR-1 and miR-133a) and protein biomarkers for the first hour after TASH (time point 0 and 1h). *** denotes p<0.0001; *, p<0.01 (Mann Whitney test) relative to the maximum value of each biomarker. Panels A-C show median values, error bars indicate interquartile range. Reproduced from Schulte et al. Circ Res 2019*

p=0.0088) (**Figure 26D**). Circulating miRNAs and proteins were measured by qPCR and enzyme-linked immunosorbent assay, respectively. To rule out that the different assay methodology impacts on the observed release kinetics, cTnI was assessed using a proximity extension assays (PEA). The PEA combines dual antibody-based detection with qPCR-based quantification. While the PEA for cTnI was less sensitive compared to cTnT, both assays revealed a similar temporal profile for the cTn release after TASH (**Figure 26C**). The PEA measurements of cTnI were not affected by heparin (**Figure 27**) due to the minute amount of sample input required compared to miRNA measurements (1µl of plasma for cTnI vs 100µl for miRNAs).

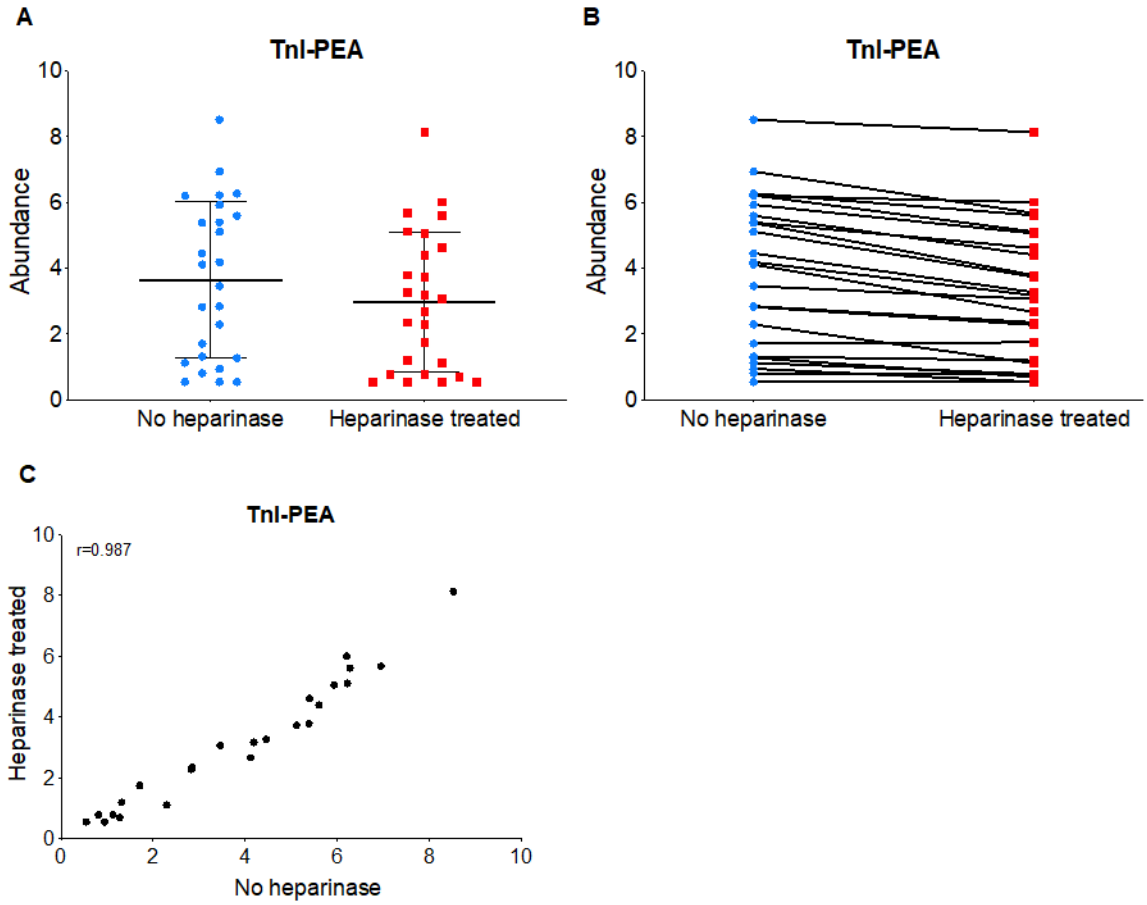

Figure 27. Comparison of PEA data in heparin and non-heparin treated samples from the TASH cohort. *As expected, after heparinase treatment slightly lower overall values were measured, caused by the dilution effect (**A** and **B**). Values between the two groups were highly correlated (**C**). PEA = Proximity Extension Assay (Olink). Reproduced from Schulte et al. Circ Res 2019*

6.1.5 Comparison of miRNAs, cMyBP-C and cTn in patients with acute MI

To compare miRNA kinetics in patients with acute MI, we analysed plasma samples from a carefully selected subcohort (n=83) of the BACC study [82], focusing on patients with initially low hs-cTnT levels who subsequently showed a steep increase within the first hour after presentation at the hospital (**Table 3**).

	All (N=83)	Non-AMI (N=45)	AMI (N=38)	p-value
Age (years)	56.0 (48.0, 68.0)	59.0 (48.0, 68.0)	55.0 (48.0, 68.0)	0.99
Male, n (%)	58 (69.9)	29 (64.4)	29 (76.3)	0.35
BMI (kg/m²)	26.3 (24.6, 29.3)	25.5 (23.7, 27.2)	28.5 (25.0, 30.7)	0.019
Systolic Blood Pressure (mmHg)	146.5 (135.4, 161.2)	145.0 (137.7, 155.0)	150.0 (135.0, 168.0)	0.46
Diastolic Blood Pressure (mmHg)	85.5 (78.0, 91.6)	84.0 (77.7, 90.0)	86.0 (78.0, 96.7)	0.33
Hyperlipoproteinemia, n (%)	27 (32.5)	13 (28.9)	14 (36.8)	0.59
Diabetes, n (%)	8 (9.8)	3 (6.7)	5 (13.5)	0.51
Current smoker, n (%)	27 (32.5)	9 (20.0)	18 (47.4)	0.016
History of AMI, n (%)	12 (14.5)	3 (6.7)	9 (23.7)	0.06
History of CAD/Bypass/PCI, n (%)	16 (19.3)	5 (11.1)	11 (28.9)	0.076
Aspirin, n (%)	22 (26.8)	7 (15.6)	15 (40.5)	0.022
Clopidogrel, Prasugrel and/or Ticagrelor, n (%)	7 (8.5)	3 (6.7)	4 (10.8)	0.79

Table 3. Clinical characteristics of the Type 1 MI cohort. *Reproduced from Schulte et al. Circ Res 2019*

Samples were taken on admission, 1h and 3 h thereafter in 38 acute MI patients. 45 patients with non-cardiac chest pain served as controls. The plasma levels of muscle- and cardiac-enriched miRNAs strongly correlated with concentrations of hs-cTnT, hs-cTNI and cMyBP-C (**Figure 28)**.

	hs-cTnT	hs-cTnI	cMyBP-C	CK-MB	CK	miR-1	miR-133a	miR-208b	miR-499
hs-cTnT	1.0000	0.8305	0.8656	0.8624	0.6043	0.665	0.6701	0.8141	0.8762
hs-cTnI		1.0000	0.8449	0.8707	0.6074	0.6994	0.6493	0.7518	0.8123
cMyBP-C			1.0000	0.8627	0.6282	0.7334	0.722	0.8047	0.88
CK-MB				1.0000	0.7897	0.7731	0.8253	0.8184	0.8218
CK					1.0000	0.5999	0.5835	0.7914	0.8397
miR-1						1.0000	0.7868	0.7965	0.8381
miR-133a							1.0000	0.8387	0.8899
miR-208b								1.0000	0.9112
miR-499									1.0000

Figure 28. Correlation of cardiac biomarkers in Type 1 MI. *All analysed biomarkers are highly correlated. Cardiac-enriched miRNAs correlate better with hs-cTnT and among each other than muscle-enriched miRNAs. Depicted are regression coefficients; p for all combinations <0.0001. CK = Creatine kinase; CK-MB = Creatine kinase muscle/brain; cMyBP-C = Cardiac myosin-binding protein C; Hs-cTnI = high sensitivity cardiac troponin I; hs-cTnT = high sensitivity cardiac troponin T, TnI-PEA = cardiac troponin I as measured by a proximity extension assay (PEA, Olink). Reproduced from Schulte et al. Circ Res 2019*

Correlations were stronger in patients with STEMI (n=20) than in patients with NSTEMI (n=18) (**Figure 29**).

A

	hs-cTnT	hs-cTnI	cMyC	TnI-PEA	CK-MB	CK	miR-1	miR-133a	miR-208b	miR-499
hs-cTnT	1,0000	0,9559	0,9237	0,9022	0,9255	0,8767	0,7485	0,8426	0,8661	0,9282
hs-cTnI		1,0000	0,9015	0,9012	0,9216	0,8448	0,6719	0,7900	0,8193	0,8457
cMyC			1,0000	0,9266	0,8513	0,8735	0,8079	0,8699	0,8530	0,8776
TnI-PEA				1,0000	0,8239	0,8630	0,7344	0,8069	0,7721	0,7672
CK-MB					1,0000	0,9585	0,7571	0,8562	0,8610	0,8890
CK						1,0000	0,7912	0,8076	0,8767	0,8886
miR-1							1,0000	0,9028	0,8796	0,8649
miR-133a								1,0000	0,9086	0,9347
miR-208b									1,0000	0,9472
miR-499										1,0000

B

	hs-cTnT	hs-cTnI	cMyC	TnI-PEA	CK-MB	CK	miR-1	miR-133a	miR-208b	miR-499
hs-cTnT	1,0000	0,9583	0,9282	0,9133	0,8785	0,7668	0,7177	0,7460	0,8106	0,8773
hs-cTnI		1,0000	0,9287	0,9230	0,8925	0,7689	0,6789	0,7107	0,7503	0,7941
cMyC			1,0000	0,9262	0,8681	0,7804	0,7924	0,7899	0,8002	0,8748
TnI-PEA				1,0000	0,8749	0,8128	0,7609	0,7588	0,7888	0,8046
CK-MB					1,0000	0,8922	0,7321	0,8355	0,8148	0,8249
CK						1,0000	0,6826	0,6733	0,7943	0,8202
miR-1							1,0000	0,8653	0,7843	0,8350
miR-133a								1,0000	0,8391	0,8787
miR-208b									1,0000	0,9118

Figure 29. Correlation of cardiac biomarkers in patients with STEMI and NSTEMI Type 1. *All analysed biomarkers are highly correlated. Cardiac-enriched miRNAs correlated better with hs-cTnT and among each other than with muscle-enriched miRNAs. These correlations were higher in patients with STEMI (**A**) than in patients with NSTEMI Type 1 (**B**). Depicted are regression coefficients; p for all combinations <0.0001. CK = Creatine kinase; CK-MB = Creatine kinase muscle/brain; cMyBP-C = cardiac myosin-binding protein C; Hs-cTnI = high sensitivity cardiac troponin I; hs-cTnT = high sensitivity cardiac troponin T, NSTEMI = non-ST-elevation myocardial infarction; STEMI = ST-elevation myocardial infarction; TnI-PEA = cardiac troponin I as measured by a proximity extension assay (PEA, Olink). Reproduced from Schulte et al. Circ Res 2019*

As expected, given their cardiac enrichment, the highest correlation with hs-cTnT was observed for the two cardiac-enriched miRNAs, miR-208b and miR-499 (r=0.81 and r=0.88, respectively, p<0.0001). This correlation is as high as the correlation between hs-cTnT and cMyBP-C and hs-cTnT and hs-cTnI

(r=0.87 and r=0.83, respectively, p<0.0001). The correlation was substantially weaker for the two muscle-enriched miRNAs, miR-1 and miR-133a (r=0.67 for both, p<0.0001). Correlations of miRNAs with cMyBP-C were comparable with correlations of miRNAs with hs-cTnT. Since the diagnosis of acute MI was adjudicated based upon hs-cTnT, hs-cTnI was also measured. Data for hs-cTnI were comparable with hs-cTnT **(Figure 30 A** and **B**).

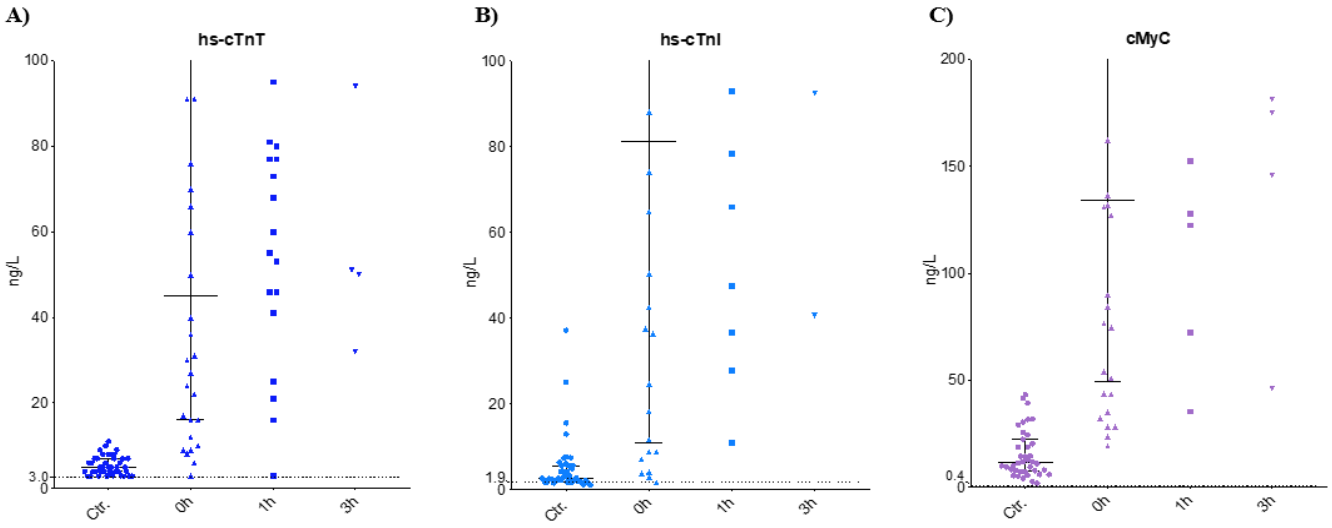

Figure 30. Release kinetics of cardiac protein biomarkers in the Type 1 MI cohort. *Values are depicted only for levels up to 100ng/L (troponins) and 200ng/L (cMyBP-C) in order to facilitate visualization of the lower concentration range. Cardiac troponins and cMyBP-C are depicted in control patients (Ctr.) vs. acute MI patients at hospital presentation (0h) and 1 hour and 3 hours after. Diagnosis of MI is adjudicated based upon hs-cTnT. hs-cTnT (A) detects all patients with acute MI at 3h after admission. Data for hs-cTnI (B) and cMyBP-C (C) are shown in comparison. The black dotted line indicates the lower limit of detection (LLoD). hs-cTnT = high-sensitivity cardiac troponin T; Hs-cTnI = high-sensitivity cardiac troponin I; cMyBP-C = cardiac myosin-binding protein C. Reproduced from Schulte et al. Circ Res 2019*

At time point 0h and 1h, one sample was below the LOD for hs-cTnT for each time point, while hs-cTnT was detectable in all MI patients at 3h. In contrast, all miRNAs showed numerous undetectable values in the MI group (**Figure 31**). This was more pronounced in NSTEMI patients than in STEMI patients (**Figure 32**).

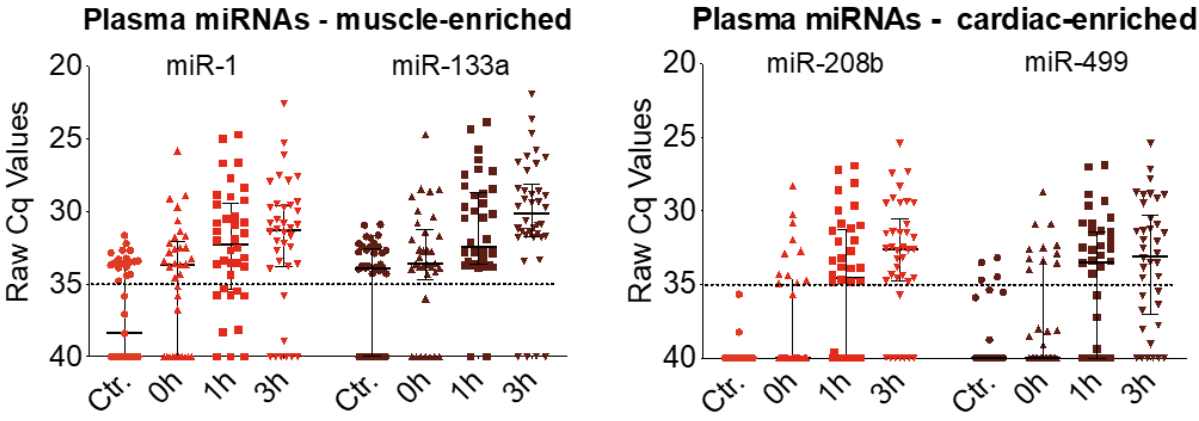

Figure 31. miRNA raw expression data in the Type 1 MI cohort. *Raw Cq values of miRNAs for control patients (Ctr) and MI patients according to time of admission to hospital (0h on presentation at hospital, 1 h and 3 hrs after presentation). At every time point, there were undetectable values (Cq>35) for each miRNA. Black dotted line denotes lower limit of detection (Cq>35). Reproduced from Schulte et al. Circ Res 2019*

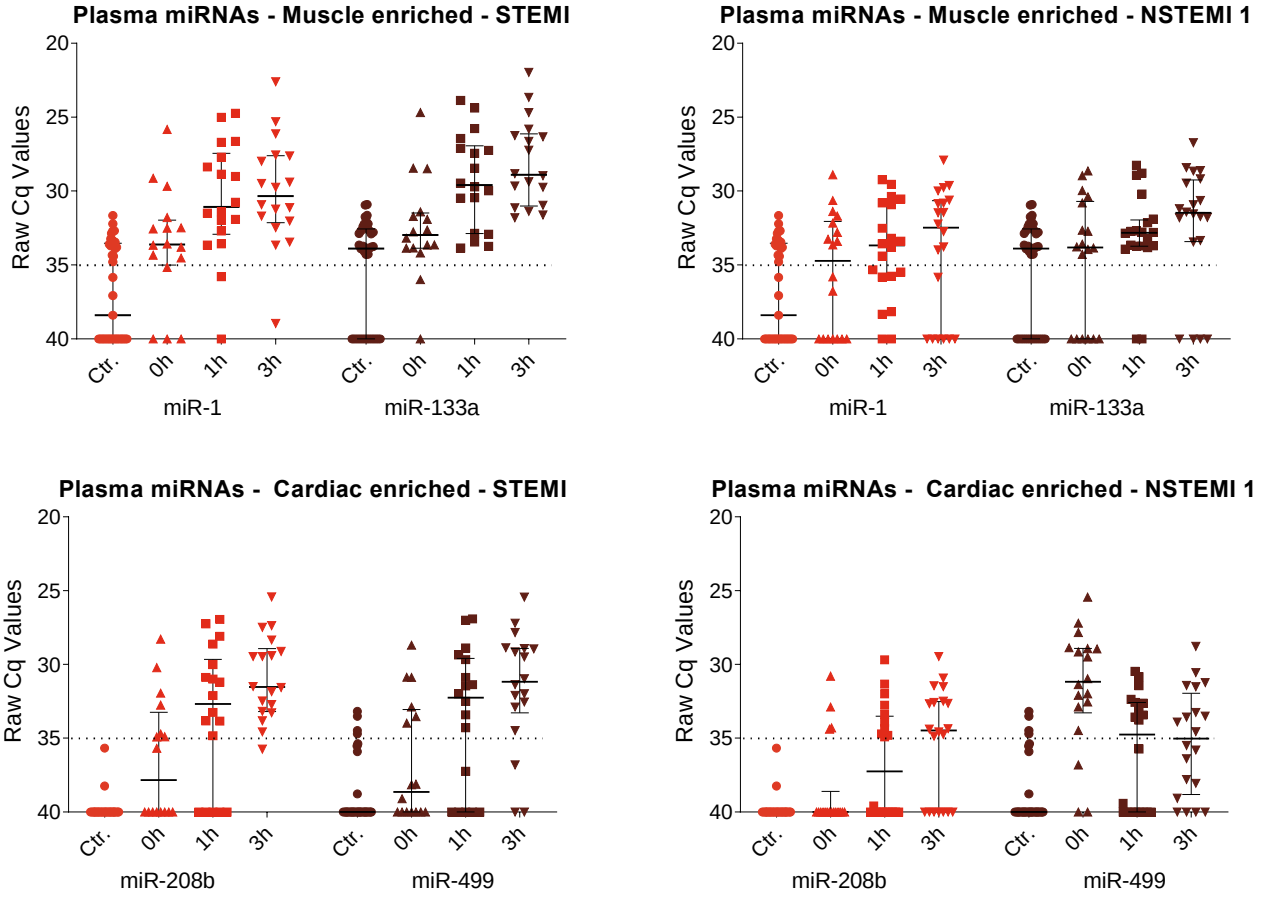

Figure 32. miRNA raw expression data in the Type 1 MI cohort. *Raw Cq values of miRNAs stratified for STEMI and NSTEMI Type 1 patients compared with control patients (Ctr.) according to time of admission to hospital: 0h on presentation at hospital, 1 h and 3 hrs after presentation. At every time point, there were undetectable values (Cq>35) for each miRNA. This is more pronounced in NSTEMI Type 1 patients compared with STEMI patients. Reproduced from Schulte et al. Circ Res 2019*

Hs-cTnT was above the lower limit of detection in 85% of the control patients (n=45), while cMyBP-C levels were above the lower limit of detection in 100% of the measurements, including control patients (**Figure 33**).

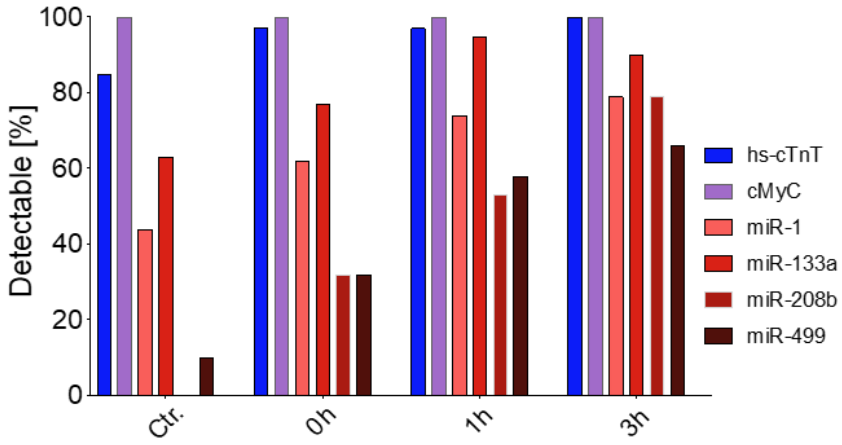

Figure 33. Detectibility of cardiac protein and miRNA biomarkers in the Type 1 MI cohort*. Shown are percentages of detectable biomarker levels in the MI cohort. Values are depicted for control patients (Ctr.) and at time point 0 h, 1 h and 3 hrs relative to presentation at hospital. cMyBP-C was detectable at all conditions / time points. Muscle-enriched miRNAs miR-1 and miR-133a are better detectable than cardiac-enriched miR-208b and miR-499, especially in the control group. hs-cTnT = high-sensitivity cardiac troponin T; Hs-cTnI = high-sensitivity cardiac troponin I; cMyBP-C = cardiac myosin-binding protein C. Reproduced from Schulte et al. Circ Res 2019*

Next, miRNA levels were reported for defined hs-cTnT groups (**Figure 34**). Only at high hs-cTnT concentrations (>1000ng/L), miRNAs were detectable in all MI patients. At low-positive hs-cTnT levels (comprising hs-cTnT levels between 21 and 50ng/L), miR-1, miR-133a, miR-208b and miR-499 were detectable in 47%, 87%, 7% and 13% of patients, respectively. In patients with hs-cTnT concentrations below 10ng/ml, miR-208b and miR-499 remained below the detection threshold (Cq of >35) whereas miR-1 and miR-133a were detectable in 39% and 64% of patients, respectively. To validate this finding, we included an additional group of 19 carefully selected MI patients with hs-cTnT levels of <1000ng/L at all 3 time points (n=57 samples, **Table 4**). In order to maximize detectability, we doubled the input of RNA for the RT-qPCR reaction. The rise in miR-1, miR-133a, miR-208b and miR-499, however, was mainly detectable at hs-cTnT levels >50-100 ng/L (**Figure 35**).

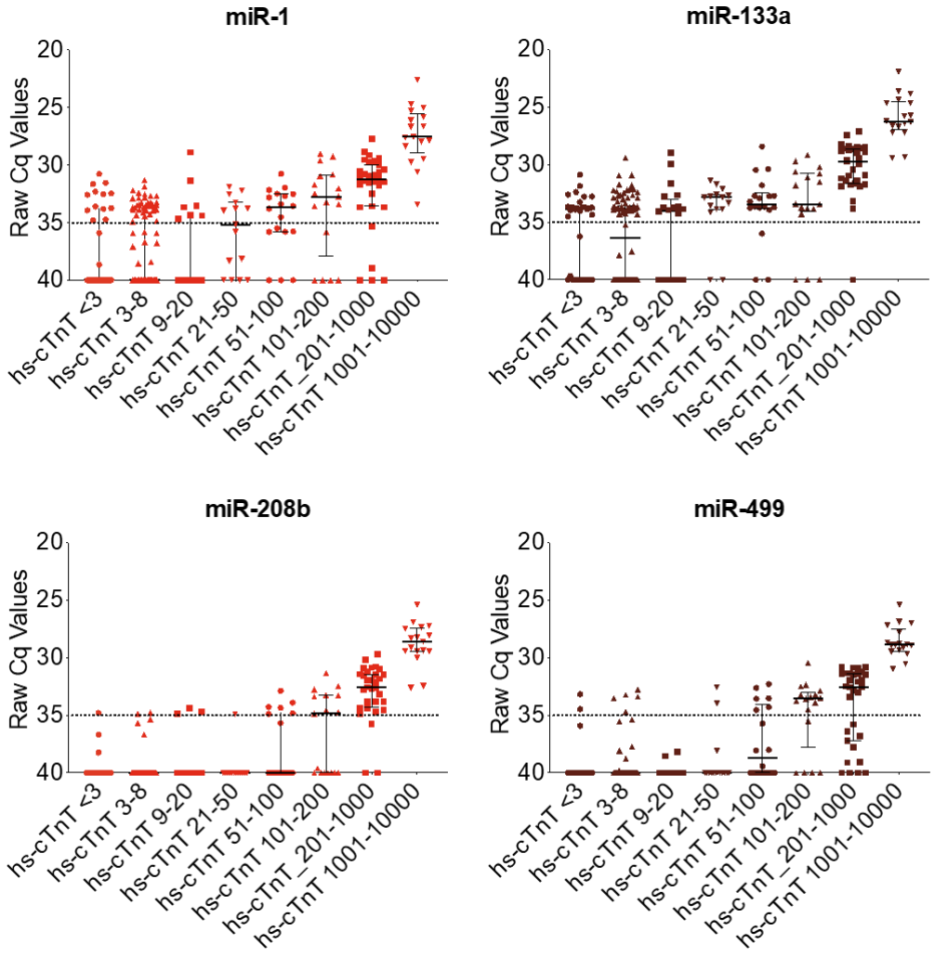

Figure 34. miRNA raw expression data corresponding to hs-cTnT groups in the Type 1 MI cohort. *miRNA raw Cq values corresponding to different ranges of hs-cTnT concentrations (ng/L). Only for hs-cTnT levels above 1000ng/L miRNAs showed 100% detectability. Black dotted line denotes lower limit of detection (Cq>35). Reproduced from Schulte et al. Circ Res 2019*

	All AMI (N=57)	AMI_discovery (N=38)	AMI_validation (N=19)	p-value
Age (years)	62.0 (49.7, 69.0)	55.0 (48.0, 68.0)	67.0 (59.2, 70.7)	0.13
Male, n (%)	46 (80.7)	29 (76.3)	17 (89.5)	0.41
BMI (kg/m²)	27.5 (24.8, 30.4)	28.5 (25.0, 30.7)	27.1 (24.7, 28.8)	0.4
Systolic Blood Pressure (mmHg)	150.0 (138.7, 169.0)	150.0 (135.0, 168.0)	152.5 (141.0, 174.5)	0.52
Diastolic Blood Pressure (mmHg)	88.0 (79.3, 98.7)	86.0 (78.0, 96.7)	96.0 (81.8, 105.1)	0.10
Hyperlipoproteinemia, n (%)	21 (36.8)	14 (36.8)	7 (36.8)	1
Diabetes, n (%)	8 (14.3)	5 (13.5)	3 (15.8)	1
Current smoker, n (%)	28 (49.1)	18 (47.4)	10 (52.6)	0.93
History of AMI, n (%)	13 (22.8)	9 (23.7)	4 (21.1)	1
History of CAD/Bypass/PCI, n (%)	18 (31.6)	11 (28.9)	7 (36.8)	0.76
Aspirin, n (%)	22 (39.3)	15 (40.5)	7 (36.8)	1
Clopidogrel, Prasugrel and/or Ticagrelor, n (%)	6 (10.7)	4 (10.8)	2 (10.5)	1

Table 4. Clinical Characteristics of Type 1 MI Discovery and Type 1 MI Validation Cohorts. *Reproduced from Schulte et al. Circ Res 2019*

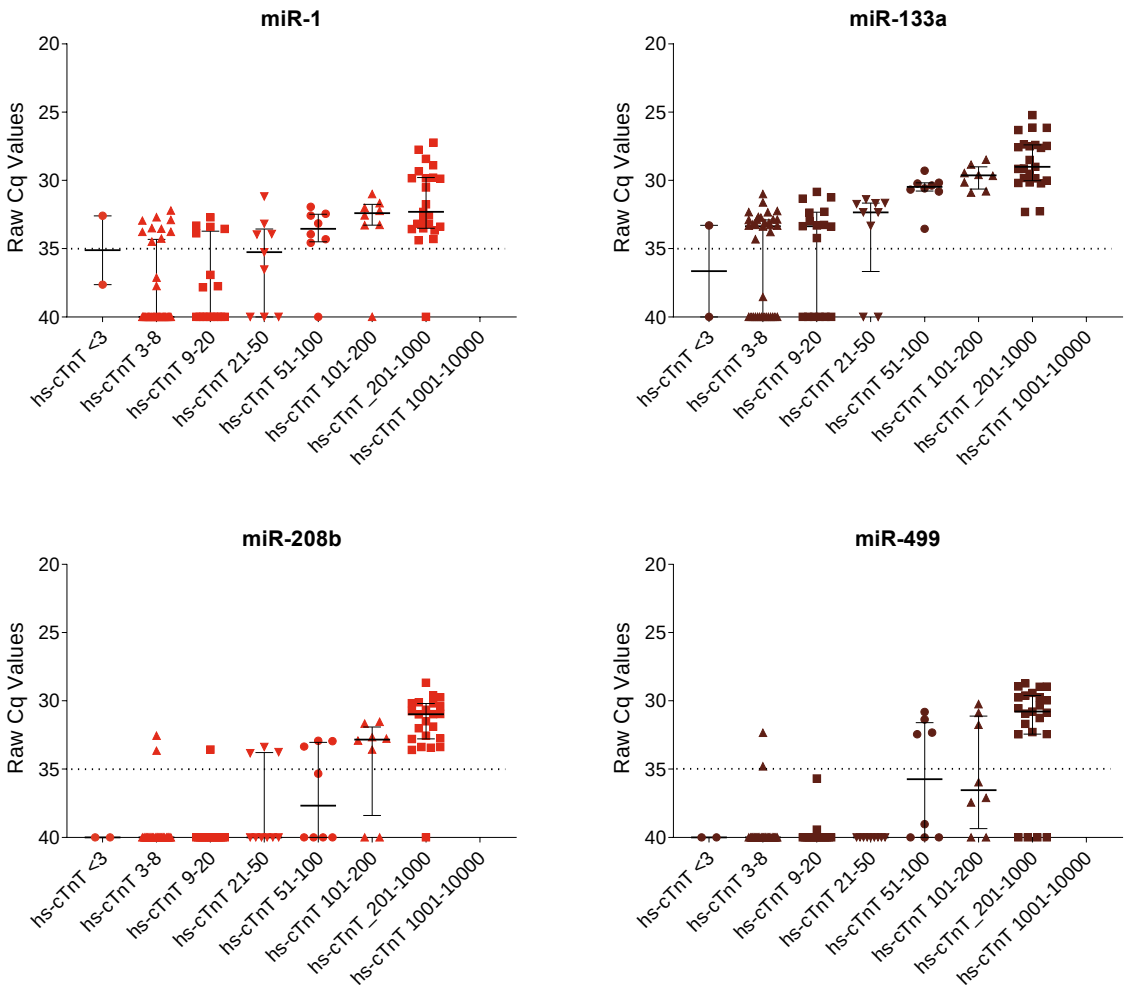

Figure 35. miRNA raw expression data corresponding to different ranges of hs-cTnT concentrations (ng/L) with increased RNA input. *An additional patient group comprising 57 carefully selected MI samples (n=19 patients at three time points) with hs-cTnT levels of <1,000ng/L was selected and miRNAs quantified. In order to improve detectability, an increased RNA input (2-fold increase) was used. However, detectability remained poor at hs-cTnT levels <50-100ng/L. Reproduced from Schulte et al. Circ Res 2019*

Thus, analogous to the TASH results, miR-1 (44%) and miR-133a (63%) were also more readily detectable in the control group compared to miR-208b (0%) and miR-499 (10%) (**Figure 32**). cMyBP-C was detectable in all control and MI samples. Confirming the results from the TASH patients, cMyBP-C showed a steeper increase in the MI cohort shortly after hospital presentation than hs-cTnT with yet smaller coefficients of variation at all time points in the MI cohort (**Figure 36A)**. Curve fitting analysis revealed significantly higher regression coefficients for cMyBP-C than for hs-cTnT and muscle- and cardiac miRNAs (**Figure 36B**).

6.1.6 Comparison of receiver operating characteristic analyses based on the TASH and MI cohorts

When comparing patients before the TASH procedure with any of the time points after (1h, 8h, 24h), both cardiac miRNAs -208b and -499 showed a higher predictive value (area under the curve, AUC

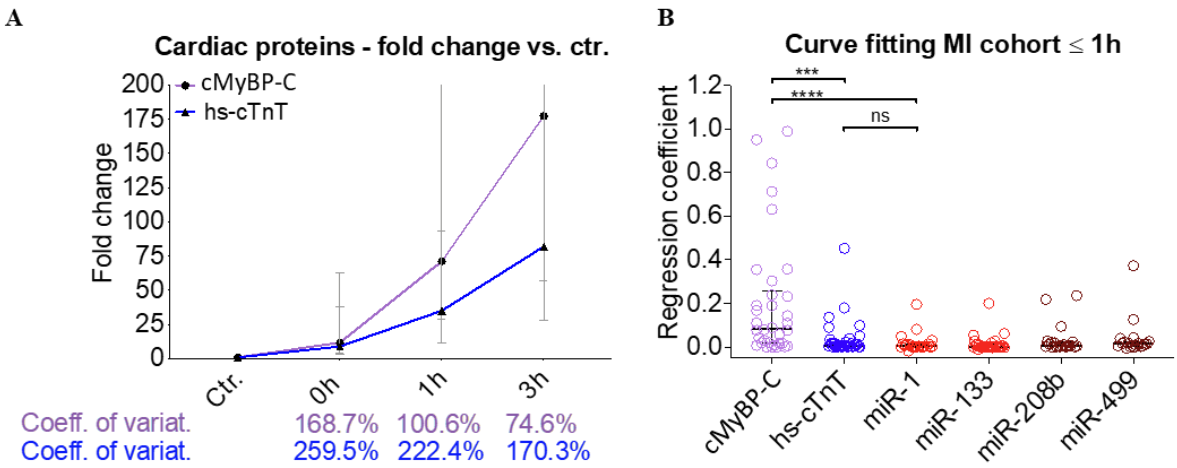

Figure 36. Release kinetics of cardiac protein biomarkers and curve fitting in Type 1 MI cohort. A) *cMyBP-C rose more quickly after onset of MI compared with hs-cTnT with a smaller coefficient of variation (values depicted are median with interquartile range). B) Curve fitting analysis of the first hour after hospital presentation revealed significant higher regression coefficients for cMyBP-C than all other biomarkers. **** denotes p<0.0001; ***, p=0.0002; ns, not significant (Mann Whitney test). Reproduced from Schulte et al. Circ Res 2019*

0.934 and 0.948, respectively) than hs-cTnT (0.918) for the detection of myocardial injury (**Figures 37, 38, Table 5**). The combination of hs-cTnT with cardiac miR-208b or cardiac miR-499 improved AUC values to 0.943 and 0.957, respectively. A combination of both cardiac miRNAs offered no further improvement in the predictive value. AUC values for muscle miR-1 and miR-133a were lower (0.824 and 0.790, respectively) despite their higher sensitivity. cMyBP-C was the cardiac protein biomarker with the highest predictive power (0.967).

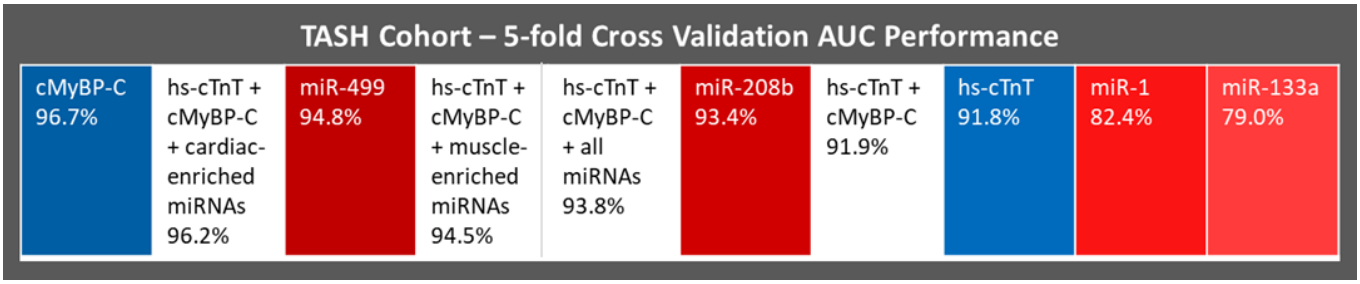

Figure 37. ROC analysis comparing predictive power of protein and miRNA biomarkers in the TASH cohort. *Blue colour for proteins, red for miRNAs, white for combinations of 2 or more biomarkers. The biomarkers are ranked from left to right (highest to lowest AUC value). The intensity of the blue and red colour increases with increasing AUC values. Reproduced from Schulte et al. Circ Res 2019*

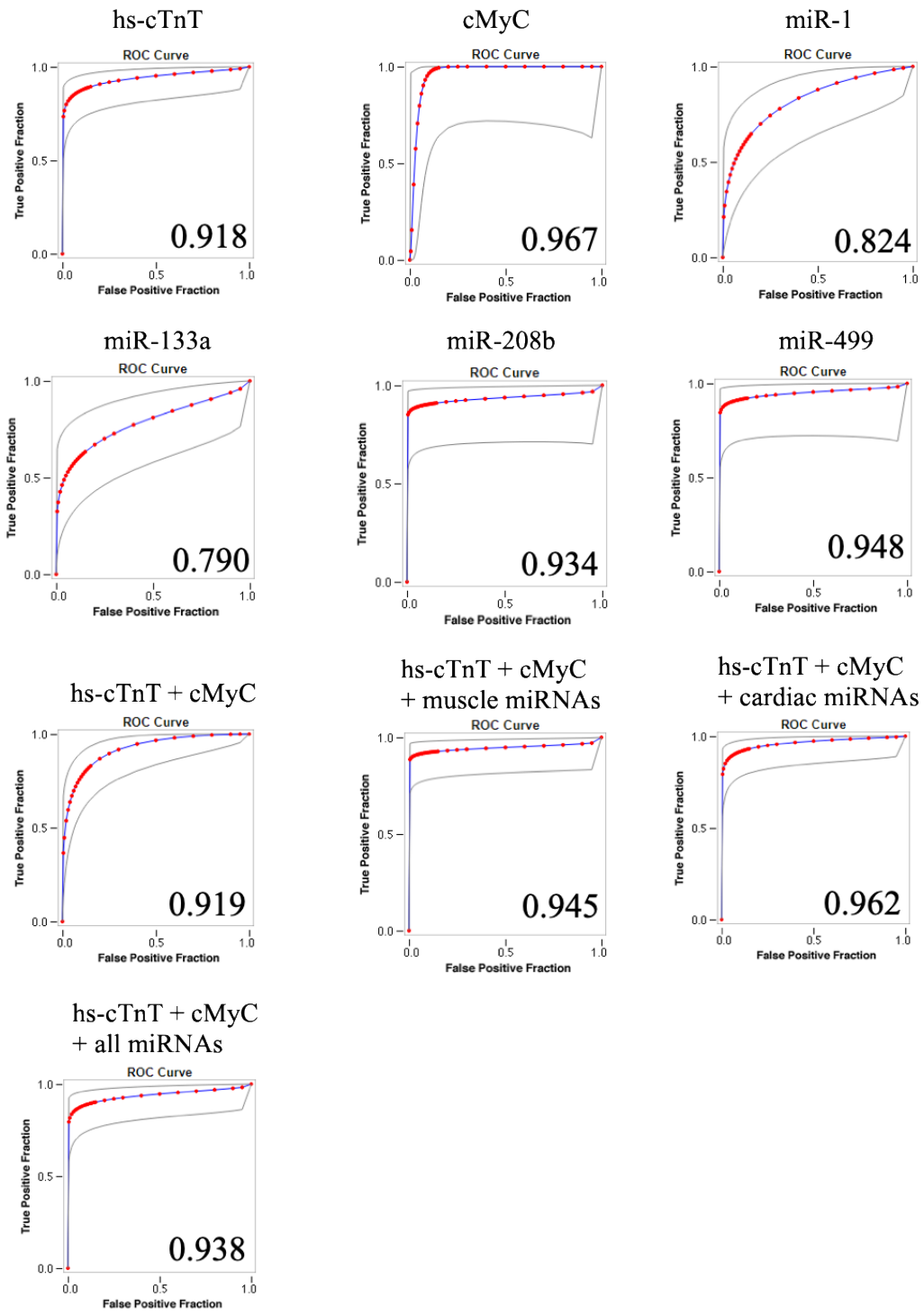

Figure 38. ROC curves for TASH cohort. *Grey lines depict the 95% confidence interval of the fitted ROC curve. hs-cTnT, high-sensitivity cardiac troponin T; cMyBP-C, cardiac myosin-binding protein C. Reproduced from Schulte et al. Circ Res 2019*

Biomarker	AUC
hs-cTnT	0.918
cMyBP-C	**0.967**
Tnl-PEA	0.912
miR-1	0.824
miR-133a	**0.790**
miR-208b	0.934
miR-499	0.948
hs-cTnT + cMyBP-C	0.919
hs-cTnT+TnI-PEA	0.918
hs-cTnT+miR-1	0.869
hs-cTnT+miR-133a	0.888
hs-cTnT+miR-208b	0.943
hs-cTnT+miR-499	0.957
miR-1+miR-133	0.874
miR-208+miR-499	0.952
hs-cTnT+miR-1+miR-133a	0.904
hs-cTnT+miR-208b+miR-499	0.939
hs-cTnT+cMyBP-C+miR-1+miR133a	0.945
hs-cTnT+cMyBP-C+miR-208b+miR499	0.962
hs-cTnT+cMyBP-C+miR-1+miR133a+miR-208b+miR-499	0.938
hs-cTnT+Tnl-PEA+miR-1+miR133a	0.848
hs-cTnT+Tnl-PEA+miR-208b+miR499	0.936
hs-cTnT+Tnl-PEA+cMyBP-C+miR-1+miR133a	0.941
hs-cTnT+Tnl-PEA+cMyBP-C+miR-208b+miR499	0.900
hs-cTnT+Tnl-PEA+miR-1+miR-133a+miR-208b+miR-499	0.886
hs-cTnT+Tnl-PEA+cMyBP-C+miR-1+miR-133a+miR-208b+miR-499	0.942

Table 5. ROC Analysis in TASH Cohort. *Green font = best-performing biomarker; Red font = worst-performing biomarker. AUC, area under the curve; cMyBP-C, cardiac myosin-binding protein C; hs-cTnT, high-sensitivity cardiac troponin T. Reproduced from Schulte et al. Circ Res 2019*

Next, the MI cohort was used as an independent validation cohort for the predictive analytics from TASH. Thus, the most promising regression models of the different combinations of proteins and miRNAs were applied to the MI cohort. When comparing control patients with acute MI patients at any of the time points (0h, 1h, 3h), both cardiac miRNAs -208b and -499 showed similar predictive power (AUC values of 0.920 and 0.921, respectively) as hs-cTnT (0.925), for the prediction of MI. This result

is comparable to the receiver operating characteristic (ROC) analyses in the TASH cohort. AUC values for muscle miR-1 and miR-133a were lower (0.825 and 0.734, respectively) despite their higher sensitivity in plasma, demonstrating the lack of cardiac specificity of muscle-enriched miRNAs (**Figure 39A, Figure 40, Table 6**). The highest AUC value in TASH was observed for cMyBP-C (0.967), while in the MI cohort, the best performance in the ROC analysis was observed for the combination of hsTnT, cMyBP-C and muscle-enriched miRNAs (0.969). Finally, cases of STEMI and NSTEMI (excluding T2MI) were assessed separately to explore different aetiologies of myocardial injury. The ROC analyses presented in **Figure 39B** and **39C** indicate that the performance of the diagnostic models is better in STEMI patients. The performance in the NSTEMI group was inferior to both STEMI and all MI cases. Importantly, the ranking of biomarker performance was consistent in all three comparisons, independent of the overall performance of the model.

A

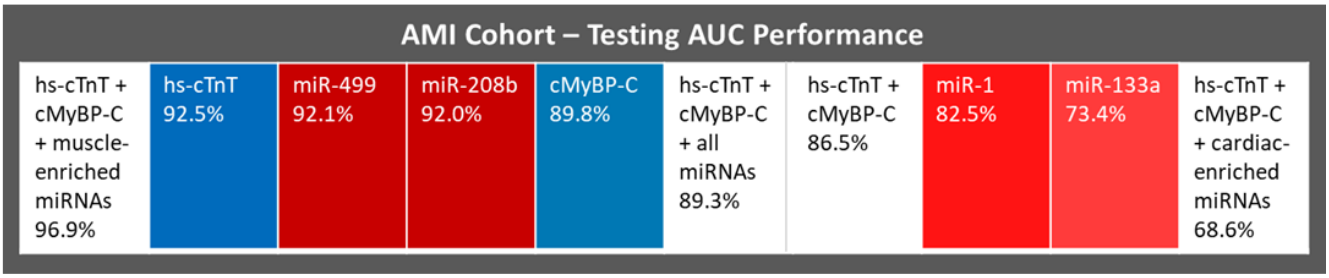

B

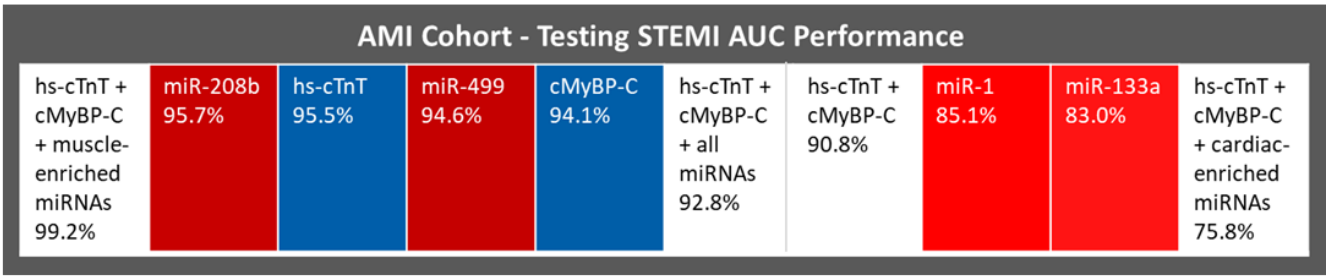

C

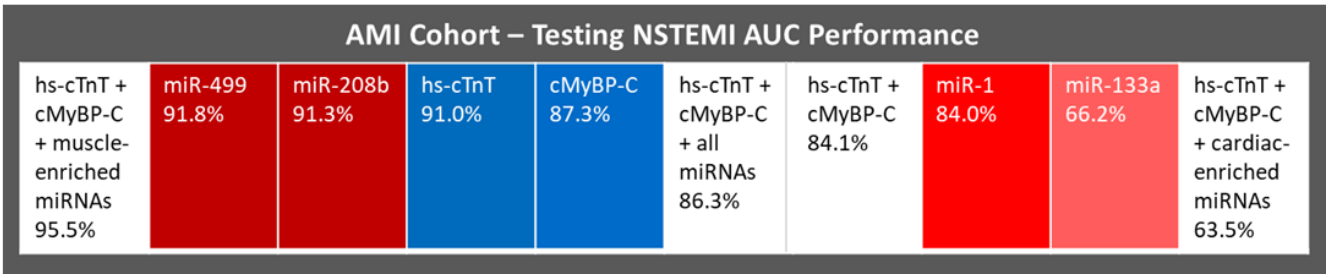

Figure 39. ROC analysis comparing predictive power of protein and miRNA biomarkers in the Type 1MI cohort. A) *MI cohort with subanalysis for* ***B)*** *STEMI patients.* ***C)*** *NSTEMI patients. Blue colour for proteins, red for miRNAs, white for combinations of 2 or more biomarkers. The biomarkers are ranked from left to right (highest to lowest AUC value). The intensity of the blue and red colour increases with increasing AUC values. Reproduced from Schulte et al. Circ Res 2019*

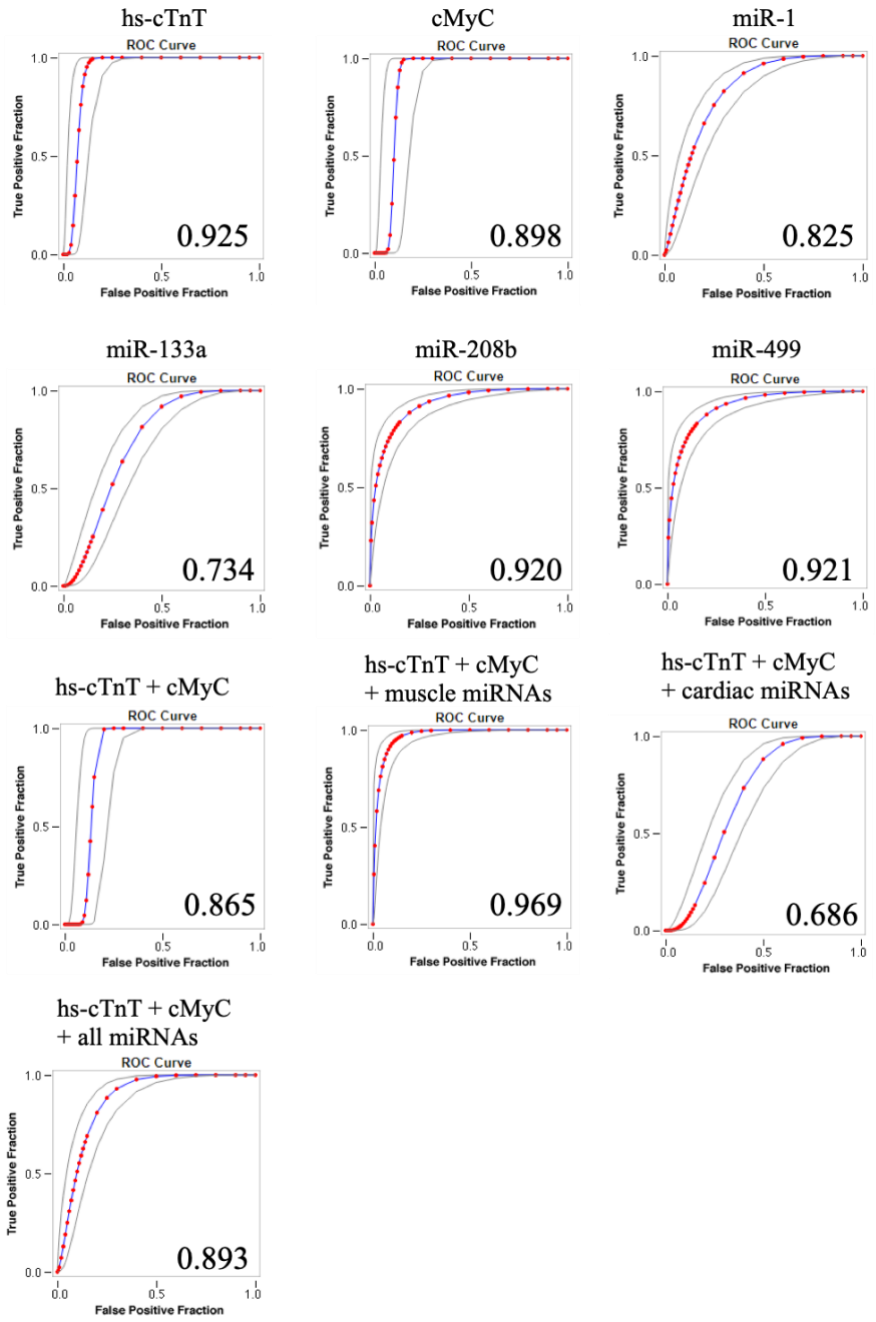

Figure 40. ROC curves forType 1 MI cohort. *Grey lines depict the 95% confidence interval of the fitted ROC curve. hs-cTnT, high-sensitivity cardiac troponin T; cMyBP-C, cardiac myosin-binding protein C. Reproduced from Schulte et al. Circ Res 2019*

Biomarker	AUC
hs-cTnT	0.925
cMyBP-C	0.898
TnI-PEA	0.695
miR-1	0.825
miR-133a	0.734
miR-208b	0.920
miR-499	0.921
hs-cTnT + cMyBP-C	0.865
hs-cTnT + cMyBP-C + miR-1 + miR-133	**0.969**
hs-cTnT + cMyBP-C + miR-208 + miR-499	**0.686**
hs-cTnT + cMyBP-C + miR-1 + miR133a + miR-208b + miR-499	0.893
hs-cTnT + TnI-PEA + cMyBP-C + miR-1 + miR-133	0.828
hs-cTnT + TnI-PEA + cMyBP-C + miR-208 + miR-499	0.917
hs-cTnT + cMyBP-C + TnI-PEA + miR-1 + miR133a + miR-208b + miR-499	0.852

Table 6. ROC Analysis in Type 1 MI Cohort. *Green font = best-performing biomarker; Red font = worst-performing biomarker. AUC, area under the curve; cMyBP-C, cardiac myosin-binding protein C; hs-cTnT, high-sensitivity cardiac troponin T. Reproduced from Schulte et al. Circ Res 2019*

6.2 Biomarkers For Assessing MI Subtypes

6.2.1 Clinical characteristics

We analysed a total of n=495 serial plasma samples across three time points i.e., on admission = baseline, 1h after admission and 3h after admission, respectively. This included n=318 serial measurements from patients with STEMI (n=31 patients), T1MI (n=26 patients), T2MI (n=31 patients), AI (n=18 patients) and n=177 sequential control samples from patients with non-cardiac chest pain (n=59 patients). Based on UDMI4, non-ischaemic cardiac conditions such as acute heart failure and Takotsubo cardiomyopathy are classified as AI (**Figure 41**). Baseline characteristics are shown in **Table 7.** Patients with T2MI and AI were older than patients with T1MI (p=0.022). AI was more common in females (p=0.015). Grace score for 6-months mortality was higher in T2MI and in AI (p=0.003) compared to T1MI (**Table 7**).

	AI (N=18)	T2MI (N=31)
Atrial Fibrillation	0	9 (29%)
Atrial Tachycardia	0	8 (26%)
Takotsubo CMP	8 (44%)	0
Heart Failure	5 (28%)	0
Hypertension	0	7 (23%)
AV Stenosis	2 (11%)	0
PE	3 (17%)	0
Prinzmetal	0	1 (3%)
VT	0	3 (10%)
Anaemia	0	1 (3%)
Embolus	0	1 (3%)
HOCM	0	1 (3%)

Figure 41. UDMI4 discharge diagnosis of Type 2 MI and acute injury. *Abbreviations – UDMI4: Fourth universal definition of myocardial infarction; AV: Aortic valve; PE: Pulmonary embolism, VT: Ventricular tachycardia; HOCM: Hypertrophic obstructive cardiomyopathy. AI = Acute Injury, T2MI = Type 2 MI. Reproduced from Schulte et al. J Mol Cell Cardiol Plus 2022*

BACC Clinical Characteristics	**All MI Patients (N=106)**	**Control (N=59)**	**STEMI (N=31)**	**T1MI (N=26)**	**T2MI (N=31)**	**AI (N=18)**	***P* value (T1MI vs T1MI)**	***P* value (T1MI vs AI)**
Demographics								
Sex (% Female)	34%	71%	16%	23%	45%	61%	0.101	**0.015**
Age (in Years)	66 (54, 75)	59 (50, 69)	65 (49.5, 68.5)	61 (52.3, 70.3)	73 (58.5, 78)	74 (64, 80.3)	**0.019**	**0.022**
BMI (Kg/m^2)	27.5 (24.6, 29.9)	26 (23.6, 27.7)	26.9 (24.8, 30.4)	28.3 (25.2, 29.2)	27.9 (25.7, 29.8)	24.8 (21.5, 28.0)	0.88	**0.037**
GRACE score (6-months mortality)	105.5 (79.3, 133)	81 (67.5, 105)	79 (60, 104)	93 (64.5, 118)	134 (103, 149.5)	122 (107.3, 145.5)	**0.0003**	**0.003**
Hypertension (%)	70%	47%	71%	62%	81%	61%	0.144	1.00

Hyperlipoproteinemia (%)	30%	27%	32%	42%	29%	11%	0.405	**0.043**
History of Smoking (%)	55%	39%	52%	81%	42%	44%	**0.003**	**0.023**
Comorbidities and baseline clinical parameters								
History of AMI (%)	17%	10%	16%	31%	13%	6%	0.117	0.060
Congestive Heart failure (%)	11%	2%	3%	8%	19%	17%	0.269	0.386
Stroke (%)	3%	5%	0%	0%	6%	6%	0.495	0.409
Atrial fibrillation (%)	18%	7%	10%	4%	42%	11%	**0.001**	0.558
Heart rate (/min)	82.5 (72.8, 101.3)	74 (64, 85)	78 (71, 87)	79 (68.3, 88.5)	97 (79, 130.5)	95 (80, 101)	**0.004**	**0.050**
Systolic blood pressure (mmHg)	150 (126, 164)	144 (136, 155)	150 (141, 170)	151 (137, 161)	140 (119, 158)	150 (125, 157)	0.147	0.970
Baseline medication								
Anti-platelet drugs (%)	39%	29%	33%	54%	42%	22%	0.431	0.061
Anti-hypertensive drugs (%)	56%	36%	43%	50%	81%	44%	**0.023**	0.767
ACE-I/ARB (%)	46%	27%	37%	42%	61%	39%	0.189	1.00
Beta Blocker (%)	39%	22%	27%	46%	61%	11%	0.294	0.021
Diuretics (%)	19%	12%	10%	12%	32%	22%	0.111	0.419
Calcium Channel Blocker (%)	13%	14%	10%	12%	16%	17%	0.715	0.676
Antidiabetics (%)	11%	7%	17%	12%	10%	6%	1.000	0.634
If Coronary Angiography: PCI (%)	67%	0%	100%	92%	0%	8%	**<0.001**	**<0.001**
Clinical cardiac biomarkers								
CK 0h (U/l)	154 (113, 222)	104 (72, 145)	193 (128, 345)	152.5 (104, 196)	142.5 (106, 178)	178 (129, 205)	0.628	0.397
CK 1h (U/l)	175	98	262	194	134	167.5	**0.047**	0.483

	(122, 292)	(69, 136)	(165, 571)	(147, 211)	(90, 182)	(135, 194)		
CK 3h (U/l)	222	91	510	261	142	165	**0.003**	0.075
	(137, 410)	(67, 128.5)	(239, 1182)	(178, 325)	(103, 205)	(126, 248)		
hs-TnT 0h (ng/L)	40	5	32	32	23	195	0.608	**0.0001**
	(16, 168)	(4, 7)	(16, 232)	(12, 89)	(13, 57)	(133, 377)		
hs-TnT 1h (ng/L)	92	5	184	78.5	36	287.5	**0.005**	**0.022**
	(42, 299)	(3.5, 7)	(95, 437)	(43, 198)	(26, 68)	(165, 440)		
hs-TnT 3h (ng/L)	178	5	519	213	78	307	**<0.001**	0.685
	(91, 517)	(4, 6)	(283, 1838)	(104, 546)	(42, 113)	(152, 502)		
hs-TnI 0h (ng/L)	68	3	108	50	22	1149	0.267	**0.0002**
	(18, 690)	(2, 5.5)	(22, 949)	(18, 263)	(10, 73)	(302, 2160)		
hs-TnI 1h (ng/L)	266	3	476	383	53	1045	**0.0008**	0.184
	(65, 1021)	(2, 4.3)	(206, 2459)	(112, 867)	(33, 211)	(155, 2306)		
hs-TnI 3h (ng/L)	1072	3	4775	2198	241	1902	**<0.001**	0.952
	(286, 4288)	(2, 5)	(1423, 26461)	(482, 4746)	(52, 525)	(845, 3358)		

Table 7. Baseline Characteristics: STEMI vs. NSTEMI Type 1 (T1MI) vs. NSTEMI Type 2 (T2MI) vs. acute myocardial injury (AI). *Continuous variables are presented as median (25th and 75th percentile). P value computed for NSTEMI Type1 (T1MI) vs NSTEMI Type2 (T2MI) and NSTEMI Type1 (T1MI) vs Acute Injury (AI) using Mann-Whitney test for continuous variables and Fisher exact test for binary variables. Abbreviations: MI: Myocardial infarction; T1MI: NSTEMI type1; T2MI: NSTEMI type2; AI: Acute Injury; GRACE: Global Registry of Acute Coronary Events; CK: creatine kinase; hs-TnT: high-sensitivity Troponin T; hs-TnI: high-sensitivity Troponin I. Reproduced from Schulte et al. J Mol Cell Cardiol Plus 2022*

6.2.2 Protein release kinetics

Baseline measurements of cTnI, cTnT and cMyBP-C were not different between T1MI and T2MI (**Figure 42**). All cardiac necrosis markers showed significant differences between T1MI and T2MI at 3h after admission (**Figure 42**). The release kinetics of NT-proBNP also did not show discriminative ability between T1MI and T2MI (**Figure 42**). cTnT differentiated AI from T1MI, albeit only on admission (**Figure 42**). However, NT-proBNP levels remained higher in AI than T1MI at all time points (**Figure 42**). hsTnT showed discriminative power for AI versus T2MI at all time points **(Figure 42)**. Pairwise statistical comparison of hsTnT and NT-proBNP at each time point for MI subtypes and control patients with non-cardiac chest pain is presented in **Figure 43.** Box plots include hsTnT and NT-proBNP values in STEMI patients for reference.

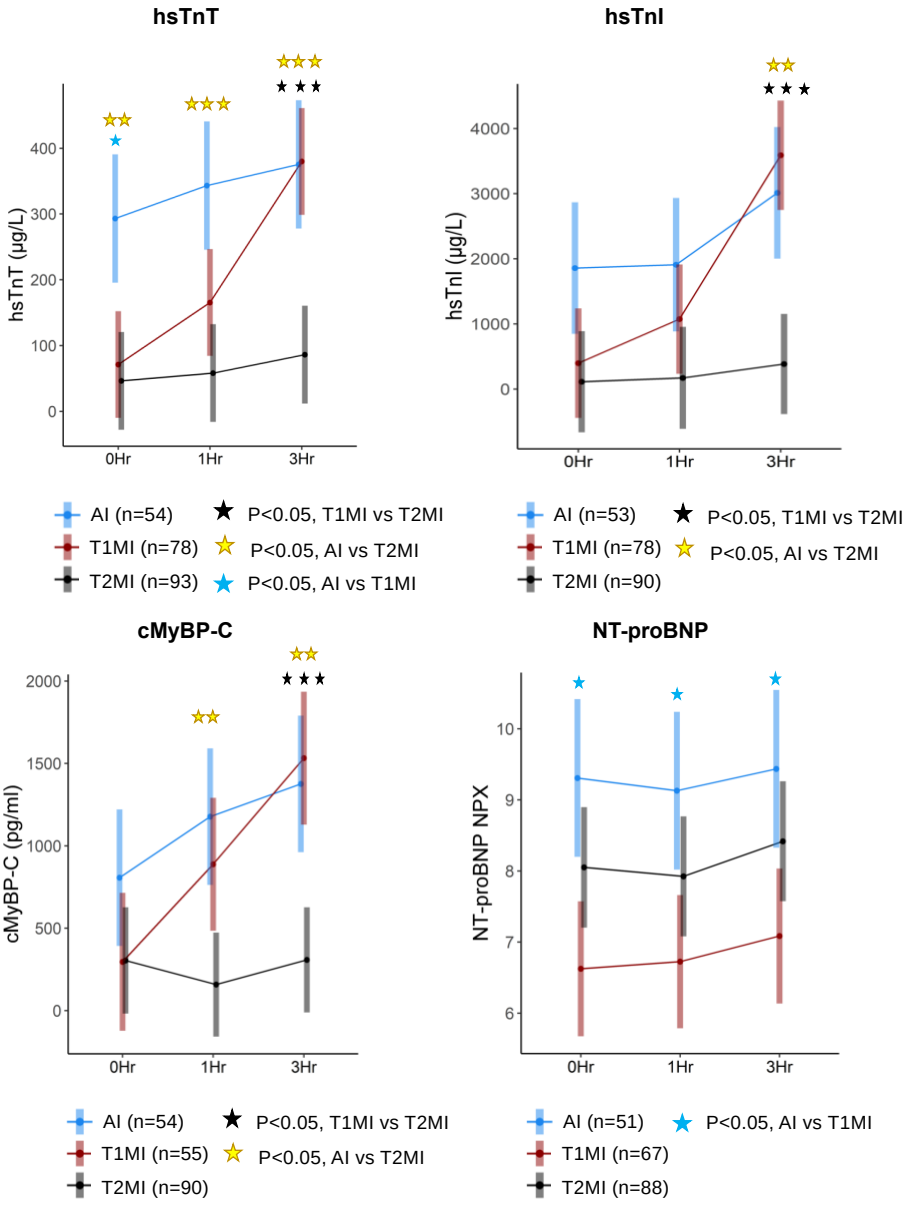

Figure 42. Protein kinetics in MI subtypes using linear mixed effects model. *Y-axis shows fitted value using linear mixed effects regression (lmer). X-axis shows sampling time in hours. Interaction style plots were generated using R package 'emmip' with dots in the plot indicating the estimated marginal mean i.e., mean adjusted for individual random effect for within subject variance and lines show the 95% confidence interval. n numbers indicate the serial measurements quantified across the 3 time points for each of the MI subtypes. Satterthwaite degrees-of-freedom method was used. Contrasts were generated using R package 'emmeans'. P values were adjusted using Tukey's method for comparing a family of 9 estimates. * P value<0.05 , **<0.01 and *** <0.001. MI: Myocardial infarction; AI: Acute Injury; T1MI: NSTEMI Type1; T2MI: NSTEMI Type2; NPX: Normalized Protein eXpression, Olink's® arbitrary unit in Log2 scale. hsTnT: high-sensitivity cardiac Troponin T; hsTnI: high-sensitivity cardiac Troponin I; cMyBP-C: cardiac myosin-binding protein C; NT-proBNP: N-terminal pro-brain natriuretic peptide. Reproduced from Schulte et al. J Mol Cell Cardiol Plus 2022*

6.2.3 Kinetics of miRNAs

miRNAs with cardiac and muscle origin as well as plasma miRNAs previously associated with cardiovascular diseases (CVD) (**Table 8**) were quantified in the 495 samples from all three time points. The selection of miRNAs was based on 1) known tissue origin (in particular cardiac/muscle vs circulating cells or other organs) and 2) detectability in the circulation.

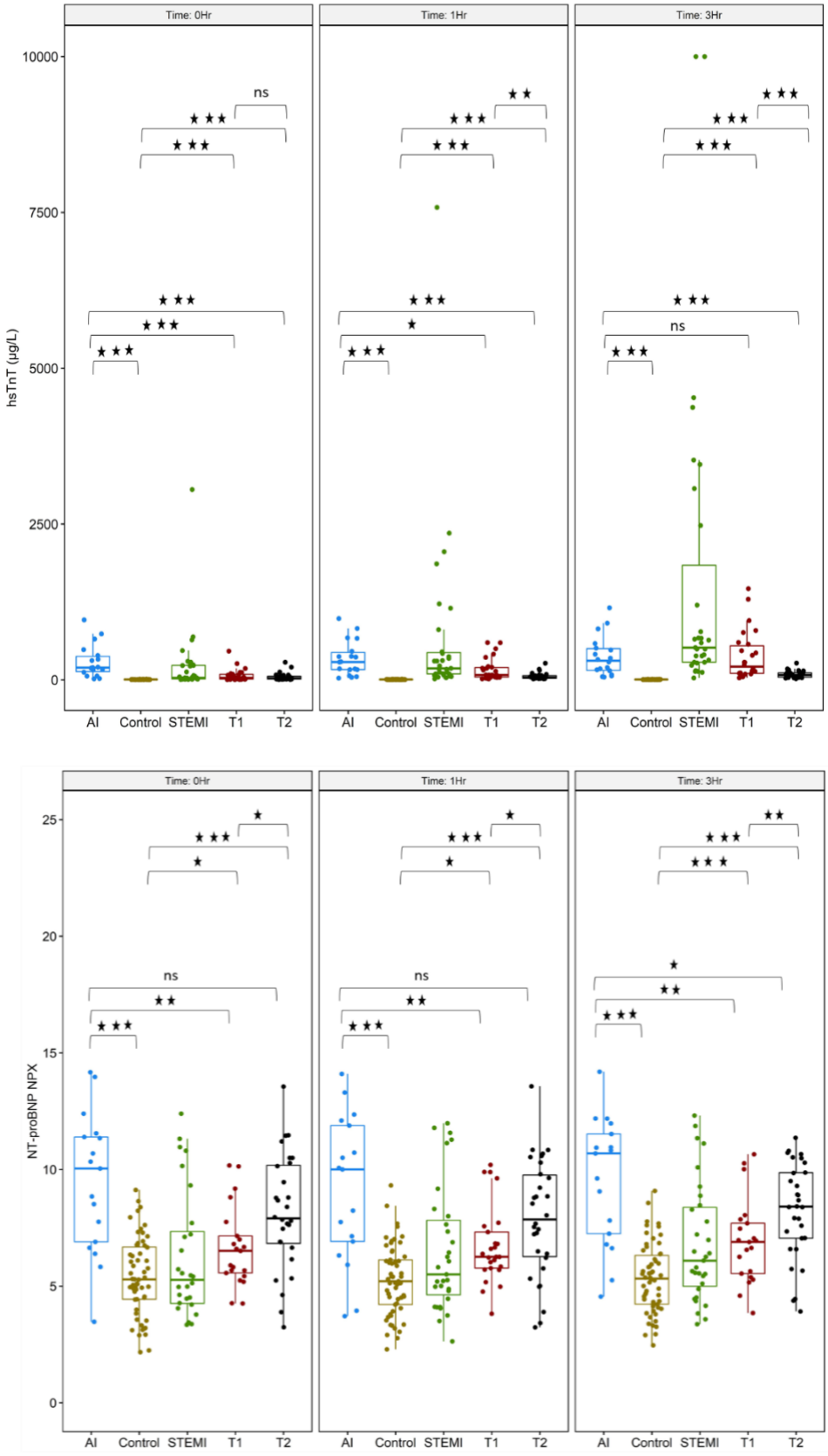

Figure 43. Comparison of release kinetics of all MI subtypes. *hsTnT (n=493) and NT-proBNP (n=467) box plots with visual summary of the data including median, first quartile (Q1), and third quartile (Q3). Pairwise statistical comparison done using Mann-Whitney test for Control vs AI, AI vs T1MI, AI vs T2, Control vs T1MI, Control vs T2, T1MI vs T2. Values for STEMI are shown as reference. Stars indicate P value: * for <0.05 ** for <0.01 and *** for <0.001. Abbreviations – ns: not significant; AI: Acute Injury; T1MI: NSTEMI type1; T2: NSTEMI type2. Reproduced from Schulte et al. J Mol Cell Cardiol Plus 2022*

miRNA	Tissue association	CVD biomarker
miR-1	Muscle – cardiac/skeletal [98]	MI [19]
miR-21	Platelets [99]	Fibrosis [19]
miR-122	Liver [100]	Card. Shock [19]
miR-126-3p	EC, Platelets [99][101]	CVD risk [19]
miR-133a	Muscle – cardiac/skeletal [98]	MI [19]
miR-150	Leukocytes, Platelets [99]	CVD risk [19]
miR-197	Platelets [102]	CVD risk [50]
miR-208	Muscle – cardiac [103]	MI [19]
miR-223	Platelets [99]	CVD risk [19]
miR-499a	Muscle – cardiac [104]	MI [19]

Table 8. miRNAs quantified in plasma of MI patients and controls. *The selection of miRNAs was based on 1) known tissue origin (cardiac/muscle vs circulating cells or other organs) and 2) detectability in the circulation. EC = Endothelial cell; MI = myocardial infarction; miRNA = microRNA. Reproduced from Schulte et al. J Mol Cell Cardiol Plus 2022*

Compared to STEMI, cardiac-specific (miR-208 and miR-499) and muscle-enriched miRNAs (miR-1 and miR-133a) were less well detectable in NSTEMI. Detectability for cardiac-specific miR-208 and miR-499 was <50%, even at 3h. Correlation analysis revealed clustering of muscle-enriched miRNAs

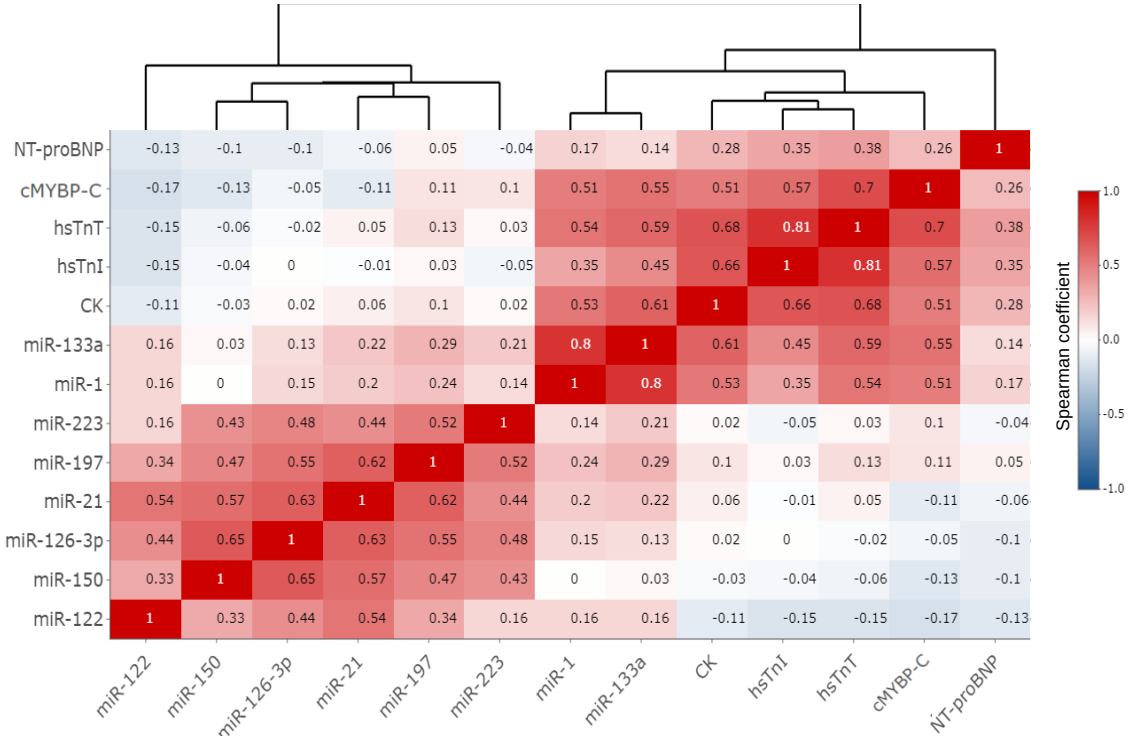

Figure 44. Correlation of protein and miRNA biomarkers. *The pairwise Spearman correlation was calculated between proteins and miRNAs adjusted for individual effects (repeated measure). Hierarchical clustering analysis and heatmap matrix illustrates positive and negative co-expression and clusters. Red and blue colours indicate a positive and negative correlation, respectively (P value < 0.05). White indicates no significant correlation (P value >0.05). P values were adjusted using the Benjamini-Hochberg FDR correction. Reproduced from Schulte et al. J Mol Cell Cardiol Plus 2022*

with cardiac necrosis markers in NSTEMI (**Figure 44**), consistent with our previous study in STEMI [8].

However, release kinetics of miR-1 and miR-133a did not offer discrimination between T1MI, T2MI and AI (**Figure 45)**. Other abundant plasma miRNAs clustered together (**Figure 44**) but their release kinetics also failed to discriminate T1MI, T2MI and AI (**Figure 45).**

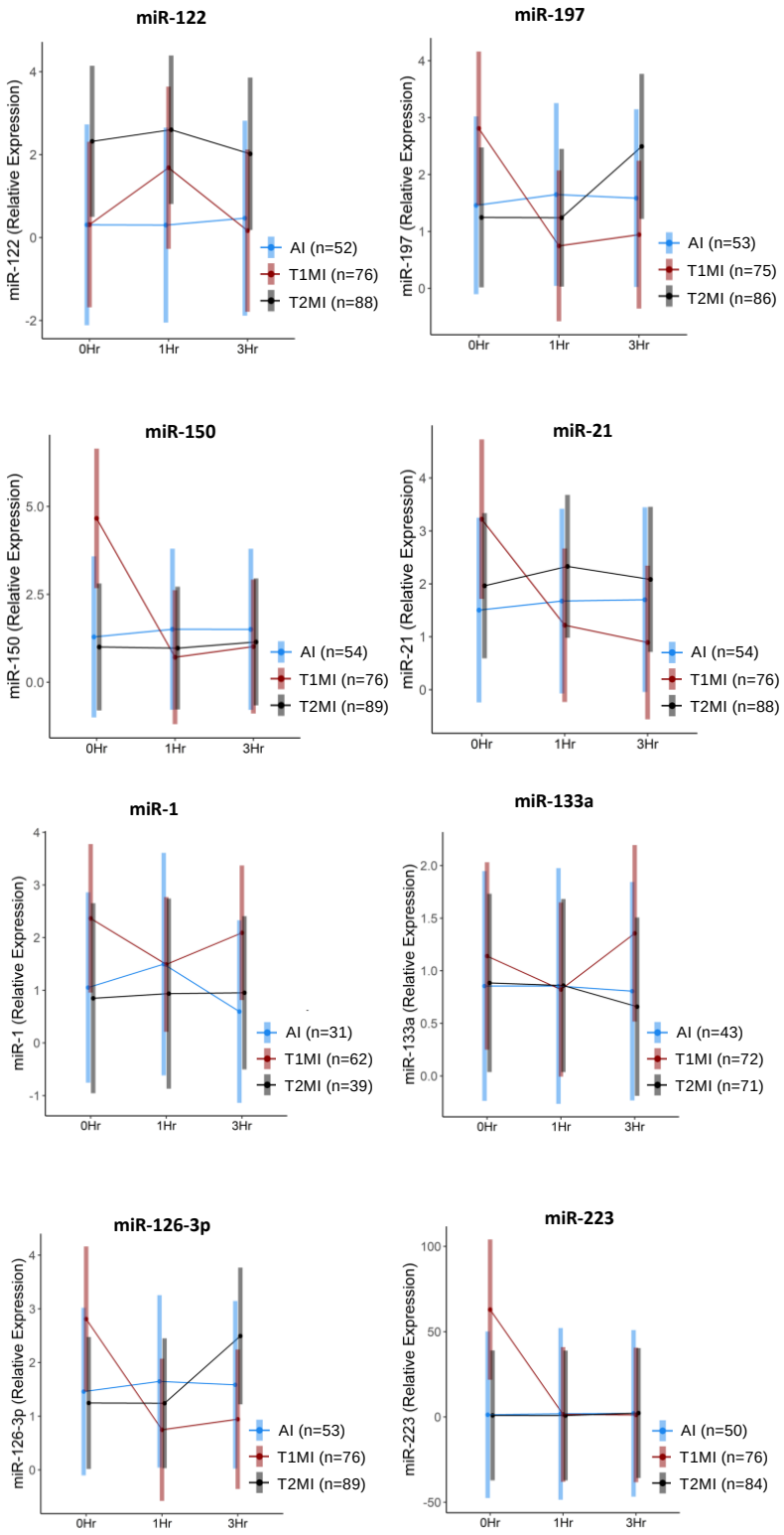

Figure 45. Circulating miRNA kinetics using linear mixed effects model. *Y-axis shows fitted value using linear mixed effects regression (lmer). X-axis shows sampling time in hours. Interaction style plots were generated using R package 'emmip' with dots in the plot indicating the estimated marginal mean i.e., mean adjusted for individual random effect for within subject variance and lines show the 95% confidence interval. n numbers indicate the serial measurements quantified across the 3 time points for each of the MI subtypes. Satterthwaite degrees-of-freedom method was used. Contrasts were generated using R package 'emmeans'. P value shows adjusted value using tukey method for comparing a family of 9 estimates. Significance stars for P value: one star for <0.05 , two for <0.01 and three for <0.001. MI: Myocardial infarction; AI: Acute Injury; T1MI: NSTEMI Type1; T2MI: NSTEMI Type2. Reproduced from Schulte et al. J Mol Cell Cardiol Plus 2022*

6.2.4 Combining NT-proBNP with cardiac necrosis markers in T1MI, T2MI and AI.

Given the distinct release kinetics of cardiac necrosis markers and NT-proBNP, we analysed their biomarker potential in a combinatorial approach. The scatterplot of hs-TnT and NT-proBNP displays how a combination of hs-TnT and NT-proBNP separates MI patients into T1MI (high hs-TnT, low NT-proBNP), T2MI (low hs-TnT, high NT-proBNP) and AI (high hs-TnT and high NT-proBNP) (**Figure 46A**). This discrimination is also apparent in the individual kinetics of hs-TnT and NT-proBNP (**Figure 42**). Hence, the integrated signature of hs-TnT, NT-proBNP and age was compared to standalone signatures of 'hs-TnT, age' and 'NT-proBNP, age' using one-vs-all multi-class random forest model in a leave-one-out cross validation with bootstrapping (**Figures 46B and 47)**.

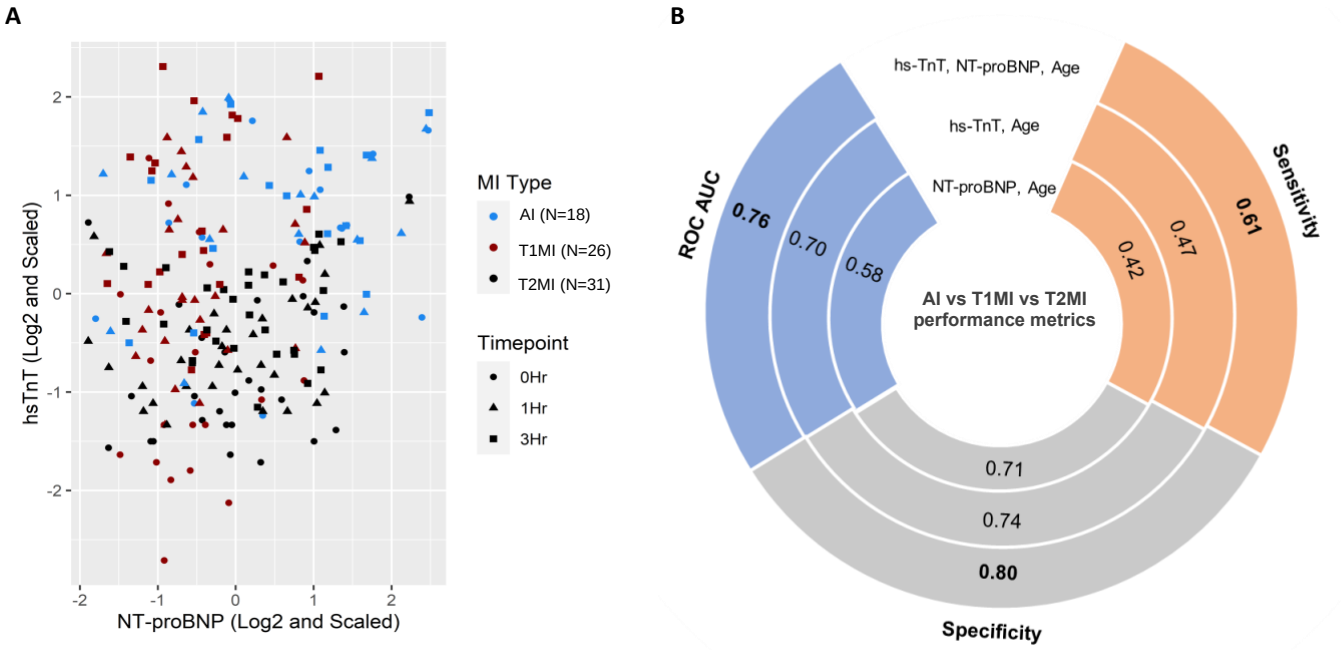

Figure 46. Discriminative value of hsTnT and NT-proBNP to differentiate T1MI, T2MI and AI. A*. Scatterplot for hs-TnT and NT-proBNP illustrates the ability of combined biomarkers in clustering T1MI (high hs-TnT, low NT-proBNP), T2MI (low hs-TnT, high NT-proBNP) and AI (high hs-TnT and high NT-proBNP). Legends shown are in combination of shape (triangle, square and circle) for timepoints and color (red, blue, black) for MI subtypes. For example, a blue square denotes AI at 3hr while a red square indicates T2MI at 3hr.* ***B.*** *Sensitivity, specificity and ROC AUC comparing predictive power of biomarkers in discriminating T1MI, T2MI and AI. ROC AUC of 0.58 with 'NT-proBNP, age' was inferior compared to ROC AUC of 0.76 with the combined signature of 'hs-TnT, NT-proBNP, age'. The low sensitivity (high false negatives) of 0.47 with 'hs-TnT, age' and 0.42 with 'NT-proBNP, age' makes these signatures unsuitable in discriminating T1MI, T2MI and AI. The combined signature of hs-TnT, NT-proBNP and age returned an overall AUC of 0.76 for discriminating T1MI, T2MI and AI with a more balanced overall sensitivity of 0.61, outperforming measurements of either hs-TnT or NT-proBNP alone. Abbreviations - ROC AUC: Receiver operating characteristic area under the curve; AI: Acute Injury; T1MI: NSTEMI Type1; T2MI: NSTEMI Type2. Reproduced from Schulte et al. J Mol Cell Cardiol Plus 2022*

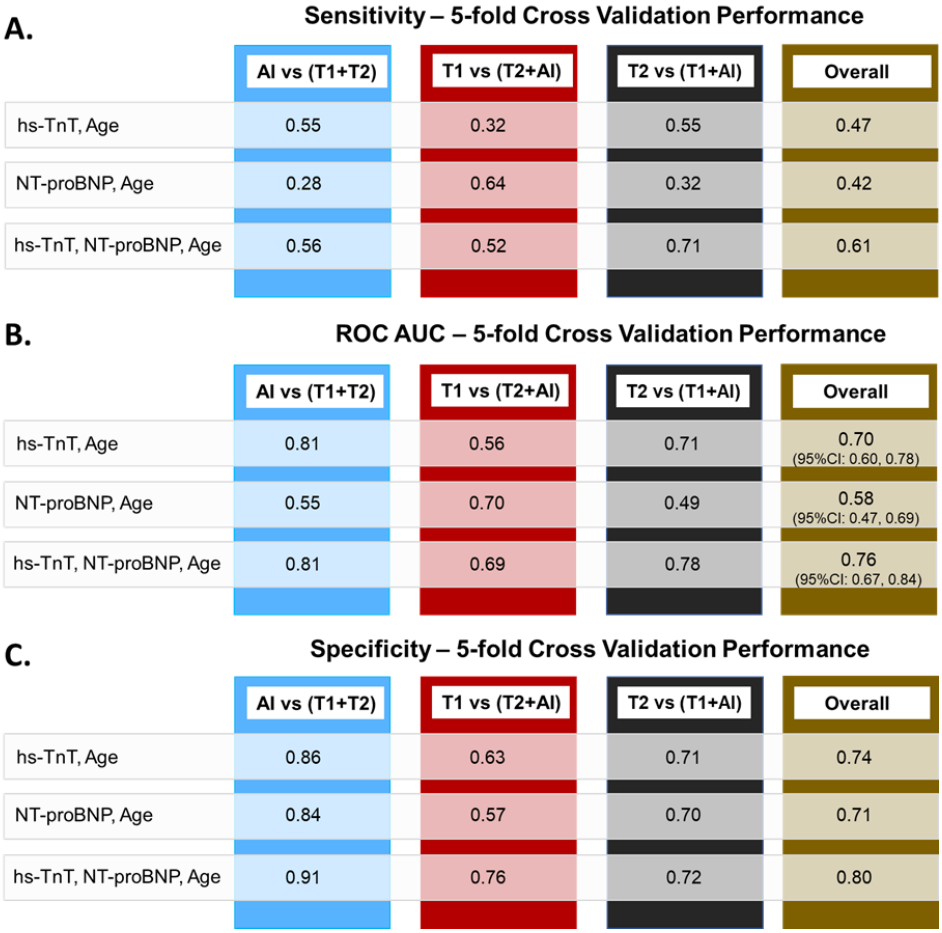

Figure 47. Sensitivity (A), ROC AUC (B) and specificity (C) comparing the predictive power of biomarkers in discriminating T1MI, T2MI and AI*. Performance metrics were computed using one-vs-all comparison with weightage to account for data imbalance. Each of the three one-vs-all and the overall performance metrics is shown. Abbreviations - ROC AUC: Receiver operating characteristic area under the curve; AI: Acute Injury; T1: NSTEMI Type1; T2: NSTEMI Type2. Reproduced from Schulte et al. J Mol Cell Cardiol Plus 2022*

One-vs-all comparison was undertaken for T1MI, T2MI and AI, thus presenting not only the overall performance of the model but also the comparative performances for T1MI vs (T2MI +AI), T2MI vs (T1MI+AI) and AI vs (T1MI+T2MI). Sex as a feature was not supported by Boruta feature selection. Hence, only age was retained in the prediction signature with individual and combination biomarkers. The AUC of 0.58 [95%CI: 0.47-0.69] with 'NT-proBNP, age' was inferior compared to the combined signature of 'hs-TnT, NT-proBNP, age', AUC 0.76 (**Figures 46B and 47B**). Further, the low sensitivity (high false negatives) of 0.47 with 'hs-TnT, age' and 0.42 with 'NT-proBNP, age' makes these signatures unsuitable in discriminating T1MI, T2MI and AI (**Figures 46B and 47A**). The combined signature of hs-TnT, NT-proBNP and age returned an overall AUC of 0.76 [95%CI: 0.67-0.84] for discriminating T1MI (AUC: 0.69), T2MI (AUC: 0.78) and AI (AUC: 0.81) with a more balanced overall sensitivity of 0.61, outperforming measurements of either hs-TnT or NT-proBNP alone (**Figures 46B, 47 and 48**).

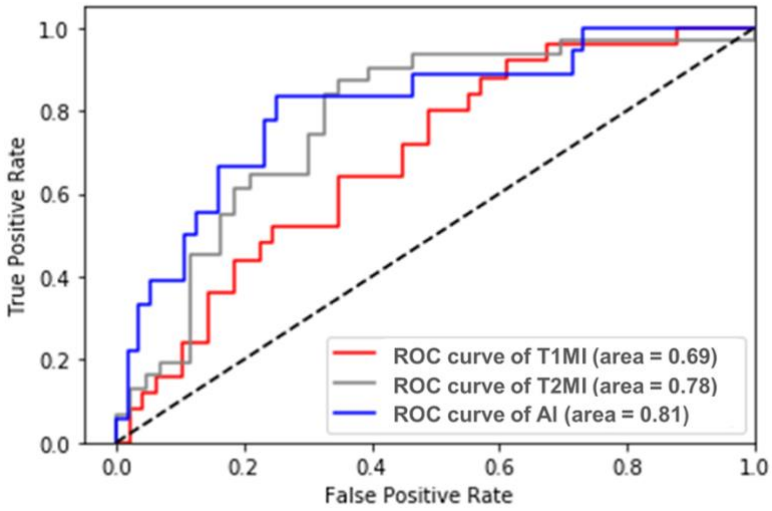

Figure 48. ROC curves for the discrimination of T1MI, T2MI and AI. *The majority vote multi-class random forest classifier used an average prediction probability of 0.52 for T1MI and T2MI, and 0.55 for AI. Abbreviations - T1MI: Type 1 myocardial infarction; T2MI: Type 2 myocardial infarction; AI: Acute injury. Reproduced from Schulte et al. J Mol Cell Cardiol Plus 2022*

7 DISCUSSION

ncRNAs are a novel entity of promising circulating biomarkers. In CVD, ncRNAs have been suggested as potential valuable prognostic as well as diagnostic biomarkers. Thus far, most attention has focused on miRNAs although new classes of ncRNAs have been identified in the circulation [105,106]. In addition to miRNAs, we assessed the potential of selected lncRNAs and circRNAs to serve as biomarkers of myocardial injury. To the best of our knowledge, no study has directly compared these classes of ncRNAs with cardiac protein biomarkers. Using heparinase-treated samples, we assessed the release of ncRNAs after TASH in a well-controlled context of myocardial injury and of miRNAs in the most relevant clinical setting of MI cases presenting with low initial cTn values. We further extended our studies to compare the discriminative ability of ncRNAs and protein biomarker trajectories for MI subtypes including AI. Measurements of established and novel protein biomarkers alongside miRNA-based biomarker candidates were performed at three serial time points: on admission, after 1h and after 3h. We then applied linear mixed effects model to compare patient subgroups and biomarker kinetics. Finally, we harnessed machine learning methods to combine independent biomarkers and identify the best serial biomarker combination in discriminating T1MI, T2MI and AI.

7.1 HEPARINASE TREATMENT TO OVERCOME CONFOUNDING BY HEPARIN

Heparin inhibits qPCR-based ncRNA quantitation [45]. Confounding by heparin is evidenced by decreased detectability, higher variation or spurious correlations of ncRNA measurements. Recent data reporting heparin to interfer with RNA detectability, focused on miRNAs [45,77]. But also mRNA [107] as well as DNA [108] quantification is hampered by the presence of heparin in the samples, indicating that the detrimental effect of heparin on RNA and DNA quantification is independent of the RNA species. Indeed, the heparin effect is based on an interference of the large, negatively charged heparin molecule (polyanion) with any type of RNA/DNA, which then leads to a strong inhibitory effect on DNA and RNA polymerase, directly affecting the reverse transcription process [108,109]. Thus, it is apparent that the inhibitory effect of heparin on DNA/RNA quantification is caused by the dependency of the RT and RT-qPCR on the required enzyme – polymerase, which is independent of the RNA species. Therefore, it can be assumed that any type of RNA quantification based on RT-qPCR (including lncRNAs and circRNAs) will be affected by the presence of heparin. Given the poor detectability of muscle-/cardiac miRNAs in healthy individuals, their assessment in the controlled heparin experiment is not possible. Apart from endogenous miRNAs, heparin predominantly affects the quantification of the exogenous *Cel-miR-39* spike-in control. As pointed out previously [110], the inter-sample deviation of *Cel-miR-39* measurements should be less than 1 cycle. However, within the first hour after administration of the heparin bolus, the detectability of *Cel-miR-39* decreases and can span up to 4 cycles. This variability is related to the half-life of heparin in the circulation. Most publications

assessing miRNAs in patients with MI failed to address this important confounding factor (**Table 2**). If unnoticed, heparin-induced suppression of the *Cel-miR-39* normalisation control results in spuriously higher levels of endogenous miRNAs, especially within the first hour after heparin administration (**Figure 20**). Heparinase treatment can overcome the confounding introduced by heparin in samples from MI patients [47]. This is the first study in which heparinise-treatment was performed in an MI cohort prior to ncRNA quantification. Our analyses of miRNAs in MI patients returned substantially higher correlation coefficients with cTn than previous publications that did not use heparinase [47].

7.2 NCRNAS AND PROTEIN BIOMARKERS IN TYPE 1 MI

Assays for cTnI and cTnT are the gold standard for detection of myocardial injury [111]. The excellent sensitivity of these assays is the result of decades of optimisation [9,112]. Using proteomics, the Mayr lab has previously identified a new cardiac biomarker, cMyBP-C. cMyBP-C may allow for an earlier detection and better rule-in/rule-out of MI [14,15]. In this study, cMyBP-C detected myocardial injury with a higher accuracy than hs-cTnT and hs-cTnI in the controlled TASH model. This finding is supported by a steeper rise within the first hour after TASH and in all time intervals (0h to 1h, 1h to 3h) in the MI cohort. cMyBP-C showed a higher detectability among control patients compared with hs-cTnT (100% vs. 85% respectively). A possible explanation for this advanced detectability could be the fact, that cMyBP-C is released from cardiomyocytes and detected in the circulation as a proteolytic fragment, potentially accelerating its release as opposed to a larger, intact protein. On the other hand, ROC analysis in the validation cohort of MI revealed lower AUC for cMyBP-C compared with hs-cTnT (0.898 vs. 0.925). This finding is most likely attributable to two factors: First, as opposed to TASH, the diagnosis of MI was adjudicated based on hs-cTnT and secondly, the selection of the MI patients from the BACC cohort was determined by initially low and then steeply rising hs-cTnT levels. Importantly, cMyBP-C has been reported as more sensitive compared with cTn [15]. This is supported by our finding that cMyBP-C shows a steeper rise in the first hour after onset of myocardial injury. The better detectability of cMyBP-C in controls also suggests that cMyBP-C might be a biomarker for cardiac disease in non-acute settings.

In addition to cardiac proteins, miRNAs offer a new opportunity for the detection of myocardial injury. The muscle-enriched miRNAs, miR-1 and miR-133a, have been implicated as markers for myocardial injury but are not specific for the heart. In contrast, miR-499 and miR-208a/b have higher cardiac specificity but are less abundant in heart and in plasma [32]. By spiking plasma with human myocardial tissue, we demonstrate that qPCR assays for ncRNAs detect the presence of smaller amounts of myocardial tissue than cardiac proteins. The regression curves for ncRNAs compared to protein biomarkers indicated a potentially higher sensitivity of qPCR-based measurements of ncRNAs. In a tightly controlled clinical setting of induced myocardial injury after TASH, muscle- and cardiac-enriched miRNAs showed an earlier rise than hs-cTn, which was similar to the release kinetics of

cMyBP-C (**Figure 21** and **Figure 26A, B**). To exclude that this difference is due to the mode of measurement, we also performed additional cTnI measurements with PEA, which combines antibody-based detection with qPCR-based quantification. Another important aspect for biomarker performance is the clearance of cardiac proteins and miRNAs from the circulation. Similar to cMyBP-C, miRNA levels peaked at 8h and declined or plateaued thereafter. In contrast, hs-cTnT concentrations were still rising at 24h after TASH. While single miRNAs failed to outperform cardiac protein biomarkers in detecting early MI, a multi-biomarker combination of two muscle-enriched miRNAs with hs-cTnT and cMyBP-C returned the highest predictive power for the detection of MI in a subcohort of the BACC study. This was consistent across different aetiologies of myocardial injury (STEMI and NSTEMI type 1). While the biomarker selection and their ranking did not change, the overall performance of the prediction model was largely dependent on infarct severity.

7.2.1 miRNAs

7.2.1.1 Cardiac and Muscle-enriched miRNAs

Although cardiac and muscle-enriched miRNAs have been previously studied as biomarker candidates for myocardial injury, our findings in heparinase-treated samples highlight important aspects that to our knowledge have not been addressed so far. First, the muscle-enriched miRNAs, miR-1 and miR-133a are more readily detectable at baseline. miR-1 and miR-133a are enriched in skeletal muscle and in cardiac muscle. The reason why we refer to them as 'muscle' miRNAs is that they are much more abundant in skeletal muscle than in cardiac muscle [26]. Taking into account the larger mass of skeletal muscle in the body compared with cardiac muscle mass, this is most likely also the reason why these miRNAs are better-detectable in healthy controls. miR-208 and -499 reach detectable values only at higher corresponding hs-cTnT values [26]. On the other hand, cardiac miRNAs are more specific for myocardial injury. They correlate best with hs-cTnT and predict myocardial injury better in the TASH cohort and as well as hs-cTnT in the MI cohort. miR-208 and miR-499 are more abundant in the heart and their expression in the skeletal muscle is so low, that they can be referred to as being (almost) cardiac-specific. This is further reflected in their detectability in healthy controls, which is extremely low – comparable to hs-cTnT/I and cMyBP-C. The differences in the specificity for the heart muscle is further validated in the correlation of these miRNAs with cardiac specific proteins (**Figure 28**). While miR-208 and miR-499 correlate with hs-cTnT similar to hs-cTnI and cMyBP-C, the correlation of miR-1 and miR-133a is substantially weaker. This is in consistent with previous reports of miR-208 and miR-499 being elevated in plasma only in cases of MI or myocardial injury, while miR-1 and miR-133a can rise in different cardiac pathologies [27,113]. In a ROC analysis of the TASH cohort, cardiac-enriched miRNAs returned higher AUC values than muscle-enriched miRNAs. Secondly, cardiac miRNA measurements in patients with MI reached the detection limit of Cq<35 cycles only at high hs-cTnT values (>50-100ng/L). Thus, miRNAs failed to identify patients with MI that initially present

with low or negative cTn values. A critical evaluation of publications is required as lower thresholds of detection may have been used in some studies, especially when confounding by heparin was not taken into consideration (**Table 2**). Given their favourable release kinetics, this shortcoming of cardiac miRNA biomarkers might be attributed to the low miRNA yield from plasma, miRNA degradation after release into circulation and inadequate detection methods compared to high-sensitivity protein assays.

7.2.1.2 Non-Cardiac and Muscle-enriched miRNAs

The remaining 7 miRNAs were selected upon their good detectability in the circulation on the one hand and the fact that they had previously been described to be associated with MI – although not muscle/cardiac-enriched. For the first time, we present data (**Figure 16**) refuting dysregulation of these miRNAs after MI. Thus, changes in their circulating levels are not caused by cardiac release but rather by a systemic response, which questions their potential as early biomarkers for myocardial injury. This is consistent with the lack of a rise of non-cardiac and muscle-enriched miRNAs with increasing spike-in concentrations of cardiac tissue. These miRNAs may well be dysregulated after MI, but the patho-mechanism seems to differ from cardiac release, as we see in muscle/cardiac miRNAs. A large number of these miRNAs is highly abundant in circulating cells such as platelets [86] and leukocytes [114]. The fact that these miRNAs indeed are detectable in cardiac tissue but are not contributing to higher quantification when spiked into plasma is most likely caused by their high abundance in plasma on the one hand and the comparably small amounts present in cardiac tissue on the other. In this respect the lack of tissue-specificity hampers the utilisation of these miRNAs as early biomarkers for myocardial injury. On the other hand, being generally dysregulated after MI hints at their potential as biomarkers in MI subtypes with more systemic responses such as T2MI.

7.2.2 lncRNAs

LncRNAs are a heterogenous group of RNAs >200 nucleotides in length [52]. Unlike miRNAs, lncRNAs are mainly located within the nucleus or in mitochondria [28,53]. Regardless, lncRNAs are readily detected in the circulation. This either indicates the presence of protective mechanisms against RNase-mediated degradation similar to those of miRNAs [52] or an abundant source with constant release.

LIPCAR was found to predict adverse cardiac remodeling and death in the aftermath of MI [28]. LIPCAR has been proposed as a biomarker of cardiac disease. However, the cardiac origin of this lncRNA in plasma has not been confirmed. In our experiments, LIPCAR showed a comparable regression curve to cardiac miRNAs in the myocardial tissue spike-in and good detectability in plasma. LIPCAR levels, however, did not increase after TASH, refuting a cardiac origin. Since LIPCAR is of mitochondrial origin and ubiquitously expressed, it seems likely that other cells and tissues contribute to circulating LIPCAR levels, such as platelets, leukocytes and erythrocytes [115], rather than myocardial injury. Given our findings of absent lncRNA plasma elevation up to 24 hours after TASH,

it seems unlikely that cardiac tissue is a major source of circulating lncRNAs. Furthermore, Thum and colleagues demonstrated a down-regulation of LIPCAR 5 days after MI but an upregulation after 1, 3 months and 1 year in patients with cardiac remodeling [28]. Given their underlying clinical assessments, the authors' suggestion that LIPCAR is of cardiac origin is counter-intuitive, at least in our opinion. An increase in plasma levels of LIPCAR as a *cardiac-derived* molecule in a subsequent chronic state seems highly unlikely if there is no detectable release upon severe myocardial injury. In a second publication, Thum and colleagues have found that '*time since diagnosis of diabetes, plasma fasting insulin, HDL-C and ultra-sensitive-CRP, … were significantly associated with circulating LIPCAR levels*' [116] in type 2 diabetes mellitus patients, indicating a more systemic response to an underlying condition, instead of a cardiac-specific release, which would concur with our data. In our experiments we found LIPCAR plasma levels to be detectable at quantification cycle (Cq) levels around 25-28 cycles, which is an indicator for high abundance in the circulation and comparable with i.e. miRNAs enriched in circulating cells such as platelet-enriched miR-126 (Cq 25-27), miR-223 (Cq 22-27) or leucocyte-enriched miR-150 (Cq 26-30). These levels are not directly comparable but provide an approximation to the abundance of circulating, cell-derived ncRNAs. Secondly, we offer data for LIPCAR's detection in myocardial tissue on a plasma matrix. Whilst LIPCAR increased in a linear fashion in our spike-in experiment of myocardial tissue, the concentration of myocardium used in this experiment (0.025-0.25ug/ul) is orders of magnitude higher than that generated in MI, which is precisely why we undertook further validation in TASH. There is no doubt that LIPCAR is detectable in myocardial tissue, but it is also, unsurprisingly, detectable in other cell types. For example, we have quantified LIPCAR in isolated circulating platelets (Cq 16-18), in leukocytes (Cq 17-19) and in erythrocytes (Cq 21-23) (**Figure 49**), confirming their high LIPCAR content.

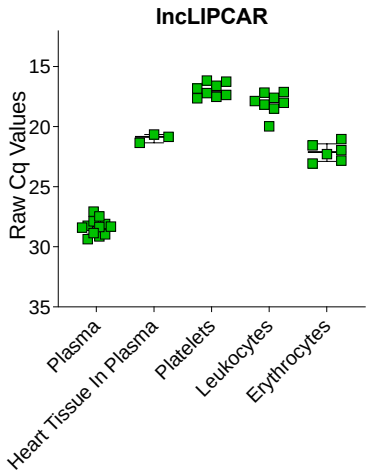

Figure 49. Raw Cq values of LIPCAR in plasma, heart tissue in plasma and circulating cells. *Despite the high concentration of heart tissue spiked into human plasma, LIPCAR levels are several magnitudes higher in isolated platelets and leukocytes. Reproduced from Schulte et al. Circ Res 2019*

The exclusive contribution of the myocardium to plasma levels of LIPCAR is therefore refuted. Haematopoietic cell turn-over, cell activation and haemolysis, especially during the conditions of

plasma generation from whole blood, could provide alternative explanations for the high abundance of circulating mitochondrial lncRNAs – such as LIPCAR. The fact that LIPCAR is readily detectable at baseline even in patients without myocardial injury argues for another abundant source. This explanation can be generalized to other ncRNA species. Human platelet turnover is on average 100bn platelets/day [117,118] and erythrocytes are produced at roughly 200 bn cells/day. Not all circulating cell content is shed into the circulation *in vivo.* However, even taking into account the smaller size of circulating cells compared with cardiomyocytes, myocardial injury may not be sufficient to result in a significant plasma contribution of circulating ncRNA contents if the transcript of interest is ubiquitously expressed and highly abundant in other cells. In contrast, cardiac- and muscle-enriched miRNAs show low baseline levels and the expected rise upon cardiomyocyte death alongside cardiac specific protein biomarkers.

To further exemplify this issue, recently, two circulating lncRNAs (lncRNA ZFAS1 and lncRNA CDR1AS) were discovered as independent predictors for MI [119]. However, since the lncRNAs were derived from whole blood, their origin or mechanistic link to MI remain unclear. Furthermore, lower levels of lncRNA HOTAIR were found in plasma of MI patients [120] and were described to be cardio-protective through interacting with miR-1. Nevertheless, lower levels of a lncRNA after MI again question its cardiac origin. It is a common misconception that circulating ncRNA changes in disease are related to the diseased tissue. In many cases, these reflect secondary changes, i.e. due to medication, inflammatory responses, or differences in sampling (peripheral venous blood versus arterial blood collected during coronary angiography). Besides the abovementioned lncRNAs, additional transcripts have been suggested as potential circulating biomarkers in CVD [52,121,122].

7.2.3 circRNAs

circRNAs are expressed in a tissue- and developmental-specific manner and can either emerge from exons or introns of pre-mRNA and are products of alternative splicing known as ‘backsplicing’ [29]. circRNAs have diverse functions [65,66] and are tissue-specific [31]. Sequencing data revealed the presence of more than 15,000 circRNAs in the human heart, some in high abundance [30]. circRNAs have previously been implicated in MI-related apoptosis [70].

circRNAs have been described as circulating biomarkers in the field of oncology [123]. In our study, circRNAs in plasma showed poor detectability despite high abundance in cardiac tissue. Also, circRNAs did not show a rise in plasma after myocardial injury. While circRNAs are supposedly less prone to degradation compared with their linear transcripts [62], this may differ in the circulation where circRNAs have been described as having a short half-life [62]. Thus, cardiac circRNAs were not well detectable in plasma and serum. Our sequencing data revealed the presence of more than 15,000 circRNAs in the human heart, some in high abundance [30]. While intron-derived circRNAs are primarily found in the nucleus [65], the majority of circRNAs, in particular those with exonic origin (**Figure 2**), are located in the cytoplasm [69]. This may increase the likelihood of their early release

into the circulation upon myocardial injury. Some studies have also described a mechanistic role for cardiac circRNAs in MI-induced apoptosis [70,71]. When evaluating circRNAs as potential biomarkers for acute MI [3], several candidate circRNAs, that we found well detectable in cardiac tissue, were undetectable in cell-free plasma or serum even after extensive myocardial injury such as TASH. Other reports implicate circulating circRNAs as biomarkers for CVD in less acute settings [72,73]. Interestingly, the authors did not use plasma or serum samples but instead used RNA isolated from whole blood, increasing the likelihood of the detected transcripts being blood cell-derived. Similar to LIPCAR, the findings may reflect changes in inflammatory or other hematopoietic cells either as a potential consequence of a systemic response after MI [72] or effects of medication. Other studies evaluating circRNAs as biomarkers were either small in size [74], or performed normalization using a transcript of a commonly used intracellular reference gene [75]. The latter results could reflect plasma levels of residual blood cells such as platelets or leukocytes. Overall, circRNAs are difficult to detect in cell free body fluids, which currently hampers their evaluation as biomarkers. On the other hand, circRNA detection assays are in their infancy and improvements may lead to better strategies in their evaluation as circulating biomarkers.

7.3 ASSESSMENT OF NCRNAS AND PROTEIN BIOMARKERS FOR MI SUBTYPES

Our study suggests that a combination of NT-proBNP and cTnT could aid in differentiating T1MI, T2MI and AI. Established (cTnT, cTnI) and novel (cMyBP-C) cardiac necrosis markers performed well in discriminating T1MI and T2MI from AI but failed in differentiating T1MI vs T2MI at early time points. The combination of cardiac necrosis markers with NT-proBNP, however, helped to identify patients with T1MI and to differentiate MI subtypes with heart failure-like pathologies, which are common among patients with AI but infrequent in patients with T1MI.

7.3.1 Cardiac necrosis markers in MI subtypes

While mortality and morbidity in T2MI is similar or even higher than in T1MI [124,125], there are no biomarkers for the diagnosis of T2MI. This is in agreement with a recent study by Eggers et al. [126] who evaluated the prognostic potential of cTn in T2MI and report strong similarities of T1MI and T2MI. Their findings emphasise the known difficulty to differentiate MI subtypes using current clinical single biomarkers. And a similar conclusion has been made previously by Nestelberger et al. [127] supporting our observation that cTns do not differentiate between T1MI and T2MI. The study by Nestelberger et al. [127], however, did not assess AI. AI patients have a worse outcome than T1MI patients as reflected by their elevated GRACE score that is comparable to T2MI (**Table 2**). Therefore, we assessed not only T2MI patients but also AI patients to account for this important MI subtype. Our data reveal discriminative ability of cTnT for differentiating T1MI vs. AI very early on admission. None of the cardiac necrosis markers was able to differentiate all three MI subtypes at any given time point. While

cMyBP-C shows earlier release kinetics upon myocardial injury compared with Tn [14,15], cMyBP-C was also unable to discriminate T2MI and AI subtypes. Both, cTn and cMyBP-C are sarcomeric proteins of cardiomyocytes and are predominantly released upon cardiomyocyte death. All necrosis markers including cMyBP-C showed significant differences between T1MI and T2MI only 3h after admission. This information extends the study by Nestelberger et al. [127] who assessed biomarkers up to 2 hours after admission and reported no significant differences for cardiac biomarkers between T1MI and T2MI. Our dataset comprises biomarker measurements up to 3 hours after admission. Only at 3h, cardiac necrosis markers had discriminative power for T1MI versus T2MI. Thus, biomarker combinations may be required to differentiate T1MI, T2MI and AI upon a patient's presentation at the emergency department.

7.3.2 miRNA biomarkers in MI subtypes

In current biomarker research, measurements extend beyond proteins and include ncRNAs, but the performance of miRNAs has not been evaluated in T1MI and AI to date. Our group has previously studied miRNAs as biomarker candidates for prediction of primary [48] and secondary [50] CVD events. Many of those miRNAs, however, are not released from cardiomyocytes [3], but platelets and other circulating cells. A systemic response is the most likely explanation for post-MI changes of these miRNAs [128,129]. In the present study, neither cardiac- and/or muscle miRNAs, nor other selected miRNAs returned discriminative power in distinguishing T1MI versus T2MI or AI. For cardiac miRNAs, their assessment is hampered by less cardiac release due to the smaller infarct size in NSTEMI compared to STEMI patients. Similarly, muscle miRNAs showed lower detectability. Other plasma miRNAs are well-detectable, but their tissue/cell origin may not reflect the underlying patho-mechanisms of most T2MI cases.

7.3.3 NT-proBNP in MI subtypes

NT-proBNP is actively secreted by cardiomyocytes upon increased wall stress and the current gold standard biomarker in the diagnosis and prognosis of heart failure. NT-proBNP also has potential as a prognostic marker for post-MI outcome [130]. Interestingly, NT-proBNP has been reported to facilitate the diagnosis of low-cTn ACS when used in combination with TnT [131]. Another report suggested that NT-proBNP identified a *'previously unrecognised group of patients'* among patients presenting to the emergency department for cardiac symptoms [132]. These early reports highlight that NT-proBNP may have diagnostic value in subtypes of MI, although the differential diagnosis of T2MI was not yet established at the time. Nestelberger et al. reported results for single NT-proBNP: Baseline NT-proBNP was amongst the best performing biomarkers but still only ranged in moderate levels of predictive power [127]. While the study by Nestelberger et al. includes more patients than our study, their analysis was focussed on the performance of single biomarkers, predominantly on admission. Also, AI, comprising patients with heart failure-like diagnoses, was not assessed. Neumann et al. [133] reported baseline NT-

proBNP in combination with cTn and other non-cardiac specific protein biomarkers to show most discriminatory potential between T1MI and T2MI or MI (T1MI, T1MI combined) and myocardial injury. The study by Neumann et al. [133] was also focused on the performance of biomarkers at baseline, i.e. on admission, while biomarker kinetics are important in the clinical evaluation of myocardial damage [134]. Our dataset comprises biomarker serial measurements up to 3 hours after admission, thus providing release kinetics.

7.3.4 Biomarker combinations for differentiation of MI subtypes

Recent studies indicate modest ability of individual routine biomarkers to differentiate T2MI [135], while biomarker combinations have only been tested at baseline, but not in serial measurements [133]. In our BACC sub cohort, serial measurements of all biomarkers were performed at all time points providing an opportunity for a direct comparison of their release kinetics. Despite the limited value of cardiac necrosis markers in the early differentiation of T2MI, their high specificity assisted in a combinatorial approach to distinguish T1MI and T2MI. When cTn and NT-proBNP were assessed in combination, their release kinetics depicted different patterns with high cTnT and low NT-proBNP in T1MI, but low cTnT and high NT-proBNP in T2MI and high cTnT and high NT-proBNP in AI. These results highlight potential for a combinatory use of cTnT and NT-proBNP in the diagnosis of all three MI subtypes i.e., T1MI, T2MI and AI. Such a combination of routine clinical biomarkers is feasible and can reduce the time needed to make a clear and differentiated MI diagnosis. An early diagnosis of T2MI and AI would have important clinical implications, i.e., 1) guidance on the necessity of invasive diagnostic procedures and 2) focus on specific treatment options for T2MI and/or AI.

7.4 CONSIDERATIONS ON OUR STUDY DESIGN

Our study provides the first rigorous assessment of miRNA vs protein biomarkers in the setting of myocardial injury (TASH and acute MI). Previous publications did not take the *confounding by heparin* into consideration, nor did they use stringent *Cq values cut-offs* for qPCR measurements. Importantly, the performance of miRNAs was not assessed in the clinically most relevant setting of *MI patients with initial low cTn* values. We have summarised the limitations of the published literature in **Table 2.** We compared characteristics of a broad range of biomarkers (miRNAs, *lncRNAs circRNAs* as well as *the novel protein biomarker cMyBP-C*), evaluated their characteristics to serve as biomarkers for myocardial injury and optimised measuring techniques (overcome heparin bias), before testing the most promising candidates in clinical settings. Therefore, we believe our data represent a stringent, methodological approach of comparing biomarkers in an unbiased way. Our study includes validation in clinical settings and provides evidence that at present miRNAs are still the best-suitable ncRNA species as circulating biomarkers for the detection of myocardial injury. At the same time their ability to differentiate MI subtypes is currently limited and, as opposed to previous studies, their detectability

cannot challenge the sensitivity offered by established or novel protein biomarkers (hs-cTn, cMyBP-C). Once technical advances will have made it possible to overcome this lack in detectability, then large scale studies are needed to validate the initial and promising results from our analysis.

To address the different aetiologies of myocardial injury, we included raw Cq values of muscle/cardiac miRNAs separately stratified for STEMI vs NSTEMI patients. As expected, STEMI patients show more Cq values above the detectability threshold, given the usually larger infarct size. We stratified the correlation analysis for STEMI and NSTEMI patients and observed that correlations could be validated in both groups. Correlations of miRNAs with cardiac proteins, however, were weaker in the NSTEMI group compared with STEMI group. This was expected given the higher number of undetectable miRNA values in NSTEMI samples with smaller infarcts. MI patients from the BACC cohort were carefully chosen regarding the disease entity: In the first assessment, non-NSTEMI Type 1 patients were excluded and STEMI patients and NSTEMI Type 1 patients were selected in a balanced ratio (20 vs. 18, respectively). In the second part of the study we assessed non-Type 1 MI to further analyse a broader range of biomarker candidates in the unmet need to differentiate more MI subtypes.

We performed separate ROC analyses for STEMI patients compared with NSTEMI patients. Overall, the performance of the ROC model increased with severity of the disease (STEMI vs. NSTEMI) and with increasing hs-cTnT values. Importantly, within the analysed subgroups, the comparability of the ranking of single markers and their combinations was largely unchanged. Given that our cohort size was low, we increased the patient numbers by 50%. Another cohort of MI patients, all with hs-cTnT values < 1,000ng/L at any time point were included (n=19 with serial measurements at three time points) in order to further focus on patients presenting within the lower hs-cTnT range. Additionally, we performed miRNA measurements with an increased (2-fold) RNA input in the reverse transcription reaction to the maximum possible input volume as a further attempt to improve detectability. The rise in miR-1, miR-133a, miR-208b and miR-499, however, remained mainly detectable at hs-cTnT levels >100 ng/L. The overall strategy for our study was to carefully select the most informative MI cases from the large BACC cohort to answer the clinically relevant question if miRNAs outperform current hs-cTn measurements. Then we assessed non-Type 1 MI to further analyse a broader range of biomarker candidates in the unmet need to differentiate more MI subtypes.

7.5 Technical Issues Hampering The Utility of ncRNAs as Biomarkers

Besides the discussed heparin issue, other technical issues have hampered the utility of ncRNAs as biomarkers, including reliable isolation methods at scale, cross-platform accuracy, and rigorous normalization methods. In our study, besides solving the heparin issue, we took these other issues into account:

Reliable isolation methods – In order to provide the best possible input material for ncRNA quantification, we chose a column-based RNA extraction method, as it is the most efficient. The chosen miRNeasy kit ranges amongst the best available kits [136]. In order to prove the reliability and efficiency of the RNA extractions **Figure 4** depicts the raw Cq values of the Cel-miR-39 spike in from the TASH cohort and the MI cohort. The standard deviation is below 0.5 and the coefficient of variation below 2% in both groups, confirming consistency of the RNA isolation.

Cross-platform accuracy – We compared the most widely used kits for RT and qPCR: Qiagen miRCURY LNA RT kit and miRCURY SYBR green qPCR versus Thermo Fisher TaqMan assays. We then compared results in TASH serum samples and decided to proceed with the Qiagen kit because miR-1 detectability was better with the Qiagen kit (**Figure 5**). Unlike the TaqMan kit, the LNA-based Qiagen RT kit does not require an extra pre-amplification step, which avoids a potential source for errors. With respect to lncRNAs and circRNAs, for cDNA synthesis, we used the highly efficient RT VILO (Variable Input – Linear Output) by Thermo Fisher, which produces a linear cDNA transcription product independent of low or high RNA content. In our case, this is of great importance given the low RNA content in plasma.

Normalisation methods – Normalisation strategy has great influence on RNA quantification. Evaluating ncRNA kinetics after myocardial injury can hamper efforts to identify endogenous miRNAs with expression stable enough to use as a normalisation control. To the best of our knowledge, no endogenous miRNA has been identified, that is stably expressed under physiological or pathological conditions and is at the same time well detectable in the circulation. Nevertheless, in order to identify potential endogenous candidates to be used as normalisation controls, we analysed expression levels of some of the most abundant plasma miRNAs in the TASH cohort. None of them returned expression profiles, which can be considered suitable as normalisation controls, especially compared with Cel-miR-39 which was extremely stable (**Figures 4 and 8**). We performed normalization using the average of all ncRNAs instead of Cel-miR-39 as normalizer. For the four central miRNAs of our interest, we conducted correlation analysis between the RQ values obtained from each one of the normalization strategies and in all cases we found strong correlation ($R2>0.5$) indicating that the selection of the normalization method does not impact the results.

7.6 STRENGTHS AND LIMITATIONS

Discrimination of patients with T1MI, T2MI and AI is an unmet clinical need. A strength of our study is that a comparison across the 3 timepoints has not been done before. Also, biomarker performance was compared for all 3 MI subtypes i.e., T1MI, T2MI and AI which has not been evaluated thus far. With biomarker measurements up to 3 hours after admission, our results extend the study by Nestelberger et al. who assessed biomarkers up to 2 hours after admission and reported no significant differences for cardiac biomarkers between T1MI and T1MI. The causes of T1MI and AI are

multifactorial and comprise systemic responses to circulatory insufficiency [3]. T2MI is defined as a mismatch of cardiac oxygen demand and supply in the absence of acute coronary plaque rupture. Thus, other biomarkers beyond the ones tested in the present study may better capture the distinct patho-mechanisms leading to cardiac ischemia in T2MI distinguishing it from AI and T1MI. Finally, serial measurements at 3 time points in all patient groups allow for a direct, exploratory comparison of existing and novel clinical cardiac necrosis and strain markers as well as miRNAs that has not been done before across T1MI, T1MI and AI subtypes.

We recognize the low patient number per group and the absence of external validation as a limitation. Thus, our findings await validation in larger patient cohorts in the future. On the other hand, this study is exploratory, searching for novel approaches to discriminate T1MI, T2MI and AI. However, generalization ability of the trained models was evaluated using cross-validation, while the data completeness allowed for a combinatory biomarker approach. Moreover, screening techniques may provide a more comprehensive assessment of novel potential biomarker candidates. We focused on comparative performance of known miRNAs and protein biomarkers in the manuscript. We have selected 10 miRNAs with a well described tissue origin and good detectability in plasma: cardiac/muscle-derived miRNAs (i.e., miR-1, -133a, -208, and -499), endothelial cell-, leukocyte- and platelet-associated miRNAs (miR-21, -126, -150, -197 and -223) as well as liver-associated miR-122 as stated in **Table 8**.

7.7 CHALLENGES IN IMPLEMENTING NCRNA BIOMARKERS

Current protein biomarker assays (i.e. current hs-cTn) have been improved over the past 30 years. Despite advances in ncRNA research, ncRNA detection is still inferior compared to cardiac proteins [3]. Furthermore, the lack of reproducibility of published ncRNA data is a concern. Tissue specific miRNAs, such as liver-derived miR-122 show highly consistent result across studies in obesity, diabetes, metabolic syndrome, and liver injury [137,138]. However, this is not the case for other miRNAs, probably because they are blood cell-derived and subject to a higher pre-analytical variation. Some of the major sources of variation are sample preparation and storage conditions, control of RNA degradation [139], presence of residual cells in body fluids [140] and the effect of hemolysis on ncRNA levels [141]. Furthermore, different RNA isolation methods[142], normalization methods and the selection of the platform for ncRNA quantification [143] can impact on the quantification of circulating ncRNAs, in particular user-dependent parameters such as detection thresholds and calibration methods contribute to inconsistencies in ncRNA quantification. Other confounders in ncRNA biomarker research are medication related, such as heparin and anti-platelet drugs [144]. Attempts have been made to harmonize the reporting of ncRNA methods in the Minimum Information for publication of Quantitative real-time PCR Experiments (MIQE) guidelines [145] but the guidelines are not yet widely

implemented [146]. Additionally, ncRNA quantification, including RNA isolation, is still not sufficiently automated and too time consuming for an application in acute clinical settings.

In summary, heparinase treatment is essential when evaluating ncRNAs in clinical settings. Amongst ncRNAs, cardiac miRNAs remained the best predictor for the diagnosis of acute MI. In serial samples from TASH and acute MI patients, cardiac miRNAs showed comparable AUC values to hs-cTnT and the additional use of muscle-enriched miRNAs combined with hs-cTnT and cMyBP-C returned the highest AUC in the clinical setting of MI, pointing out their potential future use in combined protein/ncRNA biomarker approaches. On the other hand, miRNA sensitivity was well below hs-cTnT, arguing against their clinical application at the current stage of methodological advances. This may be a reason why miRNAs did not contribute to the biomarker combination in the differential diagnosis of MI subtypes. Thus, analyses in larger cohorts seem warranted. The current Covid-19 pandemic has brought the scientific and clinical use of qPCR-based diagnostics into focus and is supporting technological advances in this field. As a result, this diagnostic platform is now more widely available and the technological potential for more standardized large-scale re-assessment of our results has improved. Therefore, faster, automated ncRNA quantification may soon allow miRNAs to be used for complementing protein biomarkers. With regards to cardiac proteins, measurements of cMyBP-C could offer some of the benefits of miRNAs, as evidenced by an earlier rise and faster decline after myocardial injury and a better baseline detectability compared to cTn. The combination of biomarkers derived from different cardiac conditions and functional background (i.e. cTn = micronecrosis, NT-proBNP = hemodynamics) could aid in improved specificity for different MI etiologies, especially with respect to the most recent advances in the definition of MI and its subentities.

8 CONCLUSIONS

Currently, biomarkers are dominated by proteins. Cardiac-specific protein biomarkers cTnI and cTnT are the current gold standard for detection of myocardial injury due to their high sensitivity and acceptable specificity [8,147]. Apart from its use in the acute setting of MI, cTn is now also evaluated as a biomarker for non-acute CVD and risk stratification. cTn is already being used in clinical routine worldwide. While higher sensitivity cTn assays have improved the identification of low risk patients suitable for immediate discharge, detecting and treating minor cardiac damage may fail to result in better clinical outcomes [148]. Nevertheless, novel cardiovascular biomarker candidates are being explored. cMyBP-C shows properties as an early rule-in/ rule-out cardiac biomarker in the acute setting of MI. The high correlation of cTn and cMyBP-C may indicate some redundancy in that both markers provide similar information. On the other hand, hs cTn assays also give rise to false positive results. Further studies and validation in existing clinical trials are warranted to determine whether this can be mitigated by additional cMyBP-C measurements.

While both cTn and cMyBP-C are cardiac-specific, markers of systemic and inflammatory processes could contribute to diagnostic and prognostic performance in terms of early detection and higher predictive power i.e. GDF-15, NT-proBNP or CRP have been implicated as prognostic biomarkers for CVD. However, their added value compared to existing CVD risk scores is still limited. In this respect, circulating ncRNAs may be useful in complementing protein biomarkers, especially with respect to specificity, given their distinct tissue- and organ-enrichment combined with the large number of ncRNA transcripts expressed in different cell and tissue types. At present, miRNAs are the most promising ncRNA species. Over the past decade numerous studies have investigated miRNAs as diagnostic and prognostic circulating biomarker candidates for CVD. Nevertheless, validation of results is scarce, reflecting a need for harmonization of ncRNA quantification and reporting methods. Furthermore, current hs-cTn assays still outperform miRNA measurements in terms of sensitivity. In parallel, confounding factors such as qPCR inhibition by heparin need to be addressed by applying appropriate methods such as heparinase treatment.

Other ncRNAs such as lncRNAs as well as circRNAs have only recently attracted attention as biomarker candidates but there is less evidence compared to miRNAs. While many more lncRNA transcripts have been discovered compared with miRNAs, their evaluation as circulating biomarkers has only just begun. In this respect, initial results are promising in terms of detectability of some lncRNAs in the circulation. For circRNAs, poor detectability in body fluids currently is the limiting factor for advances in the biomarker field. On the other hand, at a cellular level circRNAs are promising biomarker candidates in the context of a liquid biopsy, evaluating the association of i.e. platelet or leukocytes-derived transcripts to CVD. Prior to large-scale clinical evaluation and application of extracellular ncRNAs as biomarkers, several major obstacles need to be overcome, including the need for automation and scaling of measurements and improving means of detection.

9 REFERENCES

1 Thygesen, K. *et al.* (2018) Fourth universal definition of myocardial infarction (2018). *Eur. Heart J.* DOI: 10.1093/eurheartj/ehy462

2 Chapman, A.R. *et al.* (2018) Long-Term Outcomes in Patients With Type 2 Myocardial Infarction and Myocardial Injury. *Circulation* 137, 1236–1245

3 Schulte, C. *et al.* (2019) Comparative analysis of circulating noncoding rnas versus protein biomarkers in the detection of myocardial injury. *Circ. Res.* 125,

4 Ellis, A.K. Serum protein measurements and the diagnosis of acute myocardial infarction. , *Circulation*, 83. (1991) , 1107–1109

5 Jaffe, A.S. *et al.* Biomarkers in Acute Cardiac Disease. The Present and the Future. , *Journal of the American College of Cardiology*, 48. 04-Jul-(2006) , 1–11

6 Adams, J.E. *et al.* (1993) Biochemical markers of myocardial injury: Is MB creatine kinase the choice for the 1990s? *Circulation* 88, 750–763

7 Chew, D.P. *et al.* (2019) A Randomized Trial of a 1-Hour Troponin T Protocol in Suspected Acute Coronary Syndromes: The Rapid Assessment of Possible Acute Coronary Syndrome in the Emergency Department With High-Sensitivity Troponin T Study (RAPID-TnT). *Circulation* 140, 1543–1556

8 Roffi, M. *et al.* (2016) 2015 ESC Guidelines for the management of acute coronary syndromes in patients presenting without persistent ST-segment elevation. *Eur. Heart J.* 37, 267–315

9 Katus, H.A. *et al.* (1989) Enzyme linked immuno assay of cardiac troponin T for the detection of acute myocardial infarction in patients. *J. Mol. Cell. Cardiol.* 21, 1349–1353

10 Ford, I. *et al.* (2016) High-Sensitivity Cardiac Troponin, Statin Therapy, and Risk of Coronary Heart Disease. *J. Am. Coll. Cardiol.* 68, 2719–2728

11 Neumann, J.T. *et al.* (2019) Application of High-Sensitivity Troponin in Suspected Myocardial Infarction. *N. Engl. J. Med.* 380, 2529–2540

12 Blankenberg, S. *et al.* (2016) Troponin I and cardiovascular risk prediction in the general population: the BiomarCaRE consortium. *Eur. Heart J.* 37, 2428–2437

13 Aye, T.T. *et al.* (2010) Proteome-wide protein concentrations in the human heart. *Mol. Biosyst.* 6, 1917

14 Jacquet, S. *et al.* (2009) Identification of cardiac myosin-binding protein C as a candidate biomarker of myocardial infarction by proteomics analysis. *Mol. Cell. Proteomics* 8, 2687–99

15 Kaier, T.E. *et al.* (2017) Direct Comparison of Cardiac Myosin-Binding Protein C With Cardiac Troponins for the Early Diagnosis of Acute Myocardial Infarction. *Circulation* 136, 1495–1508

16 Baker, J.O. *et al.* (2015) Cardiac myosin-binding protein C: a potential early biomarker of myocardial injury. *Basic Res. Cardiol.* 110, 23

17 Anand, A. *et al.* (2018) Cardiac myosin-binding protein C is a novel marker of myocardial injury and fibrosis in aortic stenosis. *Heart* 104, 1101–1108

18 Djebali, S. *et al.* (2012) Landscape of transcription in human cells. *Nature* 489, 101–108

19 Schulte, C. *et al.* (2020) Noncoding RNAs versus Protein Biomarkers in Cardiovascular Disease. *Trends Mol. Med.* DOI: 10.1016/J.MOLMED.2020.02.001

20 Devaux, Y. *et al.* Long noncoding RNAs in cardiac development and ageing. , *Nature Reviews Cardiology*, 12. 22-Jul-(2015) , Nature Publishing Group, 415–425

21 Abbas, N. *et al.* Non-coding RNAs: emerging players in cardiomyocyte proliferation and cardiac regeneration. , *Basic Research in Cardiology*, 115. 01-Sep-(2020) , Springer, 1–20

22 Mitchell, P.S. *et al.* (2008) Circulating microRNAs as stable blood-based markers for cancer detection. *Proc. Natl. Acad. Sci. U. S. A.* 105, 10513–8

23 E, S. *et al.* (2018) The circulating non-coding RNA landscape for biomarker research: lessons and prospects from cardiovascular diseases. *Acta Pharmacol. Sin.* 39, 1085–1099

24 Condorelli, G. and van Rooij, E. (2019) MicroRNAs as Companion Biomarkers for the Diagnosis and Prognosis of Acute Coronary Syndromes. *Circ. Res.* 125, 341–342

25 Zeller, T. *et al.* (2014) Assessment of microRNAs in patients with unstable angina pectoris. *Eur. Heart J.* 35, 2106–2114

26 Wang, G.-K. *et al.* (2010) Circulating microRNA: a novel potential biomarker for early diagnosis of acute myocardial infarction in humans. *Eur. Heart J.* 31, 659–666

27 Kuwabara, Y. *et al.* (2011) Increased MicroRNA-1 and MicroRNA-133a Levels in Serum of Patients With Cardiovascular Disease Indicate Myocardial Damage. *Circ. Cardiovasc. Genet.* 4, 446–454

28 Kumarswamy, R. *et al.* (2014) Circulating long noncoding RNA, LIPCAR, predicts survival in patients with heart failure. *Circ. Res.* 114, 1569–1575

29 Memczak, S. *et al.* (2013) Circular RNAs are a large class of animal RNAs with regulatory potency. *Nature* 495, 333–338

30 Tan, W.L.W. *et al.* (2017) A landscape of circular RNA expression in the human heart. *Cardiovasc. Res.* 113, 298–309

31 Rybak-Wolf, A. *et al.* (2015) Circular RNAs in the Mammalian Brain Are Highly Abundant, Conserved, and Dynamically Expressed. *Mol. Cell* 58, 870–885

32 Kaudewitz, D. *et al.* (2015) MicroRNA Biomarkers for Coronary Artery Disease? *Curr. Atheroscler. Rep.* 17, 70

33 Baek, D. *et al.* (2008) The impact of microRNAs on protein output. *Nature* 455, 64–71

34 Fiedler, J. *et al.* (2011) MicroRNA-24 Regulates Vascularity After Myocardial Infarction. *Circulation* 124, 720–730

35 Hinkel, R. *et al.* (2013) Inhibition of microRNA-92a protects against ischemia/reperfusion injury in a large-animal model. *Circulation* 128, 1066–1075

36 Täubel, J. *et al.* (2020) OUP accepted manuscript. *Eur. Heart J.* DOI: 10.1093/eurheartj/ehaa898

37 Arroyo, J.D. *et al.* (2011) Argonaute2 complexes carry a population of circulating microRNAs independent of vesicles in human plasma. *Proc. Natl. Acad. Sci. U. S. A.* 108, 5003–8

38 Vickers, K.C. *et al.* (2011) MicroRNAs are transported in plasma and delivered to recipient cells by high-density lipoproteins. *Nat. Cell Biol.* 13, 423–33

39 Turchinovich, A. *et al.* (2011) Characterization of extracellular circulating microRNA. *Nucleic Acids Res.* 39, 7223–33

40 Reid, G. *et al.* (2011) Circulating microRNAs: Association with disease and potential use as biomarkers. *Crit. Rev. Oncol. Hematol.* 80, 193–208

41 Goretti, E. *et al.* (2014) miRNAs as biomarkers of myocardial infarction: a step forward towards personalized medicine? *Trends Mol. Med.* 20, 716–25

42 van Rooij, E. *et al.* (2006) A signature pattern of stress-responsive microRNAs that can evoke cardiac hypertrophy and heart failure. *Proc. Natl. Acad. Sci. U. S. A.* 103, 18255–60

43 van Rooij, E. *et al.* (2008) Dysregulation of microRNAs after myocardial infarction reveals a role of miR-29 in cardiac fibrosis. *Proc. Natl. Acad. Sci. U. S. A.* 105, 13027–32

44 Liebetrau, C. *et al.* (2013) Release kinetics of circulating muscle-enriched microRNAs in

patients undergoing transcoronary ablation of septal hypertrophy. *J. Am. Coll. Cardiol.* 62, 992–8

45 Kaudewitz, D. *et al.* (2013) Impact of intravenous heparin on quantification of circulating microRNAs in patients with coronary artery disease. *Thromb Haemost* 110, 609–615

46 Boileau, A. *et al.* (2018) Endogenous Heparin Interferes with Quantification of MicroRNAs by RT-qPCR. *Clin. Chem.* 64, 863–865

47 Coelho-Lima, J. *et al.* (2018) Overcoming Heparin-Associated RT-qPCR Inhibition and Normalization Issues for microRNA Quantification in Patients with Acute Myocardial Infarction. *Thromb. Haemost.* DOI: 10.1055/s-0038-1660437

48 Zampetaki, A. *et al.* (2012) Prospective Study on Circulating MicroRNAs and Risk of Myocardial Infarction. *J. Am. Coll. Cardiol.* 60, 290–299

49 Jansen, F. *et al.* (2014) MicroRNA expression in circulating microvesicles predicts cardiovascular events in patients with coronary artery disease. *J. Am. Heart Assoc.* 3, e001249

50 Schulte, C. *et al.* (2015) miRNA-197 and miRNA-223 Predict Cardiovascular Death in a Cohort of Patients with Symptomatic Coronary Artery Disease. *PLoS One* 10, e0145930

51 Bye, A. *et al.* (2016) Circulating microRNAs predict future fatal myocardial infarction in healthy individuals – The HUNT study. *J. Mol. Cell. Cardiol.* 97, 162–168

52 Viereck, J. and Thum, T. (2017) Circulating Noncoding RNAs as Biomarkers of Cardiovascular Disease and Injury. *Circ. Res.* 120, 381–399

53 Derrien, T. *et al.* (2012) The GENCODE v7 catalog of human long noncoding RNAs: analysis of their gene structure, evolution, and expression. *Genome Res.* 22, 1775–89

54 Wilusz, J.E. *et al.* (2009) Long noncoding RNAs: functional surprises from the RNA world. *Genes Dev.* 23, 1494–504

55 Gangwar, R.S. *et al.* (2018) Noncoding RNAs in Cardiovascular Disease: Pathological Relevance and Emerging Role as Biomarkers and Therapeutics. *Am. J. Hypertens.* 31, 150–165

56 Li, D.Y. *et al.* (2018) H19 Induces Abdominal Aortic Aneurysm Development and Progression. *Circulation* 138, 1551–1568

57 Uchida, S. and Dimmeler, S. (2015) Long Noncoding RNAs in Cardiovascular Diseases. *Circ. Res.* 116, 737–750

58 Tan, P. *et al.* (2019) LncRNA-ANRIL inhibits cell senescence of vascular smooth muscle cells

by regulating miR-181a/Sirt1. *Biochem. Cell Biol.* DOI: 10.1139/bcb-2018-0126

59 Yang, F. *et al.* (2014) Reciprocal Regulation of HIF-1α and LincRNA-p21 Modulates the Warburg Effect. *Mol. Cell* 53, 88–100

60 Kimura, W. *et al.* (2015) Hypoxia fate mapping identifies cycling cardiomyocytes in the adult heart. *Nature* 523, 226–230

61 Zhang, Y. *et al.* (2013) Circular Intronic Long Noncoding RNAs. *Mol. Cell* 51, 792–806

62 Jeck, W.R. and Sharpless, N.E. (2014) Detecting and characterizing circular RNAs. *Nat. Biotechnol.* 32, 453–461

63 Suzuki, H. *et al.* (2006) Characterization of RNase R-digested cellular RNA source that consists of lariat and circular RNAs from pre-mRNA splicing. *Nucleic Acids Res.* 34, e63–e63

64 Khan, M.A.F. *et al.* (2016) RBM20 Regulates Circular RNA Production From the Titin Gene. *Circ. Res.* DOI: 10.1161/CIRCRESAHA.116.309568

65 Hansen, T.B. *et al.* (2013) Natural RNA circles function as efficient microRNA sponges. *Nature* 495, 384–388

66 Legnini, I. *et al.* (2017) Circ-ZNF609 Is a Circular RNA that Can Be Translated and Functions in Myogenesis. *Mol. Cell* 66, 22-37.e9

67 Ashwal-Fluss, R. *et al.* (2014) circRNA Biogenesis Competes with Pre-mRNA Splicing. *Mol. Cell* 56, 55–66

68 Barrett, S.P. and Salzman, J. (2016) Circular RNAs: analysis, expression and potential functions. *Development* 143, 1838–47

69 Jeck, W.R. *et al.* (2013) Circular RNAs are abundant, conserved, and associated with ALU repeats. *RNA* 19, 141–57

70 Wang, K. *et al.* (2017) Circular RNA mediates cardiomyocyte death via miRNA-dependent upregulation of MTP18 expression. *Cell Death Differ.* 24, 1111–1120

71 Geng, H.-H. *et al.* (2016) The Circular RNA Cdr1as Promotes Myocardial Infarction by Mediating the Regulation of miR-7a on Its Target Genes Expression. *PLoS One* 11, e0151753

72 Vausort, M. *et al.* (2016) Myocardial Infarction-Associated Circular RNA Predicting Left Ventricular Dysfunction. *J. Am. Coll. Cardiol.* 68, 1247–1248

73 Salgado-Somoza, A. *et al.* (2017) The circular RNA MICRA for risk stratification after myocardial infarction. *Int. J. Cardiol. Hear. Vasc.* 17, 33–36

74 Pan, R.-Y. *et al.* (2017) Circular RNAs promote TRPM3 expression by inhibiting hsa-miR-130a-3p in coronary artery disease patients. *Oncotarget* 8, 60280–60290

75 Wu, N. *et al.* (2017) Profiling and bioinformatics analyses reveal differential circular RNA expression in hypertensive patients. *Clin. Exp. Hypertens.* 39, 454–459

76 Corsten, M.F. *et al.* (2010) Circulating MicroRNA-208b and MicroRNA-499 reflect myocardial damage in cardiovascular disease. *Circ. Cardiovasc. Genet.* 3, 499–506

77 Boeckel, J.-N. *et al.* (2013) Heparin selectively affects the quantification of microRNAs in human blood samples. *Clin. Chem.* 59, 1125–7

78 Kaier, T.E. *et al.* (2017) Direct Comparison of Cardiac Myosin-Binding Protein C With Cardiac Troponins for the Early Diagnosis of Acute Myocardial Infarction. *Circulation* 136, 1495–1508

79 Sánchez-Fito, M.T. and Oltra, E. (2015) Optimized Treatment of Heparinized Blood Fractions to Make Them Suitable for Analysis. *Biopreserv. Biobank.* 13, 287–295

80 Marjot, J. *et al.* (2017) Quantifying the Release of Biomarkers of Myocardial Necrosis from Cardiac Myocytes and Intact Myocardium. *Clin. Chem.* 63, 990–996

81 Liebetrau, C. *et al.* (2012) Release kinetics of cardiac biomarkers in patients undergoing transcoronary ablation of septal hypertrophy. *Clin. Chem.* 58, 1049–54

82 Neumann, J.T. *et al.* (2016) Diagnosis of Myocardial Infarction Using a High-Sensitivity Troponin I 1-Hour Algorithm. *JAMA Cardiol.* 1, 397

83 Zeller, T. *et al.* (2015) High-sensitivity cardiac troponin I in the general population – defining reference populations for the determination of the 99th percentile in the Gutenberg Health Study. *Clin. Chem. Lab. Med.* 53, 699–706

84 Westermann, D. *et al.* (2017) High-sensitivity assays for troponin in patients with cardiac disease. *Nat. Rev. Cardiol.* 14, 472–483

85 Assarsson, E. *et al.* (2014) Homogenous 96-plex PEA immunoassay exhibiting high sensitivity, specificity, and excellent scalability. *PLoS One* 9, e95192

86 Kaudewitz, D. *et al.* (2016) Association of MicroRNAs and YRNAs With Platelet Function. *Circ. Res.* 118, 420–32

87 Marjot, J. *et al.* (2016) The development and application of a high-sensitivity immunoassay for cardiac myosin-binding protein C. *Transl. Res.* 170, 17-25.e5

88 McKnight, P.E. and Najab, J. (2010) Mann-Whitney U Test. In *The Corsini Encyclopedia of*

Psychology pp. 1–1, John Wiley & Sons, Inc.

89 Troyanskaya, O. *et al.* (2001) Missing value estimation methods for DNA microarrays. *Bioinformatics* 17, 520–5

90 Smola, A.J. and Schölkopf, B. (2004) A tutorial on support vector regression. *Stat. Comput.* 14, 199–222

91 Schölkopf, B. *et al.* (2004) *Kernel methods in computational biology*, MIT Press.

92 Deb, K. *et al.* (2002) A fast and elitist multiobjective genetic algorithm: NSGA-II. *IEEE Trans. Evol. Comput.* 6, 182–197

93 Wong, T.-T. (2015) Performance evaluation of classification algorithms by k-fold and leave-one-out cross validation. *Pattern Recognit.* 48, 2839–2846

94 CHANG and Chih-Chung "LIBSVM : a library for support vector machines," ACM Transactions on Intelligent Systems and Technology, 2:27:1--27:27, 2011. *http://www.csie.ntu.edu.tw/～cjlin/libsvm* 2,

95 Metz, C.E. *et al.* (1998) Maximum likelihood estimation of receiver operating characteristic (ROC) curves from continuously-distributed data. *Stat. Med.* 17, 1033–53

96 Galili, T. *et al.* (2018) heatmaply: an R package for creating interactive cluster heatmaps for online publishing. *Bioinformatics* 34, 1600–1602

97 Kursa, M.B. and Rudnicki, W.R. (2010) Feature selection with the boruta package. *J. Stat. Softw.* 36, 1–13

98 Kay, M. *et al.* (2022) The conserved long non-coding RNA CARMA regulates cardiomyocyte differentiation. *Cardiovasc. Res.* 118, 2339–2353

99 Pedersen, O.B. *et al.* MicroRNA as Biomarkers for Platelet Function and Maturity in Patients with Cardiovascular Disease. , *Thrombosis and Haemostasis*, 122. 01-Feb-(2022) , Georg Thieme Verlag, 181–195

100 Gebert, L.F.R. *et al.* (2021) A structured RNA motif locks Argonaute2:miR-122 onto the 5' end of the HCV genome. *Nat. Commun.* 12,

101 Cao, D. *et al.* (2020) MicroRNA-126-3p Inhibits Angiogenic Function of Human Lung Microvascular Endothelial Cells via LAT1 (L-Type Amino Acid Transporter 1)-Mediated mTOR (Mammalian Target of Rapamycin) Signaling. *Arterioscler. Thromb. Vasc. Biol.* 40, 1195–1206

102 Wakabayashi, I. *et al.* (2021) Contribution of platelet-derived microRNAs to serum

microRNAs in healthy men. *Platelets* 32, 984–987

103 Van Rooij, E. *et al.* (2007) Control of stress-dependent cardiac growth and gene expression by a microRNA. *Science (80-.).* 316, 575–579

104 Matkovich, S.J. *et al.* (2012) Direct and indirect involvement of MicroRNA-499 in clinical and experimental cardiomyopathy. *Circ. Res.* 111, 521–531

105 Lee, R.C. *et al.* (1993) The C. elegans heterochronic gene lin-4 encodes small RNAs with antisense complementarity to lin-14. *Cell* 75, 843–54

106 Barwari, T. *et al.* (2016) MicroRNAs in cardiovascular disease. *J. Am. Coll. Cardiol.* 68, 2577–2584

107 Imai, H. *et al.* (1992) Short Communication Detection of HIV-l RNA in heparinized plasma of HIV- 1 seropositive individuals. 36, 181–184

108 Satsangi, J. *et al.* (1994) Effect of heparin on polymerase chain reaction. *Lancet (London, England)* 343, 1509–10

109 Walter, G. *et al.* (1967) Initiation of DNA-dependent RNA synthesis and the effect of heparin on RNA polymerase. *Eur. J. Biochem.* 3, 194–201

110 Mayr, M. *et al.* (2014) Effects of Heparin on Temporal MicroRNA Profiles. *J. Am. Coll. Cardiol.* 63, 940–941

111 Thygesen, K. *et al.* (2019) Fourth universal definition of myocardial infarction (2018). *Eur. Heart J.* 40, 237–269

112 Adams, J.E. *et al.* (1993) Cardiac troponin I. A marker with high specificity for cardiac injury. *Circulation* 88, 101–6

113 Chistiakov, D.A. *et al.* (2016) Cardiac-specific miRNA in cardiogenesis, heart function, and cardiac pathology (with focus on myocardial infarction). *J. Mol. Cell. Cardiol.* 94, 107–121

114 Selimoglu-Buet, D. *et al.* (2018) A miR-150/TET3 pathway regulates the generation of mouse and human non-classical monocyte subset. *Nat. Commun.* 9, 5455

115 Schulte, C. *et al.* (2019) Response by Schulte et al to Letter Regarding Article, "Comparative Analysis of Circulating Noncoding RNAs Versus Protein Biomarkers in the Detection of Myocardial Injury." *Circ. Res.* 125,

116 de Gonzalo-Calvo, D. *et al.* (2019) Circulating non-coding RNAs in biomarker-guided cardiovascular therapy: a novel tool for personalized medicine? *Eur. Heart J.* 40, 1643–1650

117 Siegel, R.S. *et al.* (1989) Platelet survival and turnover: important factors in predicting response to splenectomy in immune thrombocytopenic purpura. *Am. J. Hematol.* 30, 206–12

118 Deutsch, V.R. and Tomer, A. (2006) Megakaryocyte development and platelet production. *Br. J. Haematol.* 134, 453–466

119 Zhang, Y. *et al.* (2016) Reciprocal Changes of Circulating Long Non-Coding RNAs ZFAS1 and CDR1AS Predict Acute Myocardial Infarction. *Sci. Rep.* 6, 22384

120 Gao, L. *et al.* (2017) Circulating Long Noncoding RNA HOTAIR is an Essential Mediator of Acute Myocardial Infarction. *Cell. Physiol. Biochem.* 44, 1497–1508

121 Hobuß, L. *et al.* (2019) Long Non-coding RNAs: At the Heart of Cardiac Dysfunction? *Front. Physiol.* 10, 30

122 Busch, A. *et al.* (2016) Prospective and therapeutic screening value of non-coding rna as biomarkers in cardiovascular disease. *Ann. Transl. Med.* 4, 1–12

123 Li, T. *et al.* (2018) Plasma circular RNA profiling of patients with gastric cancer and their droplet digital RT-PCR detection. *J. Mol. Med.* 96, 85–96

124 Lippi, G. *et al.* (2017) Cardiac troponins and mortality in type 1 and 2 myocardial infarction. *Clin. Chem. Lab. Med.* 55, 181–188

125 Arora, S. *et al.* (2018) Impact of Type 2 Myocardial Infarction (MI) on Hospital-Level MI Outcomes: Implications for Quality and Public Reporting. *J. Am. Heart Assoc.* 7,

126 Eggers, K.M. *et al.* (2022) Clinical and prognostic implications of high-sensitivity cardiac troponin T concentrations in type 2 non-ST elevation myocardial infarction. *IJC Hear. Vasc.* 39,

127 Nestelberger, T. *et al.* (2021) Cardiovascular Biomarkers in the Early Discrimination of Type 2 Myocardial Infarction. *JAMA Cardiol.* 6, 771–780

128 Long, G. *et al.* (2012) Human circulating microRNA-1 and microRNA-126 as potential novel indicators for acute myocardial infarction. *Int. J. Biol. Sci.* 8, 811–8

129 Devaux, Y. *et al.* (2015) Diagnostic and prognostic value of circulating microRNAs in patients with acute chest pain. *J. Intern. Med.* 277, 260–271

130 Sigurdardottir, F.D. *et al.* (2018) Relative Prognostic Value of Cardiac Troponin I and C-Reactive Protein in the General Population (from the Nord-Trøndelag Health [HUNT] Study). *Am. J. Cardiol.* 121, 949–955

131 Omland, T. *et al.* (2002) N-terminal pro-B-type natriuretic peptide and long-term mortality in

acute coronary syndromes. *Circulation* 106, 2913–2918

132 Truong, Q.A. *et al.* (2012) Multi-marker strategy of natriuretic peptide with either conventional or high-sensitivity troponin-T for acute coronary syndrome diagnosis in emergency department patients with chest pain: From the "Rule Out Myocardial Infarction Using Computer Assisted Tomography" (ROMICAT) trial. *Am. Heart J.* 163, 972-979.e1

133 Neumann, J.T. *et al.* (2021) A Biomarker Model to Distinguish Types of Myocardial Infarction and Injury. *J. Am. Coll. Cardiol.* 78, 781–790

134 Campbell, D.J. *et al.* (2001) Plasma amino-terminal pro-brain natriuretic peptide levels in subjects presenting to the Emergency Department with suspected acute coronary syndrome: possible role in selecting patients for follow up? *Intern. Med. J.* 31, 211–219

135 Wereski, R. *et al.* (2021) Cardiac Troponin Thresholds and Kinetics to Differentiate Myocardial Injury and Myocardial Infarction. *Circulation* 144, 528–538

136 Brown, R.A.M. *et al.* (2018) Total RNA extraction from tissues for microRNA and target gene expression analysis: not all kits are created equal. *BMC Biotechnol.* 18, 16

137 Willeit, P. *et al.* (2017) Circulating MicroRNA-122 is associated with the risk of new-onset metabolic syndrome and type 2 diabetes. *Diabetes* 66, 347–357

138 Shah, R. *et al.* (2017) Extracellular RNAs are associated with insulin resistance and metabolic phenotypes. *Diabetes Care* 40, 546–553

139 Ludwig, N. *et al.* (2018) Small ncRNA-Seq Results of Human Tissues: Variations Depending on Sample Integrity. *Clin. Chem.* 64, 1074–1084

140 Tung, S.L. *et al.* (2018) Regulatory T cell-derived extracellular vesicles modify dendritic cell function. *Sci. Rep.* 8, 6065

141 Kirschner, M.B. *et al.* (2013) The Impact of Hemolysis on Cell-Free microRNA Biomarkers. *Front. Genet.* 4, 94

142 Witwer, K.W. (2015) Circulating microRNA biomarker studies: pitfalls and potential solutions. *Clin. Chem.* 61, 56–63

143 Alikian, M. *et al.* (2017) RT-qPCR and RT-Digital PCR: A Comparison of Different Platforms for the Evaluation of Residual Disease in Chronic Myeloid Leukemia. *Clin. Chem.* 63, 525–531

144 Sunderland, N. *et al.* (2017) MicroRNA Biomarkers and Platelet Reactivity. *Circ. Res.* 120, 418–435

145 Bustin, S.A. *et al.* (2009) The MIQE Guidelines: Minimum Information for Publication of Quantitative Real-Time PCR Experiments. *Clin. Chem.* 55, 611–622

146 Bustin, S.A. *et al.* (2013) The need for transparency and good practices in the qPCR literature. *Nat. Methods* 10, 1063–1067

147 Thygesen, K. *et al.* (2012) Third Universal Definition of Myocardial Infarction. *J. Am. Coll. Cardiol.* 60, 1581–1598

148 Shah, A.S. V *et al.* (2018) High-sensitivity troponin in the evaluation of patients with suspected acute coronary syndrome: a stepped-wedge, cluster-randomised controlled trial. *Lancet* 392, 919–928

10 CURRICULUM VITAE

General Information

Schulte, Christian, Dr., MD, PhD candidate, 20.11.1980, male

University Medical Center Hamburg Eppendorf, University Heart and Vascular Center, Department of Cardiology, Martinistraße 52, 20246 Hamburg, Germany, phone +49 (0) 40 7410-58206,

email: c.schulte@uke.de

Current position: Postdoctoral researcher and cardiologist (clinician scientist)

University Training and Degree

Medicine (2005-2011), University of Hamburg, Germany, St. Gallen, Switzerland, University of Brisbane, Australia, Degree: Staatsexamen

Advanced academic qualifications

MD doctorate: Ergebnisse nach aortenklappenerhaltendem Ersatz der Aorta ascendens in der Technik nach David, University of Hamburg, Germany, 2013, supervisor: Prof. Dr. Dr. Hermann Reichenspurner

Postgraduate professional career

2021 – today	Cardiology specialist and postdoctoral researcher, Department of Cariology, University Heart & Vascular Center UKE
2019 – 2021	Resident physician and postdoctoral researcher, Department of Cardiology, University Heart & Vascular Center UKE
2019	Research fellowship of the Deanery of the UKE, Host: Prof. Dr.Tanja Zeller (UHZ)
2019	Postdoctoral research fellow of the DFG, Host Prof. Dr. Tanja Zeller (UHZ)
2017 – today	PhD candidate: non-coding RNAs in Cardiovascular Disease, King's College London, UK, supervisor: Prof. Dr. Manuel Mayr
2017 – 2019	Postdoctoral research fellow of the DFG, King's College London, UK
2012 – 2017	Cardiologist in Training and research fellow (UHZ, UKE)
2009	Clinical fellowship, Royal Brisbane and Women's Hospital, Brisbane, Australia
2008	Clinical fellowship, Kingston Children's Hosptial, Kingston, Jamaica

Additional information

2020 – today	Associate Editor for Frontiers in Cardiovascular Medicine
2020 – 2021	Mentoring Program (DZHK), Berlin
2019 – today	Member of the Young DZHK, Partner site Hamburg/Kiel/Lubeck
2017 – today	PhD candidate, King's College London, Cardiovascular division. Non-coding RNAs in cardiovascular disease, expected completion 2021
2017 – 2019	DFG Research Fellowship, King's College London, UK
2019	DFG Return Fellowship, University Heart and Vascular Center Hamburg
2019	Research stipend, deanery University Medical Center Hamburg (50%)
2015 – today	Reviewer for numerous scientific journals (i.e. Eur J Heart Fail, Journal of the American College of Cardiology, Scientific Reports, Molecular Biology Reports, Journal of Diabe-tes Research, International Journal of Molecular Sciences, Diabetes Vasc Dis Res, An-nals of Translational Medicine, Medicina, Plos One)
2009	Research fellowship, Institute of Experimental Pharmacology and Toxicology, University Medical Center Hamburg

Awards/Grants

2021	DZHK Post Doc Start-up Grant, EUR 80,000
2019	Best publication of the year award, James Black Centre, King's College London, UK
2019	Funding for platelet aggregometer, deanery of University Medical Center Hamburg
2016	Travel grant of the University of Hamburg to the German Cardiac Society Annual Meeting
2015	Travel grant of the University of Hamburg to the ESC 2015, London
2015	Shared session poster price and overall ESC poster price, ESC 2015

Invited congress talks as faculty member

2022 – Integrated Management of Acute and Chronic Cardiovascular Disease - 2020 - ESC Preventive Cardiology Congress; 2020 - ESC Frontiers in Cardiovascular Biomedicine; 2019 - ESC Congress, Paris; 2019 - German Heart Days (DGK), Berlin

Memberships

German Cardiac Society (DGK), European Society of Cardiology (ESC) ESC Council of Basic Cardio-vascular Science, ESC Scientists of Tomorrow

11 PUBLICATIONS RESULTING FROM THIS PHD

1. **Schulte C***, Singh, B*, Theofilatos K, Zampetaki A, Sörensen NA, Lehmacher J, Hartikainen T, Haller PM, Westermann D, Zeller T, Blankenberg S, Neumann JT & Mayr M. Serial Measurements of Protein and MicroRNA Biomarkers to Specify Myocardial Infarction Subtypes. ***JMCCPL***. 2022. DOI: 10.1016/j.jmccpl.2022.100014 *equal contribution
2. Parker WAE, **Schulte C**, Barwari T, Phoenix F, Pearson SM, Mayr M, Grant PJ, Storey RF, Ajjan RA. ***Cardiovasc Diabetol***. 2020. DOI: 10.1186/s12933-019-0981-3.
3. **Schulte C**, Barwari T, Joshi A, Zeller T, & Mayr M. Noncoding RNAs versus Protein Biomarkers in Cardiovascular Disease. ***Trends in Molecular Medicine***. 2020. vol. 26 583–596.
4. **Schulte C, Zeller T.** Biomarkers in primary prevention: Meaningful diagnosis based on biomarker scores?. ***Herz.*** 2020. DOI: 10.1007/s00059-019-04874-2.
5. Shrisvastana A, Haase T, Zeller T, **Schulte C**. Biomarkers for Heart Failure Prognosis: Proteins, Genetic Scores and Non-coding RNAs. ***Front Cardiovasc Med***. 2020. DOI: 10.3389/fcvm.2020.601364.
6. **Schulte C**, Joshi A, Mayr M. Response by Schulte et al to Letter regarding Article, "Comparative Analysis of Circulating Noncoding RNAs Versus Protein Biomarkers in the Detection of Myocardial Injury". ***Circ Res***. 2019. DOI: 10.1161/CIRCRESAHA.119.315545.
7. **Schulte C**, Barwari T, Joshi A, Theofilatos K, Zampetaki A, Barallobre-Barreiro, J, Singh, B, Sörensen, NA, Neumann JT, Zeller T, Westermann D., Blankenberg S, Marber M, Liebetrau C. & Mayr M. Comparative Analysis of Circulating Non-Coding RNAs Versus Protein Biomarkers in the Detection of Myocardial Injury. ***Circ Res***. 2019. CIRCRESAHA.119.314937.
8. **Schulte C,** Mayr M. MicroRNAs: A New Understanding of Platelet Physiology and Pathology. ***Thromb Haemost***. 2019. DOI: 10.1055/s-0038-1677505.